ISSN 2663-9084 (Print)
ISSN 2663-9092 (Online)

Ukrainian Neurosurgical Journal

Vol. 30, N3, 2024

Is a scholarly Open Access journal
Founded in April 1995. Quarterly.
State Registration Certificate KV No 23771-13611PR dated 14 February 2019

The journal is on the List of Scientific Professional Editions of Ukraine, where results of thesis research for earning academic degrees of doctor and candidate of sciences and PhD may be published (Order of the Ministry of Education and Science of Ukraine No. 1301 dated 15 October 2019)

Journal publishes peer-reviewed works.

Founders
Romodanov Neurosurgery Institute
Ukrainian Association of Neurosurgeons
National Academy of Medical Sciences of Ukraine

Publisher
Romodanov Neurosurgery Institute

Contact
32 Platona Mayborody st., Kyiv, 04050, Ukraine
tel. +380 44 483-91-98
fax +380 44 489-35-61
E-mail: unj.office@gmail.com
http://theunj.org

The journal went to press 05 September 2024
Format 60 × 841/8. Offset Paper No.1
Order No. 24-26

Circulation 300 copies

Polygraphic services
FOP Golosuy IE
Certificate AA No. 9221702
86 Kyrylivska st., Kyiv, 04080, Ukraine
Tel. +380 44 239-19-85

The master layout of the journal was approved and recommended for publication and distribution via the Internet at the joint meeting of the Editorial Board of the Ukrainian Neurosurgical Journal and the Academic Council of Romodanov Neurosurgery Institute (Meeting Minutes N. 14 dated 30 August 2024)

On the cover
Figures from the article by Vitaliy Y. Molotkovets, Oleksii S. Nekhlopochyn, Myroslava O. Marushchenko "Surgical Treatment of Spinal Intra-Extradural Meningioma: A Clinical Case", p. 56-60

Content

Review article

Ukr Neurosurg J. 2024;30(3):3-17
doi: 10.25305/unj.308080

Comparative evaluation of surgical procedures for trigeminal neuralgia: a literature review

Vyacheslav S. Botev, Yurii V. Hryniv, Viktoria A. Gryb

Department of Neurology and Neurosurgery, Ivano-Frankivsk National Medical University, Ivano-Frankivsk, Ukraine

Received: 09 July 2024
Accepted: 14 August 2024

Address for correspondence:
Viacheslav S. Botev, Department of Neurology and Neurosurgery, Ivano-Frankivsk National Medical University, 2 Halytska st., Ivano-Frankivsk, 76018, Ukraine, e-mail: vyacheslav56@yahoo.co.uk

Trigeminal Neuralgia (TN) has been described in the literature as one of the commonest types of craniofacial pain disorders. TN refers to recurrent lancinating pain that occurs in the distribution of one or more branches of the fifth cranial nerve. The pain perception is typically unilateral, abrupt in onset, brief in duration, and usually starts after trivial stimuli.

The overall prevalence of TN was reported around 0.7/1000 persons, but it tends to be higher in more advanced age groups since the initial onset of the symptoms most frequently starts at the age of 50–60 years.

Although TN is more commonly seen in adults, pediatric TN represents <1.5% of all cases. Pediatric TN differs from adult TN primarily being bilateral in nature (42%) and associated with compression of multiple cranial nerves (46%).

This review will evaluate the current surgical procedures used for the treatment of TN. Operative interventions for TN include microvascular decompression (MVD), balloon compression (BC), radiofrequency thermocoagulation (RF TC), glycerol rhizotomy (GR), and stereotactic radiosurgery (SRS). We review the historical development, advantages, and limitations of these operations.

Additionally, we compare specific parameters for all current surgical procedures. We evaluated the short- and long-term outcomes, risk factors, complications and side effects in patients with TN who underwent operations. Arguments for and against the use of surgery for TN are presented.

Next, surgical decision-making algorithm for refractory classical or idiopathic TN is proposed for patients who require surgery. This algorithm may be used by neurosurgeons in selecting the best surgical treatment.

Lastly, we show the data on current clinical trials, the role of genetics to search for genes predisposing to TN. This project begins with the presumption that the risk for developing classical TN is in large part determined genetically. If so, given the power of modern genetic analysis, it should be possible to identify the underlying gene(s).

At present, there is no ideal surgical procedure for trigeminal neuralgia—one that is minimally invasive, uniformly effective, lacking complications, and without failures or recurrences. MVD still remains the standard by which all other contemporary procedures are measured. MVD provides the longest pain-free interval, yet it is not free of morbidity and mortality. Stereotactic radiosurgery provides a reasonable noninvasive option, but it has delayed onset and a recurrence interval (a few years).

Keywords: *microvascular decompression; balloon compression; radiofrequency thermocoagulation; glycerol rhizotomy; stereotactic radiosurgery*

Trigeminal Neuralgia Awareness Day is observed annually on October 7th.

History and etymology

The renowned medieval Persian scholar, philosopher, and physician Ibn Sina, also known as Avicenna (980–1037), mentioned a condition equivalent to TN in his book "Canon of Medicine"—a pain over the facial skeleton, numbness, and involuntary facial tics. His understanding that nerves conducted pain was later shared by the scholar Esmail Jorjani (1042–1137), a Persian physician. Jorjani described syndromes that were probably consistent with trigeminal neuralgia, hemifacial spasm, and Bell's palsy in his book "Treasure of the Khawarazm Shah" where he concurred with Avicenna in that pain was conducted via nerves, yet he also implicated an artery-nerve conflict as an etiology of trigeminal neuralgia. [1].

In 1756, Nicholas André introduced the term "tic douloureux," encompassing facial pain and clonic spasms in the face. The name was adopted despite the absence of facial tics in all patients suffering from the disease.

In 1773, John Fothergill published his experience treating 14 patients and identified neuralgia as a manifestation of a certain type of cancer, rather than a convulsive disorder. Due to his detailed clinical

descriptions of TN, the disease became known after its author as "Fothergill's disease."

In 1820, Scottish surgeon and anatomist Charles Bell was the first to demonstrate the connection between this syndrome and the trigeminal ganglion, introducing the term "trigeminal neuralgia" into scientific discourse.

Epidemiology

In the United States, 15,000 new cases of trigeminal neuralgia (TN) are registered annually, 1,500 in Canada, and 2,000 in Spain. In the G7 countries (USA, UK, France, Germany, Italy, Spain, and Japan), the number of patients with TN exceeds 1 million, while in China, according to Omics International, there are 4,458,090 cases, which constitutes 2.6% of the population. This figure is likely much higher due to the low rate of seeking medical care. Researchers attribute this primarily to cultural coping strategies for pain.

According to WHO data, the geriatric population is expected to reach 2 billion by 2050, compared to 900 million in 2015. This demographic shift will lead to an increase in the number of potential patients with TN [2].

TN can first appear at any age, but in more than 90% of cases, it begins after the age of 40, with peak incidence between the ages of 37 and 67. The average age of onset for classic TN is 53 years, while patients with secondary TN tend to be about 10 years younger, with an average onset age of 43.

Patients with multiple sclerosis have a 20-fold increased risk of developing TN compared to the general population. Pediatric TN is more often bilateral (42%) compared to adult TN. This is associated with the compression of multiple cranial nerves (46%) due to congenital abnormal vessels, vascular malformations, tumors, cysts, aneurysms, or arachnoiditis [3].

A painful paroxysm is usually followed by a refractory period during which pain cannot be triggered. Usually, attacks occur during the daytime with motor activities involving speech, masticatory and mimic muscles. The course of the disease is chronic and remitting. Preventive measures are lacking [4-6].

Bibliometric Analysis

Publication statistics on trigeminal neuralgia for the years 2001–2021:

4,112 articles,

12,790 authors

Most productive authors:

1. Shiting Li (China) – 56 publications
2. Zakrzewska JM (UK) – 37 publications, also the most cited author (1,284 citations)
3. Lunsford LD (USA) – 36 publications
4. Jun Zhong (China) – 34 publications

The highest number of publications comes from the USA (1,205), China (610), and Japan (230) [7].

Anatomy of the trigeminal nerve (TN)

The trigeminal nerve is the largest cranial nerve, providing sensory innervation to the face and motor impulses to the masticatory muscles. Sensory information, including touch, pain, and temperature, is transmitted through the TN nuclei in the pons before reaching the thalamus and, ultimately, the somatosensory cortex.

The TN originates from the median anterolateral surface of the pons, with a large sensory and a smaller motor root. It then passes through the prepontine and cerebellopontine cisterns and enters through the dura mater opening (porus trigeminus) into the cerebrospinal fluid-filled space known as Meckel's cave, which contains the relatively large trigeminal ganglion (Gasserian ganglion), measuring 15–18 mm. Inside Meckel's cave, the trigeminal ganglion divides into three branches: ophthalmic (V1), maxillary (V2), and mandibular (V3) ***(Fig. 1)***.

The nerve consists of five segments: the brainstem, cisternal segment, Meckel's cave, cavernous and peripheral segments. The cisternal segment is almost always the source of classic TN caused by vascular compression, identified by specific radiological criteria:

- The corresponding blood vessel is almost always an artery.
- The nerve and blood vessel cross perpendicularly.
- The contact between blood vessel and nerve occurs in the root entry zone of the nerve.

TN compression most frequently occurs due to contact with the superior cerebellar artery, less often with the anterior inferior cerebellar artery or smaller branches of the basilar artery. Only a few cases have been reported where the compression was caused by contact with an aneurysm, vertebrobasilar dolichoectasia, AVM, AV fistula, or vein.

The Redlich–Obersteiner zone, located just at the pons, contains a glial cone of residual central myelination that passes into the peripheral myelination of the nerve through Schwann cells. The junction of the central and peripheral nervous systems is particularly sensitive to mechanical stress.

Pharmacotherapy

First-line treatment includes monotherapy with sodium channel blockers. This group of drugs includes carbamazepine and oxcarbazepine. Carbamazepine is effective in more than 60% of patients, but 30% experience adverse reactions, that are severe occurring in one out of every 24 patients receiving treatment. As for oxcarbazepine, it was discontinued in Phase IV trials according to recent reports on the DrugBank website [8].

In October 2022, the FDA granted priority status (Fast Track) to a new drug under development called "Basimglurant" (NOE-101). Basimglurant is a potent inhibitor of the metabotropic glutamate receptor 5 (mGluR5), which is overproduced in cases of TN [9].

The average active period of TN lasts 49 days, followed by remission for several months (36%), weeks (16%), or days (16%). Only 6% of patients can expect remission lasting more than a year, and about 20% may suffer from continuous attacks [10].

When a patient experiences a complete absence of pain for a sufficiently long period (about 6 months, as per GECSEN recommendation), drug withdrawal may be considered. In any case, the discontinuation of treatment should be gradual. Surgical methods are recommended

This article contains some figures that are displayed in color online but in black and white in the print edition

if pharmacotherapy is ineffective, poorly tolerated, or if its effectiveness decreases over time.

The optimal time for surgery is not definitively established, though it is reasonable to avoid excessive delays. Surgery should be offered after the first year of no improvement or intolerability to pharmacotherapy. Overall, significant therapeutic outcomes should not be expected if drugs from three different classes, with different mechanisms of action, have already been tried (alone or in combination), in appropriate doses, and for a maximum period of 3 months per drug, to establish their ineffectiveness.

Surgical and other treatment methods for TN

First and foremost, it is important to note that the term "destructive" is more appropriate than "ablative." This is because "ablation" refers to the removal of tissue from its original location, but not necessarily its destruction (English dictionaries Collins, Cambridge, Macmillan English Dictionary. Ablation – the surgical removal of an organ or part).

Surgical options for treating trigeminal neuralgia include microvascular decompression and a range of destructive procedures such as percutaneous balloon compression, glycerol rhizotomy, radiofrequency thermorhizotomy, or stereotactic radiosurgery targeting the Gasserian ganglion ***(Table 1)***.

Since the end of the last century, many renowned surgeons have been involved in the treatment of TN.

The key stages of the development of surgical methods are presented in ***(Table 2)***.

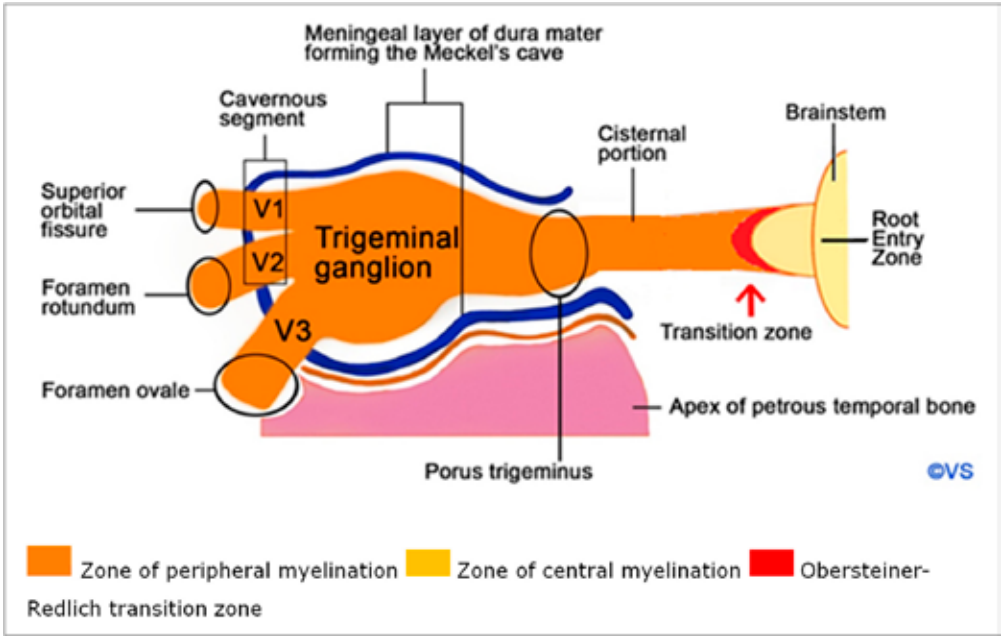

Fig. 1. Trigeminal nerve anatomy: V1- ophthalmic nerve, V2 – maxillary nerve, V3 - mandibular nerve

Table 1. Summary of available treatment modalities for trigeminal neuralgia [11, with modifications]

Surgery	Destructive	Stereotactic radiosurgery	Gamma-Knife, Cyber-Knife, LINAC
		Percutaneous rhizotomy techniques	Glycerol injection, Radiofrequency thermocoagulation, Balloon compression
		Partial sensory neurectomy	
	Non-destructive	Microvascular decompression	
Neuromodulation	Peripheral techniques	Trigeminal branch stimulation, Gasserian ganglion stimulation, Transcutaneous electrical stimulation	
	Central techniques	Motor cortex stimulation, Deep brain stimulation	
Subdermal therapies	Botulinum toxin type A, Subcutaneous alcohol blockage, Lidocaine peripheral block		
Other therapies	Cryotherapy, Streptomycin injection, Peripheral neurectomy		

Table 2. History of surgery for trigeminal neuralgia [12, with modifications]

Year	Authors	Procedures
1892	Hartley F., Krause F.	Excision of the Gasserian ganglion and its roots
1900	Cushing HW	Trigeminal ganglionectomy
1901	Spiller WG, Frazier CH	Extradural sub-temporal retrogasserian neurotomy
1911	Taptas JN	Alcohol injection into Meckel's cavity
1914	Härtel F.	Percutaneous approach to the foramen ovale
1932	Kirschner M.	Percutaneous electrocoagulation of the trigeminal ganglion
1932	Dandy WE	Posterior fossa subtotal rhizotomy
1934	Dandy WE	Recognition of vascular compression as a cause of neuralgia
1947	Olivecrona AH	Subtemporal rhizotomy
1951	Taarnhøj P.	Intradural decompression of the trigeminal ganglion and the posterior root
1952	Love JG	Extradural decompression of the trigeminal ganglion and the posterior root
1955	Shelden CH	Enlarging the foramen ovale and foramen rotundum
1959	Gardner WJ, Miklos MV	First report of vascular decompression
1966	Jannetta PJ, Rand RW	Transtentorial retrogasserian microvascular decompression
1971	Jannetta PJ	Retromastoid microvascular decompression
1971	Leksell L.	Stereotactic Gamma-Knife Radiosurgery
1974	Sweet WH, Wepsic JG	Radiofrequency thermocoagulation
1981	Håkanson S, Sweet WH	Percutaneous glycerol injection into Meckel's cavity
1983	Mullan S., Lichtor T.	Percutaneous balloon compression
1993	Meyerson BA, Lindblom U.	Motor cortex stimulation

Percutaneous destructive methods

In 1914, Fritz Härtel performed the first anterior percutaneous puncture of Meckel's cave using a spinal needle placed anterior to the coronoid process of the mandible through the foramen ovale; this approach is still in use today ***(Fig. 2)*** [13].

The needle/cannula/trocar is inserted 2.5–3 cm lateral to the corner of the mouth (3). The needle's trajectory is directed towards the intersection of two planes: one sagittal plane passing through the ipsilateral pupil (1) and the other coronal plane located 3 cm anterior to the external auditory canal (2). This point approximately corresponds to the lateral projection of the foramen ovale on the skin.

The inverted pyramid is another simple yet effective model for guiding the needle to the foramen ovale. Three of the four vertices of the pyramid are cutaneous and visible to the surgeon, while the fourth is the foramen ovale, which requires spatial imagination.

The foramen ovale is located at the posterior aspect of the greater wing of the sphenoid bone. It transmits the mandibular nerve, the accessory meningeal artery, the lesser superficial petrosal nerve, and the emissary vein. This foramen is one of the key points situated at the transition zone between intracranial and extracranial structures.

A thorough understanding of surgical anatomy and careful preoperative imaging are crucial for recognizing the potential risks of Härtel's percutaneous approach. A misaligned trajectory may lead to complications, particularly puncturing the internal carotid artery. Even with correct trajectory, the needle may penetrate the parotid duct, maxillary artery, or Eustachian tube, leading to complications such as hemoptysis, hematoma of the cheek and/or pterygoid-mandibular area, serous otitis, and others ***(Fig. 3)***.

Accessing and puncturing the foramen ovale can be challenging in certain patients, particularly those with

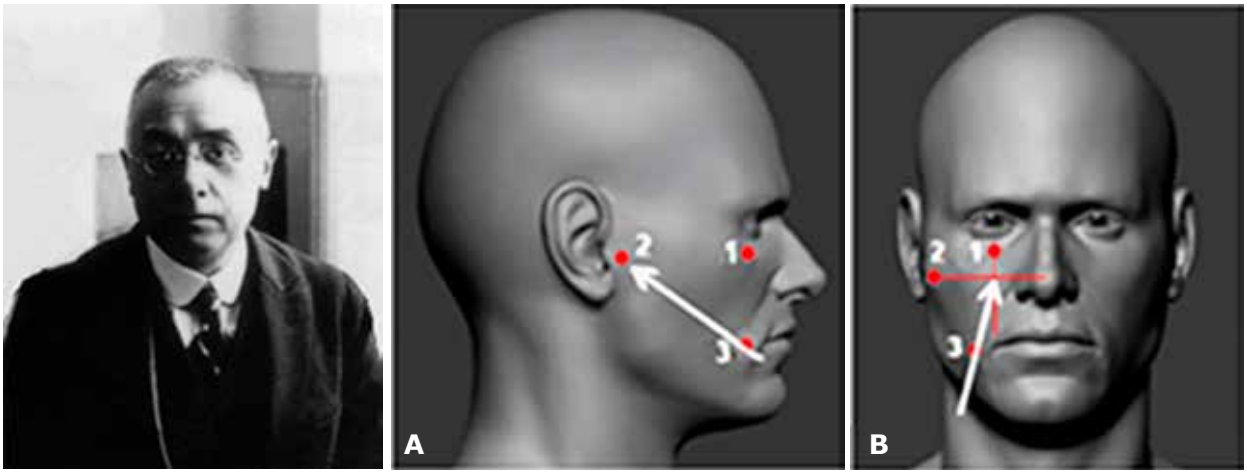

Fig. 2. Fritz Härtel (1877–1940). Härtel's approach: A – lateral view, B - anteroposterior view

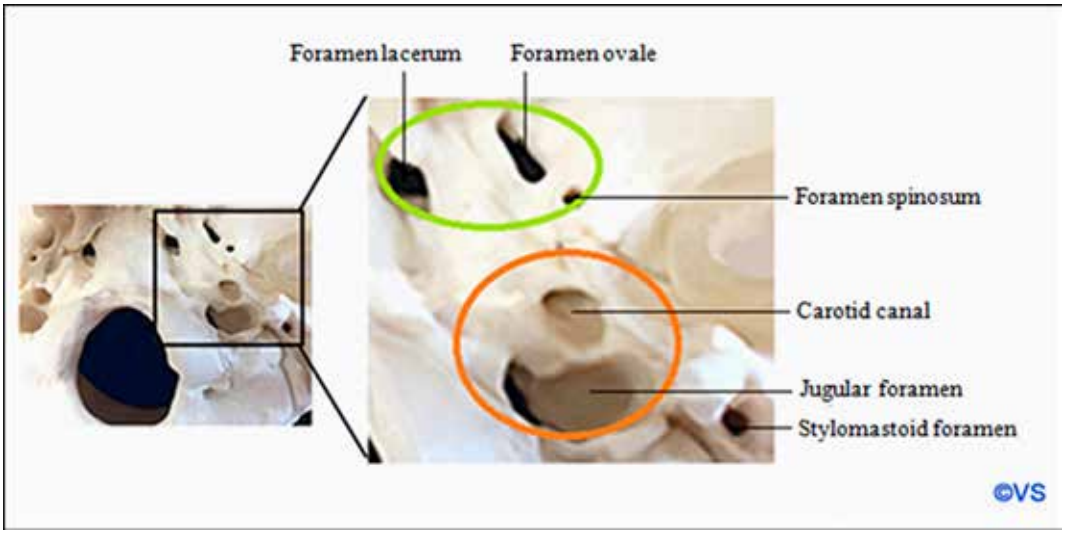

Fig. 3. The safe zones and danger zones along the periforaminal space. The green zone defines the safe zones to "walk" the needle along the skull base to find the foramen. The orange zone defines danger zones where the carotid artery or jugular vein could be injured

hypertrophic pterygoid processes or platybasia. In such cases, a trajectory guided by neuronavigation systems, or even better, catheterization of the foramen under CT guidance, may be helpful.

Thermocoagulation of the Gasserian ganglion / Radiofrequency (RF) destruction

The procedure is referred to as radiofrequency because it uses the same frequency as AM radio—approximately 500 kHz of electromagnetic radiation. Electrocoagulation for the treatment of the trigeminal nerve roots was first developed by A. Réthi in 1913. This method was associated with severe complications, including corneal ulcers that required enucleation, multiple cranial nerve palsies, carotid artery damage, cardiac arrest, meningitis, and death.

Further development of the method was continued by Martin Kirschner, who in 1931 developed a stereotactic method for inserting an insulated needle through the foramen ovale for electrocoagulation of the Gasserian ganglion. Kirschner reported on 250 cases in 1936 and 113 cases in 1942 [14, 15].

William H. Sweet ***(Fig. 4)*** and James G. Wepsic further developed the technique of radiofrequency thermal destruction of the trigeminal nerve root in 1974 [16]. They introduced various control measures—electrical stimulation of the root and temperature monitoring. In 1982, H. van Loveren, John M. Tew, and J.T. Keller presented an electrode with a curved tip ***(Fig. 5)*** [17].

Straight electrodes are preferred for third branch neuralgia, and curved electrodes for first or second branch neuralgia.

Continuous RF destruction is applied for 60-90 seconds, temperature 70-90°C. During pulsed RF destruction, intervals of short bursts of current lasting 20 ms alternate with pauses lasting 480 ms. Temperature does not exceed 42°C.

Fig. 4. William Herbert Sweet (1910–2001)

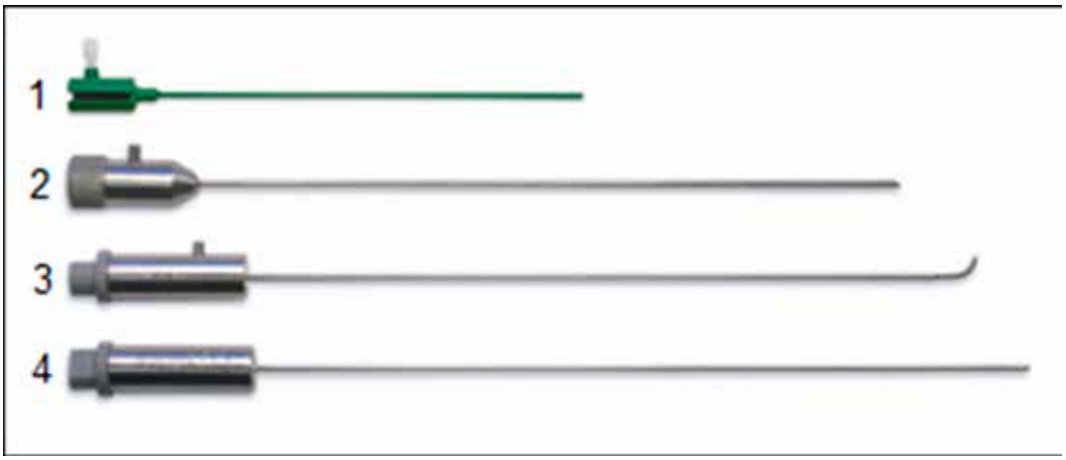

Fig. 5. Radiofrequency thermocoagulation kit: 1 - cannula, 2 - stylet, 3 - curved electrode, 4 - straight electrode

1. Yücel Kanpolat et al. (2001) described their 25-year experience in treating 1600 patients (2138 operations). 1216 patients underwent a single operation and 384 underwent multiple operations: twice in 275 patients, three times in 79, four times in 19, five times in 8 and six times in 3. Initial analgesic effect was noted in 97.6% of patients. Early recurrence of pain (< 6 months) was observed in 123 patients and late recurrence (> 6 months) in 278 patients. The recurrence rate was 25.1% during a mean follow-up period of 68 months. After 5 years, complete analgesia was maintained in 58% of patients who underwent a single procedure; this number decreased to 52% after 10 years and to 41% after 20 years. The most important complications were hypoesthesia with paresthesias in 14.6% and masticatory muscle dysfunction in 4.5% of cases. Absence or reduction of corneal reflex was observed in 91 patients (5.7%). Among them, 10 developed keratitis [18].

2. Review by M. Sindou and M. Tatli (2009) conducted by the French Neurosurgical Society (10 articles, 7483 patients) with a follow-up period of 3 to 26 years showed a mean incidence of an initial analgesic effect of 94% (81 to 99% depending on the series) and a mean long-term efficacy rate of 60.4% (20 to 93%). Side effects and complications were reported with varying frequency: bothersome facial hypoesthesia 5-98%, difficulty in mastication 4-24%, keratitis 1-8% and dysesthesia/anesthesia dolorosa 0.8-7% for later complications. Mortality was 0.1% due to carotid artery damage [19].

3. Analysis by L. Bendtsen et al. performed by the European Academy of Neurology 2019 (7 articles, 4533 patients) with a follow-up period of 3 to 9.3 years reported an initial analgesic effect of 26 to 82% of cases and a recurrence rate ranging from 16 to 74%. There were no fatal outcomes in this review. Patients with hearing loss were 6, cranial nerve palsy 36, corneal hypoesthesia 300, keratitis 55, masticatory weakness 280, facial hypoesthesia 853, anesthesia dolorosa 29 [20].

Percutaneous balloon compression of Gasserian ganglion

In 1983, Sean Mullan ***(Fig. 6)*** and Terry Lichtor performed percutaneous balloon compression (BC) of the Gasserian ganglion [21]. Mullan's kit contains a size 14 hollow metal stylet (introducer), sharp and blunt

obturators, curved and straight probes, and No.4 Fogarty balloon catheter. The balloon is inflated to a pressure of 1.0-1.5 atmospheres for 60-90 seconds. Ideally, a pear-shaped configuration of the balloon in the porus trigeminus is created during compression ***(Fig. 7)*** [22]. Some redness of the ipsilateral conjunctiva is often observed after compression.

In 2016, the FDA banned the release of Mullan kit due to manufacturing difficulties, so some surgeons use other kits or a standard liver biopsy needle, which is available in most operating rooms ***(Fig.8)*** [23-25].

1. In the review by A. Donnet et al. (2017), conducted by the French Neurosurgical Society (10 series, 1404 patients) with a follow-up period of 1–6 years, the initial pain relief effect was observed in 82–100% of patients (an average of 96%), with long-term efficacy in 54.5–91.3% of patients (an average of 67%). Hypesthesia was reported in 4–77% of cases, and transient masticatory muscle paresis occurred in 50–66% of cases. Mortality rate due to carotid artery damage was 0.2% [19].

2. S. Grewal et al. (2018) from the Mayo Clinic, in a series of 222 patients followed for 15 years with an average follow-up of 31 months, focused particularly on the timing of recurrences after BC. The likelihood of being pain-free 15 years after the procedure was only 10%. Recurrences occurred on average 12 months post-procedure. A significant number of patients reported some degree of hypesthesia (82%), though in most cases it was relatively mild. At the last follow-up, 88% of patients were pain-free, with a median follow-up of 31.1 months. Atypical pain was associated with poorer outcomes. Repeat procedures carried a higher risk of pain recurrence, but the initial effectiveness of repeat procedures did not diminish [26].

3. According to a review by L. Bendtsen et al. from the European Academy of Neurology in 2019 (5 papers, 755 patients) with a follow-up period of 5 to 10.7 years, the initial pain relief rate was 95%, which then declined to 54.5–80% (an average of 67%) at the final follow-up. Recurrence or failure rates ranged from 20 to 51.7%. The most significant reported complications were hypesthesia with paresthesia in 14.6% of cases and motor weakness of the trigeminal nerve in 4.5% [20].

4. Yi Ma, following his training in Rome under Dr. Mario Meglio from 2000 to 2017, performed 12,838 BC procedures on 12,797 patients. The initial pain relief effect was reported in 95.6% of cases. Hemorrhagic complications occurred in 11 patients, with two resulting in death. One patient died from multiple intracerebral hematomas, while the second died of a large subdural hematoma due to cavernous sinus injury. Four patients required ventriculoperitoneal shunting for hydrocephalus after subarachnoid hemorrhage, while the other five recovered spontaneously without surgery.

Five vascular complications occurred, including three cases of dural carotid-cavernous fistula (CCF) and two cases of external carotid artery system fistula. These patients were successfully treated with endovascular embolization. Ischemic stroke occurred in two cases, though the causes were not determined. Kaplan-Meier curves showed a long-term pain relief effect of over 86% five years after BC, over 83% after 10 years, and 77% after 15 years. The annual risk of recurrence was less than 7% after five years, less than 4% after 10 years, and remained stable at 2% from the 15th year post-procedure [24].

5. A. Kourilsky et al. (2022) performed a retrospective analysis of 131 patients who underwent BC for the first time between 1985 and 2019 in two French hospitals. Potential clinical and radiological predictors of time to pain recurrence and severe sensory complications were assessed using the Cox model and logistic regression, respectively. The median follow-up period was three years. Pain recurrence occurred in 77 patients (58.7%), with a median time to recurrence of two years.

Fig. 6. John Francis Mullan (1925–2015)

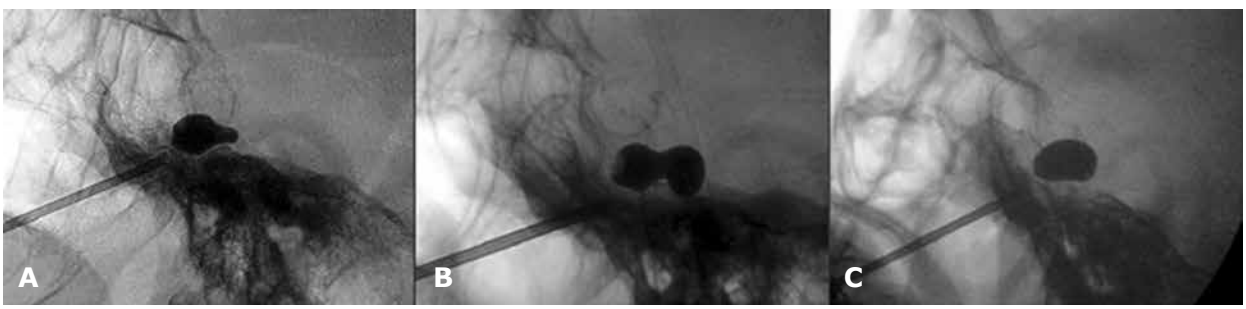

Fig. 7. Balloon shape: A - pear, B - hourglass, C - oval [22]

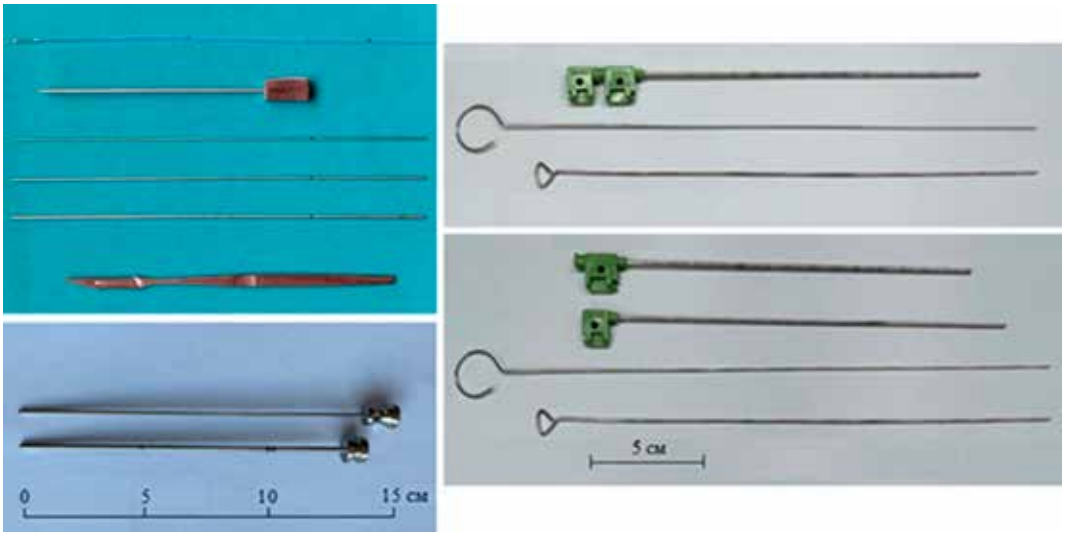

Fig. 8. Various balloon compression (BC) kits: A - O. Barlas [23], B - Y. Ma [24], C - C. Sun [25]

Multivariate analysis identified six independent factors predicting pain recurrence: 1) longer preoperative symptom duration; 2) pain location along the mandibular branch of the trigeminal nerve (V3); 3) atypical pain; 4) a history of multiple sclerosis; 5) the use of a medical device not specifically designed for BC; and 6) balloon compression duration exceeding 60 seconds [27].

Percutaneous retrogasserian glycerol rhizotomy

From 1974 to 1981, Sten Håkanson ***(Fig. 9)*** performed percutaneous puncture destruction of the Gasserian ganglion through the foramen ovale using pure glycerol.

Glycerol ($C_3H_8O_3$) is a trivalent alcohol that is colorless and odorless, serving as a precursor for the synthesis of phospholipids and triacylglycerols in the liver and adipose tissue of humans. The three hydroxyl groups and carbon backbone of glycerol form a molecule with a universal solubility profile, allowing it to dissolve easily in water and penetrate cell membranes. The mechanism of glycerol neurolysis is due to the disruption of tight junctions between Schwann cells and the external axolemma of peripheral nerves, as well as alterations in intracellular osmolality. It is also believed that anhydrous glycerol isolates the pathological section of the axon, and since it has a high dielectric constant (45.5 at 25°C), it renders the nerve a poor conductor. This causes presynaptic inhibition and delays the propagation of nerve impulses.

In the 1970s in Stockholm, during the development of stereotactic radiosurgical destruction of the Gasserian ganglion using a Gamma-Knife, radioactive tantalum powder dissolved in glycerol was used to create a stereotactic target by injecting it into the trigeminal cistern. Håkanson and his colleagues noticed that the injection of this medium itself seemed to reduce facial pain even before the Gamma-Knife procedure was administered. The group later described a method of direct glycerol injection into the trigeminal cistern and published their first case series in 1981 [28].

1. In a report by P. Asplund et al. (2016) from Umeå University (Sweden), involving 124 patients who underwent glycerol rhizotomy and were followed up for 5 years, an immediate effect was noted in 85% of cases, with a median pain-free period lasting 21 months. At the last follow-up, 47 patients (38%) were pain-free. Hypesthesia with dysesthesia was observed in 23% of patients, frequently combined with a decreased corneal reflex. Herpes outbreaks occurred in 3%, and chemical meningitis also in 3%. According to Kaplan–Meier statistical analysis, the probability of being pain-free at 5 years was less than 20% [29].

2. A literature review by the French Neurosurgical Society (2017), including 1310 cases with a follow-up period of 1–10 years (average 6.5 years), showed an effectiveness rate of 42–84%, which is maintained in the long term in 18–59% of cases (average 38.5%). The main complications include: hypesthesia with dysesthesia in 30% of cases, refractory keratitis in 5%, and herpes outbreaks in 50% [19].

3. In a series by L. Bendtsen et al. (2019), including 289 patients with a follow-up period of 4.5 to 8 years, an immediate effect was achieved in 75% of patients. Pain relief at the average follow-up period decreased to 18–59% depending on the series (average 40%), with the frequency of recurrences or failures varying from 41 to 84%. The most significant complication in these series was facial hypesthesia with varying degrees of paresthesia/dysesthesia in 39% [20].

4. Imran Noorani et al. (2016) in a series of 152 glycerol rhizotomies with long-term follow-up showed that analgesia of class I or II was noted in 53.7% of procedures, class III in 17.4%, class IV in 16.1%, and class V in 12.8%. Complete initial pain relief (with or without medication) was achieved in 72%, comparable to the 73–98% reported in previous literature. The overall complication rate was 30.3%. The most common complications were decreased corneal reflex (11.2%), recurrence of herpes simplex (8.6%), numbness (71.7%), and mild dysesthesia (5.9%). The average time to pain recurrence was 14 months. The recurrence rate at 12 months was 45.5% [30].

The 5-point Barrow Neurological Institute Pain Scale (BNI-PS) allows for the assessment of pain intensity and

the need for the patient to use medications to manage it ***(Table 3).***

Glycerol rhizotomy has an advantage compared to other methods as it does not require specialized equipment. However, the neurotoxic effects of glycerol, due to the difficulty in controlling its diffusion into the subarachnoid space, lead to side effects and complications.

Comparison of three percutaneous rhizotomy methods

Imran Noorani et al. (2021) were the first to analyze data over a 19-year period at a single neurosurgical center, involving 210 patients (a total of 392 procedures): 152 glycerol rhizotomies, 155 thermocoagulations, and 85 balloon compressions.

It was shown that balloon compression provides the longest duration of pain relief compared to glycerol rhizotomy and thermocoagulation, with the latter two showing similar durations of pain relief. It was also noted that repeated procedures offer good long-term pain relief. Recurrence of pain occurred in 25% of patients within 5 months after glycerol rhizotomy, 12 months after thermocoagulation, and 26 months after balloon compression. The average time to pain recurrence was 29 months for glycerol rhizotomy and 30 months for thermocoagulation [31].

Comparison of balloon compression (BC) with radiofrequency (RF) thermocoagulation

J. Herta et al. (2023) conducted a retrospective single-center analysis of a series involving 230 patients with TN in Austria, who underwent 202 BCs and 234 thermocoagulations between 2002 and 2019. An immediate effect was achieved after 353 (84.2%) procedures, with no significant difference between BC (83.7%) and thermocoagulation (84.9%). The pain-free period following the procedures was longer for BC at 481 days, compared to thermocoagulation at 421 days, but without statistical significance. The complication rate was 22.2%, and zero mortality showed no differences between the two procedures.

Seventeen (3.9%) operations had to be terminated due to severe bleeding (1.6%), inability to access the foramen ovale (1.4%), and anesthetic issues related to airway or circulatory function (0.9%). Diplopia occurred after four BC procedures, but never after thermocoagulation. Bradycardia, which is common with destructive procedures, had to be treated with medication in 60% of all cases. A drawback of both methods is the significant recurrence rate, which varies widely across studies, ranging from 15% to 64%. After one year, the recurrence rate was 56.1% for BC and 56% for RF. In the long term, BC showed a slightly longer recurrence-free period than thermocoagulation [32].

Comparison of percutaneous rhizotomy methods ***(Table 4).***

Fig. 9. Sten Håkanson

Microvascular decompression (MVD)

In 1966, Robert W. Rand ***(Fig. 10)*** was the first to perform microvascular decompression (MVD) of the trigeminal nerve root at the brainstem via a subtemporal approach. In 1967, Peter J. Jannetta ***(Fig. 11)*** performed MVD of the trigeminal nerve root in the prepontine cistern.

1. A large sample of 1,185 cases from 1972 to 1991, in the study by F. Barker, P. Jannetta et al. (1996), demonstrated sustained pain relief in 70% of cases, with 30% experiencing recurrences. 11% underwent repeat surgeries. Two female patients died due to hemispheric stroke and infarction of the brainstem and cerebellum. Six patients developed infarction, edema, or hemorrhage in the ipsilateral cerebellar hemisphere, five of whom underwent cerebellar resection. Two patients were found to have postoperative supratentorial hematomas (one subdural and one intracerebral). These eight patients recovered after hematoma evacuation. After the introduction of intraoperative monitoring of brainstem evoked potentials, there were no fatal complications. Female gender, symptom duration longer than eight years, venous compression, and the absence of immediate postoperative pain cessation were significant predictors of possible recurrence [34].

Table 3. Barrow Neurological Institute (BNI) Pain Intensity Scale

Score	Description
I	No pain, no medication
II	Occasional pain, not requiring medication
III	Some pain, adequately controlled with medication
IV	Some pain, not adequately controlled with medication
V	Severe pain, no pain relief

In 1999, Peter Jannetta's team published a report on 4,415 operations performed between 1969 and 1999. The authors described all the nuances of each of the six main stages of MVD in detail [35].

2. M. Sindou et al. (2018), in a meta-analysis of 17 articles (5,124 patients), showed similar results across various published articles. Immediate pain relief was achieved in 80–98% of patients (an average of 91.8%), with complete pain relief maintained in 62–89% (an average of 76.6%) by the end of the follow-up period (ranging from 5 to 11 years, with an average of 7 years). Complete pain relief after the first procedure was noted in 71% of cases. Improvement was observed in 93% patients immediately after the intervention [36].

3. In a meta-analysis by L. Bendtsen et al. (2019) from the European Academy of Neurology (21 articles, 5,149 patients) with an average follow-up period of 3 to 10.9 years, initial pain relief was reported in 80-98.2% of cases, pain-free status during follow-up in 62-89%, and recurrence rates ranging from 4-38% [20].

Complications after MVD may occur in 20% of patients, though serious complications are rare. Complications related to cranial nerves require special attention, as cranial nerves IV through XII are exposed during surgical access. Numbness and dysesthesia occur in 5% to 10% of patients. Diplopia due to manipulation of the fourth or sixth nerve is often transient, and facial nerve paralysis is rare (<1%). Hearing loss varies from 1% to 20%, depending on audiometry or subjective reports.

Other complications include cerebrospinal fluid leakage (3–4%); infections are rare and occur at the same rate as with other craniotomies. Other rare complications include aseptic meningitis, postoperative bleeding, and stroke. The mortality rate associated with the procedure is estimated at 0.2%.

4. F. Chen et al. (2021), in a meta-analysis of 74 articles (8,172 patients), noted a recurrence rate in 956 patients (11.6%). Factors contributing to a relatively higher recurrence rate included atypical symptoms of TN, absence of nerve excavation, non-arterial compression, patient age between 50-60 years, and longer disease duration. However, the recurrence rate after MVD was significantly lower than with pharmacotherapy, Gamma-Knife surgery, percutaneous balloon compression, and radiofrequency thermocoagulation. Even after successful surgery, 10% of patients experienced recurrences. The most common complications included hypoacusis (hearing loss) and TN paresis [37].

Table 4. Comparison of the percutaneous procedures [33]

	RFT	GR	PBC
Initial outcome	97 - 99%	53 – 98%	82 – 93%
Recurrence	+	+++	++
Division selectivity	+++	++	+
Nerve fiber selectivity	++	++	+++
Anesthesia	Awake	Sedation	Sedation+pacemaker
Overall complication rate	+++	++	+
Anesthesia dolorosa	0.6 – 0.8%	0 – 5%	0 – 3.4%
Masseter weakness	3 – 29%	0 – 4.1%	10 – 50%

+++: more likely, ++: moderate, +: less likely, RFT: radiofrequency thermocoagulation, GR: glycerol rhizotomy, PBC: percutaneous balloon compression

Fig. 10. Robert W. Rand (1923–2013)

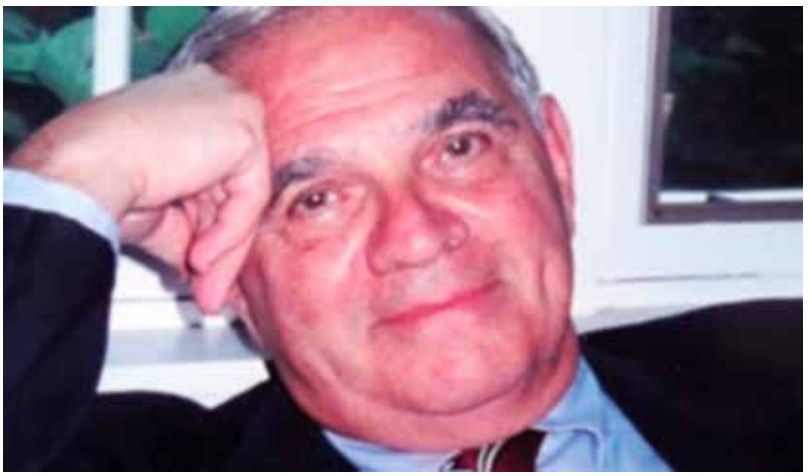

Fig. 11. Peter J. Jannetta (1932–2016)

Reproduced with the permission of prof. M. McLaughlin

Postoperative hemorrhage into the cerebellum may be a major cause of fatal complications after MVD. If a hematoma is confirmed, urgent surgery should not be delayed. Rapid hematoma evacuation, as well as ventricular drainage through the anterior horns on both sides, can save the patient.

Stereotactic radiosurgery (SRS)

Lars Leksell **(Fig. 12)** first reported on stereotactic radiosurgery (SRS) in 1951. In his initial experiments, Leksell connected a dental X-ray tube to a stereotactic arc to irradiate the trigeminal ganglion. Later, in 1971, he developed the Gamma Knife, which uses multiple focused beams from cobalt-60 sources.

1.The first large series of 117 patients was conducted at the Mayo Clinic in Rochester, published by B. Pollock et al. (2002) with an average follow-up period of 26 months (ranging from 1 to 48 months). Pharmacotherapy was unnecessary for 57% of patients after one year, and 55% after three years. Sensory disturbances were detected in approximately 25% of patients at a dose of 90 Gy [38].

2. In the Marseille series of 497 patients with long-term follow-up, S. Tuleasca, J. Regis et al. (2016) reported that 64.9% and 45.3% of patients remained pain-free and did not require medication at five and ten years, respectively. Very troubling hypoesthesia was observed in only 3 patients (0.6%) [39].

3. The same authors, in 2018, performed a systematic review of all 65 published articles up to 2015, including 6,461 patients. Gamma - Knife was used in 45 articles, LINAC in 11, and CyberKnife in 9. The efficacy was found to be similar for each method: 53% for Gamma- Knife, 49% for LINAC, and 56% for CyberKnife. Recurrence rates ranged from 24% to 32%. Between 30% and 45% of patients remained pain-free without pharmacotherapy for up to 10 years of follow-up. The most common side effect was hypoesthesia (0–68%). Other side effects included dysesthesia, paresthesia, dry eyes, deafferentation pain, and keratitis [40].

4. According to a meta-analysis (46 articles, 5,787 patients) conducted by A. Gubian et al. (2017), the efficacy of SRS for classic TN is 71%, with over 64% of patients experiencing analgesic effects for five years or more after irradiation. Complications of SRS included temporary numbness and dysesthesia in 28% of patients, and hearing loss in 0.74%. TN Recurrence occurred in 25% of cases, but repeat irradiation remained effective [41].

There is now a large body of literature detailing the outcomes, particularly when using the Gamma-Knife system. A correlation has been established between the frequency of hypoesthesia and pain relief. Reoperation is possible even for the third time, although the incidence of hypoesthesia increases with each subsequent procedure. Overall results seem comparable to percutaneous methods but inferior to MVD. The likelihood of a favorable long-term outcome after Gamma-Knife surgery is slightly less than 50%, with a 20% chance of facial numbness.

A selective series of operations performed in leading clinics ***(Table 5)***.

Algorithm for selecting surgical treatment for trigeminal neuralgia

Many universities and major centers in the USA, UK, Italy, South Korea, and other countries offer various algorithm options for selecting surgical interventions for TN. These algorithms are primarily designed for researchers, postgraduate students, and doctoral candidates, consisting of diagnostic and treatment blocks. For practicing physicians, in our opinion, a simpler algorithm would be more suitable ***(Fig. 13)***.

1.For young and healthy patients without comorbidities, MVD should be offered.

2.For elderly, less healthy patients, or those who do not wish to undergo open surgery, balloon compression is recommended as the first-line treatment.

3. If balloon compression is not possible, glycerol rhizotomy or thermocoagulation may be considered, but thermocoagulation should be avoided in patients with pain in the first branch of the TN.

Selecting the most appropriate treatment method requires an assessment of the risks and benefits of each procedure. As always in neurosurgery, proper patient selection can ensure a higher success rate.

A summary table on the effectiveness of surgical treatments for TN ***(Table 6)***.

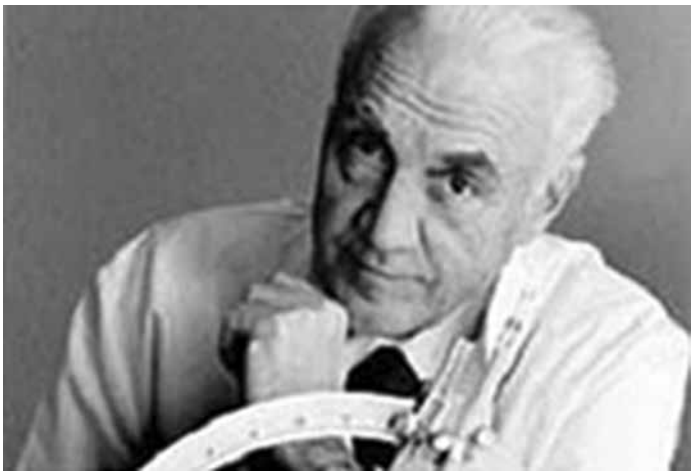

Fig. 12. Lars Leksell (1907–1986)

Medical negligence and lawsuits

A. Boyke et al. (2021) conducted a 34-year analysis of medical negligence lawsuits in the U.S. related to the treatment of TN. The report includes 49 lawsuits from 1985 to 2019. The most frequently accused medical professionals were dentists (31 cases) and neurosurgeons (10 cases). The average payout for dentists was $415,908, while for neurosurgeons it was $618,775. The most common complaints by plaintiffs after surgery involved cranial nerve injuries, loss of consortium, financial losses, and death [53].

Current clinical trials

As of December 8, 2022, there were 793 clinical trials registered on the website www.clinicaltrials.gov focusing on the treatment of neuropathic pain, of which 64 (7%) were specifically for TN [54].

Professor Joanna Zakrzewska from University College London (UCL) is, as of June 24, 2024, the lead moderator of fifteen new trials in the United Kingdom. For more information, [see https://www.hra.nhs.uk/planning-and-improving-research/application-summaries/research-summaries/?query=Trigeminal+Neuralgia&research_type=&rec_opinion=&date_from=&date_to=&relevance=true].

The most significant ones are:

1.Search for genes predisposing to TN - DNA will be collected from 500 patients with TN across multiple centers. A whole-genome analysis will be performed and compared with appropriate control standards to identify sequence variants that significantly segregate among TN patients. These sequence variants may cause TN by directly affecting the function of the proteins encoded by these genes or by altering other aspects of gene expression. If genetics indeed play a role in TN, there is a strong likelihood that this project will uncover these genes and, ultimately, the pathophysiological mechanisms involved.

2.Virtual Reality (VR) technology - this is being explored as a new tool to reduce pain perception and could become a breakthrough in cases resistant to treatment. A study will be conducted on the effectiveness of stereotactic radiosurgery with VR training. Additionally, using MRI and artificial intelligence, researchers will attempt to identify structural abnormalities in the central nervous system associated with pain.

3.Augmented Reality (AR) technology - combined with established trajectory planning software like Magic Leap 1 and Brainlab Elements, augmented reality will

Table 5. Selected large series of surgical treatment for trigeminal neuralgia

Procedure	Author	Years	Total number of operations
Balloon compression	Yi Ma (China) [24]	2000-2017	Exceeds 16 000
	O. Barlas (Turkey) [23]	2007-2021	500
Glycerol rhizotomy	LZ Chen (China) [42]	1983-2008	4012
	XH Wang (China) [43]	1983-2003	3370
	D. Kondziolka (USA) [44]	1985-2004	1174
Radiofrequency thermocoagulation	Y. Kanpolat (Turkey) [18]	1974-1999	2138
	G. Nugent (USA) [45]	1982-1997	Exceeds 1600
	M. Sindou (France) [46]	1980-2022	3250
Stereotactic radiosurgery	C. Tuleasca (France) [39]	1992-2010	497
	K. Marshall USA) [47]	1998-2008	777
	A. Niranjan (USA) [48]	1988-2016	1250
	A. Jarrahi (USA) [49]	2000-2022	587
Microvascular decompression	P. Jannetta (USA) [35]	1969-1999	4415
	J. Zhong (China) [50]	2000-2020	Exceeds 10 000

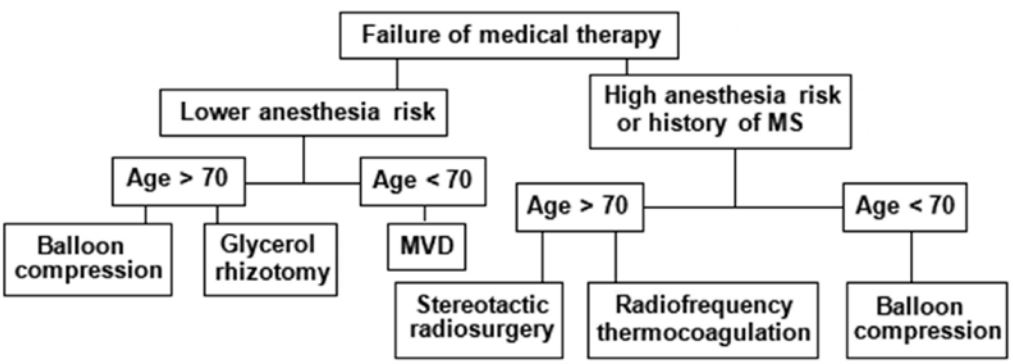

Fig. 13. An algorithm for refractory classical or idiopathic TN

Table 6. Summary of surgical outcomes in TN (according to S. Bick et al. [51], R. Kirollos et al. [52] with modifications)

Procedure	Initial Response Rate (%)	Long-Term Response Rate (%)	Recurrence Rate (%)	Mortality (%)	Side effect / Complications (%)
MVD	80.3-96.0	1 year - 84 5 years - 72-85 10 years - 74	23.4	0-1.2 (cerebellar infarct)	*Transient:* trochlear palsy 0-5, cerebellar infarct 1, CSF leakage 2-17 *Permanent:* numbness 2-7, hearing loss 2.5, facial palsy 0-2, anesthesia dolorosa 1-3
RF	97.6-99.0	1 year - 61.8 5 years - 57.7 10 years - 52.3 20 years - 41	39.6	0.1 by carotid injury	*Transient:* masseter weakness 4-24, keratitis 1-8, trochlear palsy 1-2
GR	71.0-97.9	1 year - 53-63 5 years - 43.5	61.5	0	*Permanent:* herpes eruption 50, meningeal reaction - frequent, numbness/ dysesthesia 30, corneal hypoesthesia 15, keratitis 5
BC	82.0-93.8	1 year - 74.6 5 years - 69-80 10 years - 68.1	33	0.2 by carotid injury	*Transient:* numbness 39, masseter weakness 66, aseptic meningitis 0.7
SRS	79.0-91.8 (delayed 10 d-3.4 mo)	1 year - 75-90 5 years - 44-65 10 years - 30-51.5	46	0	*Permanent:* hypoesthesia 0-54

significantly improve the accuracy of foramen ovale puncture compared to the Härtel's "freehand" approach.

4. Artificial intelligence for predicting postoperative outcomes.

5. Biomarker research - this involves studying the expression levels of inflammatory cytokines and neurotransmitters in the peripheral blood of TN patients before and after surgery. The aim is to gather information for personalizing treatment options.

6. Percutaneous balloon compression using the Sinovation R neurosurgical robot.

Conclusions

- A cure for trigeminal neuralgia is unpredictable.
- Women experience recurrences more frequently than men, and the time to recurrence is shorter.
- Female gender and younger age are independently associated with worsening pain scores at the 3-month follow-up, according to multivariate analysis.
- In 10% of patients with classical TN who underwent successful surgery, recurrence is observed.
- A shorter disease duration (≤ 5 years), arterial compression, and Type I TN predict more favorable outcomes.
- In 74% of patients, microvascular decompression (MVD) results in pain-free status for up to 10 years, with the lowest rate of rehospitalization within the first year.
- While MVD carries a higher risk of serious complications, including weakness of the masticatory muscles, hearing loss, cerebellar infarction, and cerebrospinal fluid leakage, the rate of these complications remains relatively low in experienced hands.
- Among percutaneous techniques, radiofrequency thermocoagulation provides good initial and long-term pain relief, with the advantage of selecting the exposure to the specific branch of the trigeminal nerve.
- Glycerol rhizotomy and balloon compression have similar initial pain relief and duration of effect.
- Radiofrequency thermocoagulation is likely to require follow-up procedures.
- Advanced age and postoperative numbness are predictors of good - outcomes for percutaneous surgery.
- Repeated procedures carry a higher risk of pain recurrence, but the initial effectiveness of these subsequent procedures does not decrease.
- It is becoming increasingly clear that no single method has 100% efficacy. This suggests that TN is probably a heterogeneous group of disorders that collectively manifest as facial pain.

Destructive methods are preferred if MRI does not reveal neurovascular contact. The neurosurgical arsenal offers a wide range of options, each with its own advantages and disadvantages. Careful consideration of these factors will help determine which procedure is most suitable for a specific situation.

Currently, there is no ideal surgical method for treating TN that is minimally invasive, equally effective, and free from complications, failures, and recurrences. MVD remains the standard against which all other modern procedures are measured, offering the longest pain-free intervals.

Ultimately, uncovering the molecular mechanisms underlying trigeminal neuralgia will pave the way for new, more effective, and less invasive treatments.

Disclosure

Conflict of interest

The authors declare no conflicts of interest and no personal financial interest in the preparation of this article.

Funding
The study was conducted without sponsorship.

References

1. Park K, Cho KR, editors. Trigeminal Neuralgia: A Comprehensive Guide. Springer Nature; 2023.
2. Trigeminal Neuralgia Treatment Market Growth Insight: Global Industry Analysis by Size, Share, Comprehensive Analysis, Future Trends and Competitive Landscape to Forecast by 2026 [Internet]. PharmiWeb; 2021. https://www.pharmiweb.com/press-release/2021-03-25/trigeminal-neuralgia-treatment-market-growth-insight-global-industry-analysis-by-size-share-compr
3. Xu R, Xie ME, Jackson CM. Trigeminal Neuralgia: Current Approaches and Emerging Interventions. J Pain Res. 2021 Nov 3;14:3437-3463. doi: 10.2147/JPR.S331036
4. Bendtsen L, Zakrzewska JM, Heinskou TB, Hodaie M, Leal PRL, Nurmikko T, Obermann M, Cruccu G, Maarbjerg S. Advances in diagnosis, classification, pathophysiology, and management of trigeminal neuralgia. Lancet Neurol. 2020 Sep;19(9):784-796. doi: 10.1016/S1474-4422(20)30233-7
5. Cruccu G, Di Stefano G, Truini A. Trigeminal Neuralgia. N Engl J Med. 2020 Aug 20;383(8):754-762. doi: 10.1056/NEJMra1914484
6. Lambru G, Zakrzewska J, Matharu M. Trigeminal neuralgia: a practical guide. Pract Neurol. 2021 Oct;21(5):392-402. doi: 10.1136/practneurol-2020-002782
7. Zhu G, Fu Z, Su S, Tang Y, Liu F, Yu W. Global Trends and Hotspots in Trigeminal Neuralgia Research From 2001 to 2021: A Bibliometric Analysis. Front Neurol. 2022 May 10;13:894006. doi: 10.3389/fneur.2022.894006
8. Oxcarbazepine Withdrawn Phase 4 Trials for Trigeminal Neuralgia (TN) Treatment [Internet]. DrugBank. 2024. https://go.drugbank.com/drugs/DB00776/clinical_trials?conditions=DBCOND0081925&phase=4&purpose=treatment&status=withdrawn
9. An Efficacy and Safety Study of Basimglurant in Patients With Trigeminal Neuralgia [Internet]. ClinicalTrials.gov. 2024. https://clinicaltrials.gov/study/NCT05217628
10. Benoliel R, Zini A, Khan J, Almoznino G, Sharav Y, Haviv Y. Trigeminal neuralgia (part II): Factors affecting early pharmacotherapeutic outcome. Cephalalgia. 2016 Jul;36(8):747-59. doi: 10.1177/0333102415611406
11. Spina A, Mortini P, Alemanno F, Houdayer E, Iannaccone S. Trigeminal Neuralgia: Toward a Multimodal Approach. World Neurosurg. 2017 Jul;103:220-230. doi: 10.1016/j.wneu.2017.03.126
12. Toda H, Goto M, Iwasaki K. Patterns and variations in microvascular decompression for trigeminal neuralgia. Neurol Med Chir (Tokyo). 2015;55(5):432-41. doi: 10.2176/nmc.ra.2014-0393
13. Härtel F. Die Behandlung der Trigeminusneuralgie mit intrakraniellen Alkoholeinspritzungen. Deutsche Zeitschrift für Chirurgie. 1914 Feb;126(5–6):429–552. doi: 10.1007/bf02800919
14. Kirschner M. Zur Behandlung der Trigeminusneuralgie: Erfahrungen an 250 Fallen. Arch Klin Chir. 1936;186:325-34.
15. Kirschner M. Die Behandlung der Trigeminusneuralgie (Nach Erfahrungen an 113 Kranken). Munch Med Wochenschr. 1942;89:235-9.
16. Sweet WH, Wepsic JG. Controlled thermocoagulation of trigeminal ganglion and rootlets for differential destruction of pain fibers. 1. Trigeminal neuralgia. J Neurosurg. 1974 Feb;40(2):143-56. doi: 10.3171/jns.1974.40.2.0143
17. van Loveren H, Tew JM Jr, Keller JT, Nurre MA. A 10-year experience in the treatment of trigeminal neuralgia. Comparison of percutaneous stereotaxic rhizotomy and posterior fossa exploration. J Neurosurg. 1982 Dec;57(6):757-64. doi: 10.3171/jns.1982.57.6.0757
18. Kanpolat Y, Savas A, Bekar A, Berk C. Percutaneous controlled radiofrequency trigeminal rhizotomy for the treatment of idiopathic trigeminal neuralgia: 25-year experience with 1,600 patients. Neurosurgery. 2001 Mar;48(3):524-32; discussion 532-4. doi: 10.1097/00006123-200103000-00013
19. Sindou M, Tatli M. Traitement de la névralgie trigéminale par thermorhizotomie [Treatment of trigeminal neuralgia with thermorhizotomy]. Neurochirurgie. 2009 Apr;55(2):203-10. French. doi: 10.1016/j.neuchi.2009.01.015
20. Bendtsen L, Zakrzewska JM, Abbott J, Braschinsky M, Di Stefano G, Donnet A, Eide PK, Leal PRL, Maarbjerg S, May A, Nurmikko T, Obermann M, Jensen TS, Cruccu G. European Academy of Neurology guideline on trigeminal neuralgia. Eur J Neurol. 2019 Jun;26(6):831-849. doi: 10.1111/ene.13950
21. Mullan S, Lichtor T. Percutaneous microcompression of the trigeminal ganglion for trigeminal neuralgia. J Neurosurg. 1983 Dec;59(6):1007-12. doi: 10.3171/jns.1983.59.6.1007
22. Gonzales-Portillo Showing M, Huamán Tanta LA. Compresión percutánea del ganglio de Gasser y raíz trigeminal con balón en el tratamiento de la neuralgia del trigémino. Revista Argentina de Neurocirugía. 2020 Sep 10;34(03). doi: 10.59156/revista.v34i03.121
23. Barlas O, Unal TC. A technique to facilitate the cannulation of the foramen ovale for balloon compression. Br J Neurosurg. 2023 Dec;37(6):1918-1921. doi: 10.1080/02688697.2021.1907308
24. Ma Y, Li Y, Huang H, Wang B, Wang Q. Percutaneous Microcompression for Idiopathic Trigeminal Neuralgia: curative effects and complications. Research Square. 2020; Mar 28. doi: 10.21203/rs.3.rs-19565/v1
25. Sun C, Zheng W, Zhu Q, Du Q, Yu W. The Transformation of the Balloon Shape in Percutaneous Balloon Compression for Trigeminal Neuralgia. J Pain Res. 2021 Dec 14;14:3805-3814. doi: 10.2147/JPR.S343783
26. Grewal SS, Kerezoudis P, Garcia O, Quinones-Hinojosa A, Reimer R, Wharen RE. Results of Percutaneous Balloon Compression in Trigeminal Pain Syndromes. World Neurosurg. 2018 Jun;114:e892-e899. doi: 10.1016/j.wneu.2018.03.111
27. Kourilsky A, Palpacuer C, Rogers A, Chauvet D, Wiart C, Bourdillon P, Le Guérinel C. Multivariate models to predict pain recurrence and sensitive complications after percutaneous balloon compression in trigeminal neuralgia. J Neurosurg. 2022 Apr 22;137(5):1396-1405. doi: 10.3171/2022.2.JNS212644
28. Håkanson S. Trigeminal neuralgia treated by the injection of glycerol into the trigeminal cistern. Neurosurgery. 1981 Dec;9(6):638-46. doi: 10.1227/00006123-198112000-00005
29. Asplund P, Blomstedt P, Bergenheim AT. Percutaneous Balloon Compression vs Percutaneous Retrogasserian Glycerol Rhizotomy for the Primary Treatment of Trigeminal Neuralgia. Neurosurgery. 2016 Mar;78(3):421-8; discussion 428. doi: 10.1227/NEU.0000000000001059
30. Noorani I, Lodge A, Vajramani G, Sparrow O. Comparing Percutaneous Treatments of Trigeminal Neuralgia: 19 Years of Experience in a Single Centre. Stereotact Funct Neurosurg. 2016;94(2):75-85. doi: 10.1159/000445077
31. Noorani I, Lodge A, Durnford A, Vajramani G, Sparrow O. Comparison of first-time microvascular decompression with percutaneous surgery for trigeminal neuralgia: long-term outcomes and prognostic factors. Acta Neurochir (Wien). 2021 Jun;163(6):1623-1634. doi: 10.1007/s00701-021-04793-4
32. Herta J, Loidl TB, Schmied T, Tomschik M, Khalaveh F, Wang WT, Dorfer C. Retrospective comparison of percutaneous balloon compression and radiofrequency-thermocoagulation in the management of trigeminal neuralgia. Acta Neurochir (Wien). 2023 Jul;165(7):1943-1954. doi: 10.1007/s00701-023-05656-w
33. Chang KW, Jung HH, Chang JW. Percutaneous Procedures for Trigeminal Neuralgia. J Korean Neurosurg Soc. 2022 Sep;65(5):622-632. doi: 10.3340/jkns.2022.0074
34. Barker FG 2nd, Jannetta PJ, Bissonette DJ, Larkins MV, Jho HD. The long-term outcome of microvascular decompression for trigeminal neuralgia. N Engl J Med. 1996 Apr 25;334(17):1077-83. doi: 10.1056/NEJM199604253341701
35. McLaughlin MR, Jannetta PJ, Clyde BL, Subach BR, Comey CH, Resnick DK. Microvascular decompression of cranial nerves: lessons learned after 4400 operations. J Neurosurg. 1999 Jan;90(1):1-8. doi: 10.3171/jns.1999.90.1.0001
36. Sindou M, Keravel Y, Simon E, Mertens P. Névralgie du trijumeau et neurochirurgie. EMC – Neurologie. 2012 Jan;9(1):1-14. doi: 10.1016/s0246-0378(12)70006-4
37. Chen F, Niu Y, Meng F, Xu P, Zhang C, Xue Y, Wu S, Wang

L. Recurrence Rates After Microvascular Decompression in Patients With Primary Trigeminal Neuralgia and Its Influencing Factors: A Systematic Review and Meta-Analysis Based on 8,172 Surgery Patients. Front Neurol. 2021 Sep 30;12:738032. doi: 10.3389/fneur.2021.738032
38. Pollock BE, Phuong LK, Gorman DA, Foote RL, Stafford SL. Stereotactic radiosurgery for idiopathic trigeminal neuralgia. J Neurosurg. 2002 Aug;97(2):347-53. doi: 10.3171/jns.2002.97.2.0347
39. Régis J, Tuleasca C, Resseguier N, Carron R, Donnet A, Gaudart J, Levivier M. Long-term safety and efficacy of Gamma Knife surgery in classical trigeminal neuralgia: a 497-patient historical cohort study. J Neurosurg. 2016 Apr;124(4):1079-87. doi: 10.3171/2015.2.JNS142144
40. Tuleasca C, Régis J, Sahgal A, De Salles A, Hayashi M, Ma L, Martínez-Álvarez R, Paddick I, Ryu S, Slotman BJ, Levivier M. Stereotactic radiosurgery for trigeminal neuralgia: a systematic review. J Neurosurg. 2019 Mar 1;130(3):733-757. doi: 10.3171/2017.9.JNS17545
41. Gubian A, Rosahl SK. Meta-Analysis on Safety and Efficacy of Microsurgical and Radiosurgical Treatment of Trigeminal Neuralgia. World Neurosurg. 2017 Jul;103:757-767. doi: 10.1016/j.wneu.2017.04.085
42. Chen L, Xu M, Zou Y. Treatment of trigeminal neuralgia with percutaneous glycerol injection into Meckel's cavity: experience in 4012 patients. Cell Biochem Biophys. 2010 Nov;58(2):85-9. doi: 10.1007/s12013-010-9094-z
43. Xu-Hui W, Chun Z, Guang-Jian S, Min-Hui X, Guang-Xin C, Yong-Wen Z, Lun-Shan X. Long-term outcomes of percutaneous retrogasserian glycerol rhizotomy in 3370 patients with trigeminal neuralgia. Turk Neurosurg. 2011 Jan;21(1):48-52. doi: 10.5137/1019-5149.JTN.3550-10.1
44. Kondziolka D, Lunsford LD. Percutaneous retrogasserian glycerol rhizotomy for trigeminal neuralgia: technique and expectations. Neurosurg Focus. 2005 May 15;18(5):E7. doi: 10.3171/foc.2005.18.5.8
45. Nugent GR. Radiofrequency treatment of trigeminal neuralgia using a cordotomy-type electrode. A method. Neurosurg Clin N Am. 1997 Jan;8(1):41-52. doi: 10.1016/S1042-3680(18)30336-X
46. Sindou M, Brinzeu A. Trigeminal Neuralgias: A Neurosurgical Illustrated Guide. Springer International Publishing; 2023. doi: 10.1007/978-3-031-25113-9
47. Marshall K, Chan MD, McCoy TP, Aubuchon AC, Bourland JD, McMullen KP, deGuzman AF, Munley MT, Shaw EG, Tatter SB, Ellis TL. Predictive variables for the successful treatment of trigeminal neuralgia with gamma knife radiosurgery. Neurosurgery. 2012 Mar;70(3):566-72; discussion 572-3. doi: 10.1227/NEU.0b013e3182320d36
48. Niranjan A, Lunsford LD. Radiosurgery for the management of refractory trigeminal neuralgia. Neurol India. 2016 Jul-Aug;64(4):624-9. doi: 10.4103/0028-3886.185393
49. Jarrahi A, Cantrell R, Norris C, Dhandapani K, Barrett J, Vender J. Trigeminal Neuralgia Treatment Outcomes Following Gamma Knife Stereotactic Radiosurgery. International Journal of Translational Medicine. 2022 Nov 22;2(4):543–54. doi: 10.3390/ijtm2040041
50. Zhong J. The simpler the better: a personal philosophy of microvascular decompression surgery. Chin Med J (Engl). 2021 Feb 15;134(4):410-412. doi: 10.1097/CM9.0000000000001233
51. Bick SKB, Eskandar EN. Surgical Treatment of Trigeminal Neuralgia. Neurosurg Clin N Am. 2017 Jul;28(3):429-438. doi: 10.1016/j.nec.2017.02.009
52. Kirollos R, Helmy A, Thomson S, Hutchinson P, editors. Oxford Textbook of Neurological Surgery. Oxford University Press; 2019. doi: 10.1093/med/9780198746706.001.0001
53. Boyke AE, Naidu I, Lam S, Alvi MA, Bader ER, Agarwal V. Medical Malpractice and Trigeminal Neuralgia: An Analysis of 49 Cases. J Oral Maxillofac Surg. 2021 May;79(5):1026.e1-1026.e8. doi: 10.1016/j.joms.2020.12.041
54. Du Z, Zhang J, Han X, Yu W, Gu X. Potential novel therapeutic strategies for neuropathic pain. Front Mol Neurosci. 2023 Apr 21;16:1138798. doi: 10.3389/fnmol.2023.1138798

Original article

Ukr Neurosurg J. 2024;30(3):18-29
doi: 10.25305/unj.301385

Results of interventions on the celiac plexus in treating patients with chronic pharmacoresistant abdominal pain

Vadym V. Biloshytsky[1,2], Dmytro M. Romanukha[1,3]

[1] Romodanov Neurosurgery Institute, Kyiv, Ukraine
[2] Pain Management Center SPRAVNO, Kyiv, Ukraine
[3] Main Medical Center of the Ministry of Internal Affairs of Ukraine, Kyiv, Ukraine

Received: 04 April 2024
Accepted: 29 May 2024

Address for correspondence:
Dmytro M. Romanukha, Main Medical Center of the Ministry of Internal Affairs of Ukraine, 1 Berdychivs'ka Street, Kyiv, 04116, Ukraine, e-mail: neuromanukha@gmail.com

Patients with chronic abdominal pain are a complex cohort of patients who undergo treatment by many specialists for a long time: surgeons, urologists, gynecologists, neurologists, psychiatrists, etc. However, despite all diagnostic and treatment measures, the pain syndrome persists or worsens.

Objective – evaluation of the effectiveness, safety and long-term results of treating patients with abdominal pain syndromes, which includes the use of various methods of minimally invasive interventions on the celiac plexus (CP) taking into account the peculiarities of the origin, nature and localization of pain.

Materials and methods. An analysis of the results of 26 interventions on CP in 21 patients was performed. Inclusion criteria for participants in the study were individuals with persistent pharmacoresistant abdominal pain for ≥3 months, aged 19 to 73 years. There were 13 (62.0%) male and 8 (38.0%) were female. Mean age was 55.2±15.2 years. Patients were divided into two groups. The first (n=16) included patients with pancreatic cancer, the second (n=5) included patients with non-oncological chronic abdominal pain syndromes: functional abdominal pain syndrome was diagnosed in three cases, and one observation each of solaritis and chronic pancreatitis.

All procedures were performed under CT. To assess the intensity of the pain syndrome, a visual analogue scale (VAS) of pain from 1 to 10 cm was used, where 0 cm is the absence of pain, 10 cm is unbearable pain; functional status (FS) - according to the Karnofsky scale (KS) from 0 to 100%. Estimation of the daily dose of opioid analgesics was estimated using the oral morphine equivalent daily dose (oMEDD). Patients were observed for 6 months, evaluations were carried out after 1 week, 1, 3 and 6 months, respectively.

Results. In the first group, 17 interventions on CP were performed in 16 participants, sympatholysis was performed twice in one patient. In the second group - 9 interventions in 5 patients: 4 Celiac Plexus Blocks (CPBs) of the central nervous system using "Depo-Medrol®" (methylprednisolone) and 5 neurolysis with 96% ethyl alcohol. Two patients were initially treated with CPB and then sympatholysis due to the recurrence of pain syndrome with the aim of a more stable sympatholytic and analgesic effect. In one patient, neurolysis of CP was performed three times. In all cases, no complications were recorded during the procedures.

VAS before the procedure in the general group (n=26) was 9.6±0.6 cm, one week after the intervention it was 4.5±1.6 cm (P<0.0001), after one month it was 3.2±1 .5 cm (P<0.0001), after 3 months – 3.0±1.6 cm (P<0.0001), after six months – 4.4±1.6 cm (P<0.0001). The FS indicator according to the KS before the procedure in the general group was 65.8±7.0%, one week after the intervention – 80.8±8.0% (P<0.0001), one month later – 81.5±8.3 % (P<0.0001), after 3 months – 75.0±9.5% (P<0.0010), after six months – 68.0±9.4% (P=0.4042). The oral morphine equivalent daily dose before the procedure in the general group was 123.8±86.0 mg per day, one week after the intervention on CP oMEDD was 57.3±61.2 mg (P<0.0001), after 1 month – 41.0±47.3 mg (P<0.0001), after 3 months – 44.0±51.3 mg (P<0.0001), after 6 months – 80.6±77.2 mg (P<0,0001).

Conclusions. Computed tomography-guided celiac plexus neurolysis is a useful and effective tool in treating patients with both abdominal pain caused by inoperable pancreatic cancer and chronic non-oncological pharmacoresistant abdominal pain. Minimally invasive interventions on CP provide a significant reduction of pain syndrome according to the VAS scale (p<0.001), reduce the need to take opioids analgesics (p<0.001) after 1, 3, 6 months and increase the FS of patients according to the KS (p<0.001) after 1, 3 months. Taking into account the high percentage of recurrence of pain syndrome in the studied patients of the group of non-oncology pain, the need for repeated interventions for the purpose of long-term pain control, interventions on CP in this cohort of patients require further research with an increase in the number of observations.

Key words*: neurolysis; sympatholysis; celiac plexus; solar plexus; pancreatic cancer; abdominal pain; solaritis; functional abdominal pain syndrome*

Introduction

According to the WHO, about 37% of people in developed countries suffer from diseases and conditions associated with chronic pain [1]. Studies conducted in Europe have shown that every fifth person reports the presence chronic pain of moderate or high intensity, with 90% of these individuals experiencing pain for more than two years, and one-third of cases not being alleviated by treatment [1]. Extrapolating these data suggests that millions of people in Ukraine, mainly of working age and elderly, have problems related to chronic pain.

Patients with chronic abdominal pain represent a challenging cohort, often undergoing long-term treatment by various specialists (surgeons, urologists, gynecologists, neurologists, psychiatrists, etc.). However, despite all diagnostic and therapeutic measures, the pain syndrome persists or worsens. A striking example is abdominal pain in patients with malignant neoplasms of the abdominal organs, as about half of cancer patients experience it, and in the later stages of the disease, this number exceeds 70% [2,3]. Its prevalence is even higher in patients with pancreatic cancer [4]. Only 12–20% of these patients are diagnosed at a stage where tumor resection is possible [5]. Pain management in these patients is usually very challenging, often requiring the chronic use of high doses of opioid and non-opioid analgesics or their combinations. Opioids are more effective and provide good pain relief but come with a range of side effects (nausea and vomiting, constipation, itching, dry mouth, pronounced sedation or delirium, hallucinogenic effects, the need to increase the dose due to the development of tolerance, intolerance to a particular drug) [6-8]. These side effects can worsen the quality of life, which is crucial for this cohort of patients, whose five-year survival rate is only 8% [9]. Inadequate pain management negatively affects the quality of life and is associated with worse clinical survival outcomes for patients [4, 10, 11].

The approach to treating patients with chronic non-oncological abdominal pain is a complex issue and is discussed in the literature. These pain syndromes are complex conditions diagnosed in a small number of patients. Often, various specialists examine the patients, but a definitive diagnosis cannot be established.

The functional abdominal pain syndrome (FAPS) is classified as a functional gastrointestinal disorder according to the Rome diagnostic criteria [12]. According to the latest revision (2016) of this diagnostic classification, FAPS is referred to as "centrally mediated abdominal syndrome." This can be a debilitating disorder characterized by constant or frequently recurring abdominal pain lasting at least six months, with some loss of daily functioning [13]. As with other functional gastrointestinal disorders, there is no evidence of structural (morphological) disease causing the symptoms.

Solar plexitis (solariitis) is rarely diagnosed in clinical practice. Patients typically describe it as pain primarily in the epigastric area between the xiphoid process of the sternum and the navel. The pain is cramp-like, not associated with food intake, and may radiate throughout the abdomen, under the ribs, and into the back. In addition to pain, the clinical picture may include spasms, atony of the stomach or intestines, abdominal distension, nausea, constipation, or diarrhea. Solar crises—episodes of intense, stabbing pain in the epigastrium—can also occur, manifesting as increased blood pressure, tachycardia, and skin redness. The etiology of solar plexitis is not well studied. It is presumed to involve infectious diseases, traumatic factors (abdominal or chest injuries), inflammatory diseases of the abdominal organs (particularly pancreatitis, cholecystitis), intoxications of various origins, etc.

The incidence of chronic pancreatitis is estimated to be 50–75 cases per 100,000 people per year [14]. About 85-90% of patients with this condition experience pain at the time of diagnosis, which worsens as the disease progresses, significantly impairing their quality of life [15]. Numerous studies on the quality of life of these patients indicate that pain dominates the quality of life indicators in all major areas [16,17]. Abdominal pain due to chronic pancreatitis is debilitating for the patient and poses a complex challenge for both gastroenterologists and pain management specialists (algologists) or surgeons.

Interventions on the structures of the autonomic nervous system are becoming increasingly common worldwide. They are safe, minimally invasive, effective, and associated with a minimal number of complications while providing a lasting therapeutic effect. However, only a small number of scientific studies have been published on minimally invasive interventions on sympathetic plexuses, particularly in cases of abdominal pain syndromes, and there is a lack of clear systematization of interventions and data on their outcomes and effectiveness.

It is important to understand the fundamental difference between CPB and neurolysis (sympatholysis) of nerve plexuses. CPB is performed with injectable corticosteroids and/or a combination of long-acting local anesthetics for a temporary block of pain impulse transmission. Neurolysis is performed using ethanol or phenol, which provides a more sustained effect by destroying nerve fibers. In some cases, radiofrequency denervation (ablation) or nerve plexus modulation is used for a longer-lasting effect.

Objective: To evaluate the effectiveness, safety, and long-term outcomes of treating patients with abdominal pain syndromes using various methods of minimally invasive interventions on the abdominal plexus, considering the nature, character, and location of the pain.

Materials and Methods

Study Design

A prospective interventional study was conducted on the basisof two medical institutions in Kyiv (Main Medical Center of the Ministry of Internal Affairs of Ukraine and Acad. A.P. Romodanov Institute of Neurosurgery of the National Academy of Medical Sciences of Ukraine) from

This article contains some figures that are displayed in color online but in black and white in the print edition

2016 to 2024. The results of 26 interventional procedures on the CP in 21 patients were analyzed. All procedures were performed using a standardized protocol by a single team consisting of three doctors (two from the hospital and one from the Institute).

The study was approved by the Ethics and Bioethics Committee of the A.P. Romodanov Institute of Neurosurgery of the National Academy of Medical Sciences of Ukraine (minutes No. 3, dated December 16, 2020). After a detailed explanation of the procedure, written informed consent was obtained from all patients. The study did not pose any increased risk to the participants and was conducted in compliance with bioethical norms and scientific standards for conducting clinical research involving patients.

Inclusion Criteria

Individuals with persistent pharmacoresistant abdominal pain lasting ≥3 months, diagnosed with pancreatic cancer, functional abdominal pain syndrome (FAPS), solaritis, or chronic pancreatitis. Patients of both sexes, aged 19 to 73 years. Lack of response to analgesics, anti-inflammatory drugs, and other treatments.

Exclusion Criteria

Age under 16 years. Patients with existing local infection at the puncture site or systemic infection (sepsis). Allergy to any anesthetic or contrast dye.

Individuals with impaired coagulation profile, presence of aneurysm, mural thrombus, or significant atherosclerotic calcification of the aorta. Patients with mental disorders under psychiatric observation. Inability to continue participation in the study throughout the observation period.

Group Characteristics

The study included 13 (62.0%) men and 8 (38.0%) women. The average age of the subjects was (55.2 ± 15.2) years. The patients were divided into two groups: the first group consisted of 16 patients with pancreatic cancer, and the second group included 5 patients with non-oncological chronic abdominal pain syndromes (three cases of FAPS, one case of solaritis, and one case of chronic pancreatitis).

Procedure Methodology

Patients were selected for empirical analysis of CP injections under computed tomography (CT) guidance, using a "GE Revolution Evo" 64/128-slice machine (General Electric, USA) at the Main Medical Center of the Ministry of Internal Affairs, and a "Toshiba Aquilion Prime" 80/160-slice machine (Toshiba, Japan) at the Institute of Neurosurgery. Prior to the procedure, all patients had their blood pressure, heart rate, and oxygen saturation levels measured. In cases of malignant pancreatic lesions, patients were cachectic, elderly, and had low blood pressure. An intravenous catheter was placed before the procedure due to the frequent complication of hypotension. For several days before the sympatholysis, all patients were advised to drink at least 1.5-2.0 liters of water per day; if this was not possible, intravenous infusion of 500-1000 ml of saline solution was administered. The neurolysis was performed under local anesthesia, with all patients undergoing cardiorespiratory monitoring (electrocardiography, blood pressure control, pulse oximetry) in the presence of an on-duty anesthesiologist during the procedure. There were no cases requiring intravenous sedation with fentanyl, midazolam, or general anesthesia with intubation.

The optimal puncture site is located 5-7 cm lateral to the midline at the level of the L1 vertebra or at the level of the lower edge of the 12th rib, with the needle directed medially at a 45° angle and upwards (cranially) at a 15° angle. Following all aseptic rules, after subcutaneous infiltration with a 2% lidocaine solution, a 22G needle with a beveled tip, 120 mm in length, was gradually advanced forward alongside the vertebral bodies. The ideal position for the needle tip is approximately 1 cm anterior to the aorta, between the diaphragmatic crura and the pancreas, at the level between the celiac trunk and the superior mesenteric artery, as confirmed by control CT scanning. On each side, 1 ml of "Tomogexol 350" (Pharmak, Ukraine) radiopaque dye diluted in saline (1:2-1:3) was injected, followed by 5 ml of 0.5% bupivacaine to reduce pain response during alcohol infusion. Then, 20 ml of 96% ethyl alcohol was slowly injected (10 ml on each side). In cases of CPB "Depo-Medrol®" 40 mg (methylprednisolone, Pfizer, USA) was used instead of alcohol (40 mg on each side, totaling 80 mg). On CT imaging it is crucial during to confirm the spread of the neurolytic agent (or hormone) along the anterolateral surface and anterior to the aorta in the retroperitoneal space, as the spread of the neurolytic agent is key to successful sympatholysis ***(Fig. 1)***.

For analysis, data were collected from patients after the procedure at intervals of 1 week, 1 month, 3 months, and 6 months. Patients who were unable to visit the clinic were contacted by phone, and their responses were recorded. Data were also analyzed from patient examinations using a preliminary survey that used the Visual Analog Scale (VAS) for pain, ranging from 1 to 10 cm, where 0 cm indicates no pain, and 10 cm indicates unbearable pain. Before and after the procedure, the functional status (FS) of patients was assessed using the Karnofsky scale (KS), which ranges from 0 to 100%. The daily dose of opioid analgesics was evaluated using the oral morphine equivalent daily dose (oMEDD). Participants were followed-up for 6 months, with assessments conducted at 1 week, 1 month, 3 months, and 6 months.

Statistical Analysis

The obtained data were processed using the MedCalc V 22016 statistical software package. Quantitative data (age, VAS score, and KS) are presented as the arithmetic mean and standard deviation. To identify differences after the interventions, the Student's t-test for related samples was used if the data followed a normal distribution, or a Wilcoxon rank sum test was used if the data distribution deviated from normal. A critical significance level of 0.05 was adopted.

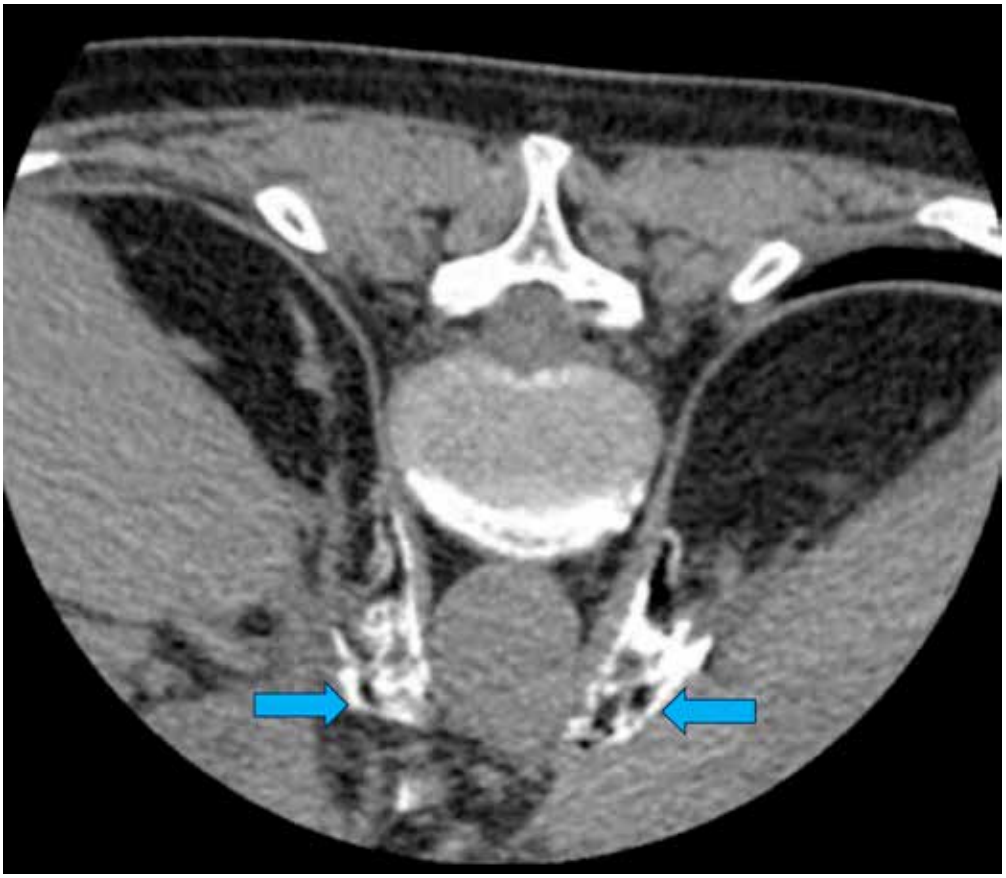

Fig. 1. Control CT Scan of a 64-year-old female patient with pancreatic cancer, undergoing celiac plexus neurolysis via bilateral posterior paravertebral antecrural access. The pre-procedure VAS pain score was 10 cm. The needles are positioned in the antecrural space at the level of the celiac artery trunk, with contrast injected to confirm their location. Arrows indicate the spread (free diffusion) of the contrast in the antecrural space along the lateral and anterior surface of the aorta and the celiac artery trunk—locations where the CP nodes are situated. Subsequently, 20 ml of 96% ethanol was injected. VAS score after the procedure: 2 cm

Results and Discussion

The total number of CP interventions was 26 in 21 patients. In most cases (76.2%), the pain was caused by malignant pancreatic lesions ***(Table 1)***.

No complications were recorded during the interventions that would lead to a deterioration of the patients' condition. There were no manifestations of neurological deficits, vascular injuries, perforations of internal organs, pleural sinuses, lungs, etc.

In 5 cases (19.2%), local pain at the injection site was reported, which regressed within 24 hours ***(Table 2)***. This complication is associated with the spread of residual ethanol from the needle into the surrounding tissues (subcutaneous tissue, muscles) at the puncture site. To prevent this complication, we recommend injecting 3-5 ml of saline before removing the needles. In 4 cases (15.4%), post-procedural pain was noted in the lower abdomen, radiating along the ureter to the lower back and groin area. In all cases, the complications regressed within 24 hours after the intervention. A possible explanation for this pain syndrome is the injury to the renal capsule as the needle passes near it or irritation of the capsule by ethanol. Two patients (7.7%) reported transient diarrhea after the procedure. This complication is likely due to the activation of the parasympathetic nervous system's influence on the gastrointestinal tract as a result of blocking the fibers of the CP. The diarrhea was transient and did not require specific treatment. In 1 case (3.8%), orthostatic post-procedural hypotension was recorded, which was resolved by intravenous administration of crystalloids and dexamethasone. This complication is caused by sympathetic denervation (CPB) of the vascular wall of the large arteries of the abdominal aorta. The patient's blood pressure normalized within a few hours of observation.

In the overall patient group, a significant reduction in pain according to the VAS was recorded one week after the procedure: from (9.6 ± 0.6) before the intervention to (4.5 ± 1.6) cm ***(Table 3)***. A persistent (up to 6 months) and noticeable decrease in pain intensity on the VAS was noted before and after the intervention ($p < 0.001$) ***(Fig. 2)***.

The average KS score before and one week after the procedure was (65.8 ± 7.0)% and (80.8 ± 8.0)%, respectively, with this indicator increasing in the first three months following the procedure (the difference was statistically significant). The decrease in functional status at six months is related to the predominance of

oncology patients in the study and the complications associated with the primary disease.

The daily dose of opioid analgesics in the general group before the procedure was (123.8 ± 86.0) mg, one week after the CP intervention, it was (57.3 ± 61.2) mg ($p < 0.0001$), one month after the procedure – (41.0 ± 47.3) mg ($p < 0.0001$), three months after – (44.0 ± 51.3) mg ($p < 0.0001$), and six months after – (80.6 ± 77.2) mg ($p < 0.0001$) ***(Fig. 3)***.

In the overall group, a repeat CP intervention was performed in 3 (14.0%) patients. In 1 (4.8%) patient, the CP neurolysis was performed three times. In the group of patients with malignant pancreatic tumors, CP neurolysis was repeated only in 1 (6.25%) case.

In all cases of malignant pancreatic lesions, neurolysis of the CP fibers with ethanol was used. In the second group, four CPBs using "Depo-Medrol®" (methylprednisolone) and five neurolyses with 96% ethyl alcohol were performed.

The average VAS score before the procedure in the first group was (9.7±0.6) cm, one week after the intervention it was (4.7±1.4) cm ($p<0.0001$), one month after it was (3.1±1.5) cm ($p<0.0001$), three months after it was (2.6±1.3) cm ($p<0.0001$), and six months after it was (4.1±1.4) cm ($p<0.0001$), the FS indicator according to the Karnofsky scale (KS) score before the procedure was (64.7±7.9)%, one week after the intervention it was (78.2±6.4)% ($p<0.0001$), one month after it was (78.8±6.9)% ($p<0.0001$), three months after it was (71.2±6.9)% ($p=0.023$), and six months after it was (63.5±6.0)% ($p=0.668$). The oMEDD before the procedure was (179.0±43.8) mg, which can be explained by the high level of opioid analgesic use in cancer patients. After the intervention, this figure decreased to (85.0±58.6) mg ($p<0.0001$); one month and three months later, it was (61.8±46.5) mg and (66.5±50.6) mg, respectively ($p<0.0001$). However, after six months, the need for opioids in this cohort of patients increased

Table 1. Characteristics of patients (n=21)

Indicator	Number	
	Abs.	%
Sex		
Males	13	62,0
Females	8	38,0
Age, years:		
mean	55,2±15,2	
min-max	19–73	
Etiology of pain:		
Pancreatic cancer	16	76,2
FAPS	3	14,2
Solaritis	1	4,8
Chronic pancreatitis	1	4,8

Table 2. Adverse events and post-procedural complications of celiac plexus interventions (n=26)

Indicator	Number	
	Abs.	%
Post-Procedural Complications:		
no complications	14	53,9
local pain at the puncture site	5	19,2
pain along the ureter	4	15,4
transient diarrhea	2	7,7
orthostatic hypotension	1	3,8

Table 3. Changes of VAS and KS scores (n=26)

Assessment period	VAS score, sm	P	KS score, %	P
Before procedure	9,6±0,6	<0,001	65,8±7,0	<0,001
After 1 week	4,5±1,6	<0,001	80,8±8,0	<0,001
After 1 month	3,2±1,5	<0,001	81,5±8,3	<0,001
After 3 months	3,0±1,6	<0,001	75,0±9,5	<0,001
After 6 months	4,4±1,6	<0,001	68,0±9,4	0,4042

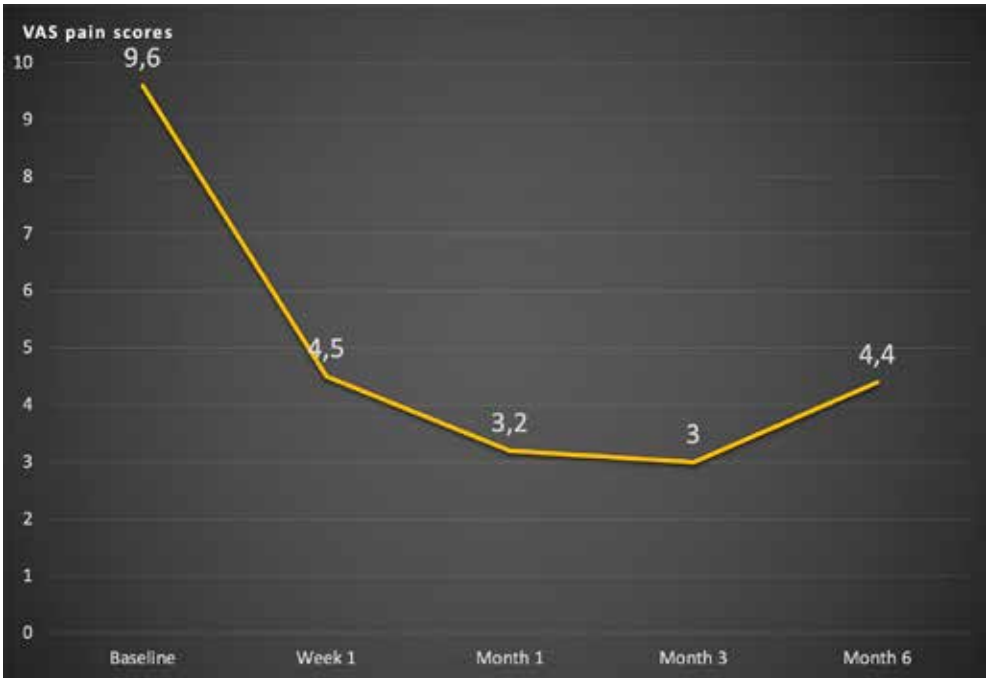

Fig. 2. Changes of average VAS value

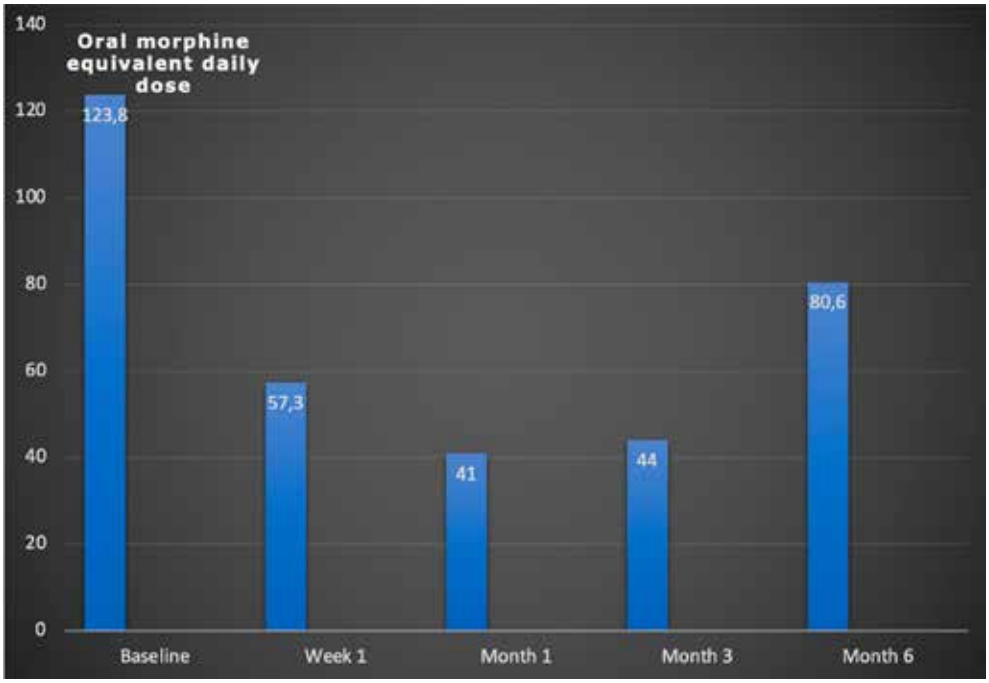

Fig. 3. Changes of the average oMEDD

again to (120.6±66.0) mg/day (p=0.025), although it remained lower than the pre-procedure level.

All patients in the second group experienced significant pain reduction according to the VAS, both one week after – from (9.4±0.5) cm before the procedure to (4.0±1.9) cm (p<0.001) – and six months after – to (4.8±1.8) cm (p<0.001). The average KS score one week after the procedure increased from (67.7±4.4)% to (86.6±8.6)% (p<0.007), and six months later to (77.7±8.3)% (p=0.017). The use of opioid analgesics was significantly lower in this group. The oMEDD before the procedure averaged (20.0±26.0) mg, after the procedure – (5.0±10.6) mg (p<0.001), and this level remained stable for six months after the intervention.

The literature mainly includes single observations of CP interventions, case series, or small patient samples. Despite the significant interest of specialists in such interventions, there are challenges in finding and selecting patients for this procedure. Healthcare professionals and patients are not well informed about

this treatment approach. A meta-analysis of 24 studies resulted in 59 publications after a literature search, with only 24 providing data on CP interventions in two or more patients [18]. In the review by S. Vig et al., a literature search yielded 686 publications, but only 44 randomized controlled trials and case series (more than 10 patients) were selected for analysis [19]. The limitations of our study include the small sample size of patients with non-oncological pain who underwent celiac plexus interventions, which can be attributed to the complex diagnosis of such abdominal pain syndromes and the selection of patients suitable for this procedure.

CP neurolysis demonstrates high efficacy in reducing pain intensity, decreasing the need for opioid medications, and minimizing associated side effects in patients with malignant abdominal organ lesions. This has been confirmed in numerous studies [8,9,20–24]. A Cochrane review involving six studies showed statistically significant evidence of the benefits of CP over conservative pain management in all patients who underwent the procedure [25]. According to S. Vig et al., CP interventions have proven to be an effective method for treating pain in malignant pancreatic lesions [19].

The pathophysiology of FAPS is unique because the pain is almost entirely caused by enhanced central perception of normal visceral signals, rather than increased peripheral stimulation from the abdominal or pelvic organs. This clinical feature often arises when gastrointestinal disorders become chronic, and the perceived pain (in the cortical centers) increasingly depends on the input from the central nervous system, which is modulated by psychosocial variables. In fact, with FAPS, gastrointestinal disorders may be minor or even absent, resulting in "abnormal perception of normal bowel function." Thus, while the pain is felt in the abdomen (and attributed to it), the nature and magnitude of the pain are predominantly regulated by cognitive and emotional centers. Recognizing this concept is crucial for understanding FAPS from the perspective of clinical manifestations, pathophysiology, diagnosis, and treatment [26-28].

According to the Rome IV criteria, FAPS must include all of the following [26]:

1. Continuous or nearly continuous abdominal pain.
2. Absence or occasional association of pain with physiological events (e.g., eating, defecation, or menses).
3. Some loss of daily functioning (e.g., missing work/school, family and social limitations/activities).
4. The pain is not fabricated (e.g., malingering).
5. Insufficient symptoms to meet the criteria for another functional gastrointestinal disorder that would explain the pain.

These criteria should be observed for the past 3 months with symptom onset at least 6 months before the diagnosis.

If the diagnostic criteria of FAPS are as specified, further diagnostic testing is not required. Unfortunately, most patients undergo extensive testing, including non-invasive procedures such as abdominal ultrasound, multislice CT, and magnetic resonance imaging (MRI) of the abdomen, as well as invasive procedures such as capsule video endoscopy, esophagogastroduodenoscopy, colonoscopy, endoscopic ultrasonography (EUS) and retrograde cholangiopancreatography etc. These tests are not only unnecessary but also pose a risk to the patient, lead to excessive healthcare costs, and can reinforce the patient's inclination to believe that a different diagnosis has not been established. Along with the lack of experience and confidence in the diagnosis on the part of the physician, this often leads to prolonged testing [27].

Thus, if the diagnostic criteria are met and there are no alarming signs, a diagnosis of FAPS can be established if there is no suspicion that the pain is feigned. Feigned pain or malingering is associated with the deliberate fabrication or gross exaggeration of physical (or psychological) symptoms, driven by external incentives. Malingering is not easy to detect, especially for physicians inexperienced with this pathology, so it may be advisable to consult a psychiatrist to confirm or refute the suspicion [27,29].

Medication therapy may be targeted at symptoms or underlying causes, that is, the central mechanisms of pain. Due to persistent debilitating abdominal pain, many patients require and receive analgesic medications, often opioids. Many overburdened emergency department physicians, faced with demanding patients without a clear cause of their pain, prescribe them [30]. Besides the obvious problems and side effects associated with excessive use of opioid analgesics, there is a less recognized potential complication: the development of opioid bowel syndrome. This syndrome is characterized by chronic or frequently recurring abdominal pain that worsens with prolonged use or increasing doses of opioids [31]. Since it presents the same symptom as FAPS, the relationship between pain and opioid use is unclear. Some researchers believe that the cause lies in paradoxical visceral hyperalgesia induced by chronic opioid use [30,32].

The basis of medical therapy for FAPS is treatment with antidepressants [27]. This is because these drugs can modulate pain perception by modulating central regulatory mechanisms and, to some extent, visceral hypersensitivity. They are successfully used to treat chronic neuropathic pain [33]. A systematic review and meta-analysis of tricyclic antidepressants, selective serotonin reuptake inhibitors, serotonin-norepinephrine reuptake inhibitors, and psychological therapy (cognitive behavioral therapy) have shown that all these treatments were effective [33].

The main issues related to antidepressant therapy for FAPS are side effects and the perception of many patients that being prescribed a "psychiatric" drug means that all their problems are "in their head." For this reason, it is important to articulate the reasons for prescribing these medications in such a way as to persuade the patient to try them while simultaneously reducing the frequency of side effects [27,28,34].

One possible treatment method for FAPS is minimally invasive intervention on the nerve structures of the sympathetic system [35,36]. However, there is a limited amount of literature on such interventions for chronic functional abdominal pain. Successful use of radiofrequency ablation of the thoracic splanchnic nerves has been reported in a 27-year-old man who had previously undergone a diagnostic CPB with lidocaine,

which showed significant pain reduction on the Visual Analog Scale (VAS). During the 8-week follow-up period, the patient was satisfied with the result and reported that his pain had decreased [37]. In a study that performed 72 minimally invasive interventions on the CP or splanchnic nerves, 5 were conducted in patients with chronic abdominal pain syndrome. A 20% (1/5) effectiveness of such interventions was reported [38].

In the International Classification of Diseases X Revision, the term "solaritis" is not present. In the Rome IV diagnostic criteria, there is no mention of a diagnosis of solaritis. In the section on functional gastrointestinal disorders, epigastric pain syndrome is described with the following diagnostic criteria [26]: it should include one or both of the following symptoms occurring at least 1 day per week:

1) bothersome pain in the epigastrium (severe enough to interfere with usual activities);

2) unpleasant burning in the epigastrium (severe enough to interfere with usual activities);

absence of signs of organic, systemic, or metabolic disease that is likely to explain the symptoms during routine investigations (e.g., fibrogastroduodenoscopy).

These criteria are considered valid if they have been observed during the last 3 months, with symptom onset at least 6 months prior to diagnosis.

Supporting criteria:

1. Pain may be induced by eating, reduced during eating, or occur during fasting.

2. Additional symptoms may include postprandial bloating in the epigastrium, belching, and nausea.

3. Persistent vomiting is likely indicative of another disorder.

4. Heartburn is not considered a dyspeptic symptom but may often be present.

5. The pain does not meet the criteria for biliary pain.

6. Symptoms that are relieved by the evacuation of stool or gas should generally not be considered as part of dyspepsia.

7. Symptoms of other diseases (e.g., gastroesophageal reflux disease and irritable bowel syndrome) may coexist with epigastric pain syndrome.

In contemporary medical literature, the term "solaritis" is scarcely mentioned. There is no data on the prevalence of this condition. Older French literature sources discuss pain arising from irritation of the fibers of the celiac nerve plexus, referred to as "solar neuralgia," "solaralgia," or "solaritis" [39]. However, due to the poorly understood etiological factors of this disease and the difficulty in diagnosing it, interest in pain originating in the solar plexus has significantly diminished. One theory for the development of solaritis was Glénard's visceroptosis, which involves the prolapse of abdominal organs, leading to the exposure of the aorta located directly beneath the abdominal wall. Tension in the intestinal mesentery irritates the nerve plexuses, causing pain as a result.

Z. Maratka examined a consecutive series of 234 patients admitted to the hospital regardless of diagnosis and 100 outpatient patients with established gastrointestinal clinics with functional disorders. The overall prevalence of a certain degree of solar tenderness in unselected patients was 28%, and 37% in patients with functional gastrointestinal disorders [40]. The author uses the term "solar tenderness" to describe pain upon palpation of the aorta and believes that, normally, the periaortic nerve plexuses are painless upon palpation. In some patients, such palpation is painful, sometimes very painful, so the author suggests considering "solar tenderness" as a pathology. "Solar tenderness" has a typical characteristic that distinguishes it from other causes of tenderness upon palpation in the epigastrium. Sensitivity is localized along the course of the aorta along the midline between the xiphoid process and the navel and bifurcates below the navel into two branches, corresponding to an inverted Y-type bifurcation. This is best detected by using the fingertips of both hands placed side by side perpendicular to the abdominal wall. Moving the hands from one side of the midline to the other, one can find that the tenderness is strictly limited to the aorta and its bifurcation. Moving the hands distally shows that the tenderness is greatest above the navel and disappears when the hands are positioned between the branches of the bifurcation. Tenderness limited to the aorta and its branches indicates that the origin of the pain is from the periaortic nerve plexuses, as there is no other organ or structure with such localized tenderness. In more complex cases, in addition to objective "solar tenderness," there is a subjective component—"solar pain," spontaneous pain arising in the solar plexus. It is felt in the epigastrium and radiates laterally along both costal margins, as well as to the back. It is often associated with a sensation of pressure and tightness in the epigastrium. A typical complaint is an unpleasant pulsation of the aorta ("epigastric pulsation"). The pain is not related to food intake, is sometimes associated with stress, rarely occurs at night, and may be accompanied by anxiety and other symptoms of neurosis. According to the author, "solar tenderness" and "solar pain" form a typical syndrome—the solar plexus syndrome, which is a specific type of neurosis characterized predominantly by the involvement of abdominal nerve plexuses, often associated with functional gastrointestinal disorders such as functional dyspepsia and irritable bowel syndrome [40].

According to Z. Maratka, the Rome criteria incorrectly interpret some pathological conditions and fail to mention typical syndromes, particularly pain resulting from solaritis [41,42]. Our patient was clinically diagnosed with "solaritis" due to the combination of pain syndrome with symptoms like abdominal bloating and constipation.

Treating pancreatic pain can be challenging and often ineffective [43]. A variety of approaches are used to manage these patients, including pancreatic enzymes, octreotide, antioxidants, opioid analgesia, minimally invasive celiac plexus interventions, and endoscopic pancreatic surgery. Endoscopic treatment involves the removal of stones from the main pancreatic duct and dilation of strictures, which facilitates decompression and drainage of the main pancreatic duct [44]. According to one popular hypothesis, the pain is caused by duct obstruction. The expected result of duct obstruction is increased pressure within the duct and gland, especially when pancreatic secretion is stimulated (e.g., after

eating). Elevated pressure can lead to pain due to increased basolateral enzymes secretion or ischemia in the pancreas resulting from pressure rising to a level that impedes its blood supply [45]. Studies conducted on both animals and humans have shown that patients with chronic pancreatitis may have increased ductal or parenchymal pressure in the pancreas. Surgical treatment is associated with a reduction in this pressure and a decrease in pain intensity [46,47]. Animal models of chronic pancreatitis also show that pancreatic blood flow decreases and ischemia develops upon stimulation of pancreatic secretion, mimicking compartment syndrome. While this mechanism of pain onset seems plausible, other studies have not found a clear relationship between pressure and pain or between pressure reduction and pain relief [47]. Extracorporeal shock wave lithotripsy of pancreatic stones reduces obstruction of the main pancreatic duct, leading to pain relief [48]. Other surgical methods include thoracoscopic splanchnicectomy (denervation of the visceral nerves, nerve plexuses, and ganglia), intraoperative CPB, radiofrequency ablation or cryoablation, and pancreatic resection [15]. However, these treatments have had varying and limited efficacy for long-term pain control. Some patients respond to combined multimodal therapy, but many patients become dependent on opioids. For this reason, the use of opioids to treat chronic pain raises resistance and concerns about potential opioid dependence and other side effects of opioids [49].

The ultimate common pathway for any pathological process causing pain in the pancreas is the visceral nerves [50]. The sympathetic nerves that innervate the pancreas pass through the CP, and blocking this innervation can be highly effective in treating pancreatic pain [7].

Celiac plexus interventions are an alternative method for reducing pain syndrome in patients with pharmacoresistant chronic pancreatitis [51-54]. M. Kaufman et al. conducted a thorough search of the Medline, Pubmed, and Embase databases for studies published in the English literature from January 1966 to December 2007 that evaluated the effectiveness of ultrasound-guided CPB in patients with chronic pancreatitis whose conservative medication therapy failed to control the pain and improve their condition [7]. Studies involving fewer than 10 patients were excluded from the analysis. Six relevant studies were identified (total number of patients = 221). It was found that ultrasound-guided CPB block was an effective tool for reducing abdominal pain in 51.46% of patients.

In a prospective randomized study on the efficacy of ultrasound-guided CPB in treating abdominal pain associated with chronic pancreatitis, conducted by F. Gress et al. [55], the procedure was performed on 90 individuals (40 men and 50 women). Significant pain reduction was reported in 55% of patients. The average pain score on the VAS decreased from 8 to 2 cm at 4 and 8 weeks post-procedure ($p<0.05$). A sustained effect was noted at 12 weeks in 26% of patients and at 24 weeks in 10%. In 3 patients, pain was absent at 35 and 48 weeks of follow-up. According to the authors, the procedure is less effective in patients who have undergone surgery for chronic pancreatitis.

M.S. Sey et al. studied the efficacy of endoscopic ultrasound-guided (EUS) interventions on the CP in 1,108 patients treated at the Indiana University Medical Center (USA). A total of 248 patients with chronic pancreatitis, who underwent two or more CP interventions, were selected. After the first procedure, 76% of patients reported a reduction in pain intensity. The average duration of pain relief was 10 weeks. Subsequent procedures contributed to a prolonged period of pain relief (12–20 weeks). Older age ($p = 0.026$) and pain reduction after the first block ($p = 0.0024$) were associated with pain reduction following subsequent procedures. Considering the near absence of complications (3 minor transient complications), the study by M.S. Sey et al. demonstrates the feasibility and effectiveness of repeated celiac plexus interventions for pain control in patients with chronic pancreatitis [56].

Various minimally invasive intervention techniques targeting structures of the sympathetic autonomic nervous system (SANS) for treating pain caused by chronic pancreatitis are compared. For instance, D. Santosh et al. compared CP using a percutaneous technique under fluoroscopic control of an image intensifier (fluoroscopy) and under endoscopic ultrasound guidance [57]. The study involved 56 patients with chronic pancreatitis and abdominal pain requiring daily analgesic intake for 4 weeks or more. CPB was performed in 27 patients using EUS, and in 29 patients using fluoroscopy. Improvement in pain score on the VAS was observed in 70% of individuals who underwent the EUS-guided technique and in 30% of the percutaneous access group ($p=0.044$).

A case involved the use of botulinum toxin for CP in a 32-year-old patient with pharmacoresistant chronic pancreatitis who continued to experience pain even after surgical treatment, such as pancreatic duct drainage [58]. This treatment option for persistent chronic pancreatic pain was considered because clinical studies on botulinum toxin have shown good efficacy in treating peripheral and central neuropathic pain, particularly in cases of postherpetic neuralgia, trigeminal neuralgia, and neuropathic pain caused by spinal cord injury. After the injection of 100 units of onabotulinumtoxin A into the CP under X-ray guidance, the pain disappeared, the patient did not request any opioid medications, and was discharged. A sustained result was demonstrated for 15 weeks following the intervention. The patient reported that pain intensity was 0 cm on the VAS without the use of analgesics.

As with the use of CP neurolysis for pain caused by pancreatic cancer, some researchers recommend performing CPB in the early stages of pain management for pancreatitis, especially before the patient becomes dependent on opioid medications [60]. Most authors believe that in cases of chronic pancreatitis, CP interventions should be limited to situations where pain does not respond to other treatments (medical and surgical) or for managing exacerbations of chronic pain [61, 62].

The current (2023) American Gastroenterological Association guidelines for endoscopic treatment of acute and recurrent chronic pancreatitis recommend CP interventions for patients with debilitating pain that

significantly worsens their quality of life and for whom other therapeutic measures have been ineffective [6]. The rationale is based on observational studies suggesting that pain relief lasting about 6 months can be achieved in 50-60% of patients [7, 54, 64].

Conclusions

1. CT-guided CP neurolysis is a useful and effective tool in treating patients with both abdominal pain caused by inoperable pancreatic cancer and chronic non-cancer pharmacoresistant abdominal pain.

2. Minimally invasive CP interventions significantly reduce pain according to the VAS ($p<0.001$), decrease the need for opioid analgesics ($p<0.001$) at 1, 3, and 6 months, and improve patients' FS according to the KS ($p<0.001$) at 3 months.

3. Taking into account the high frequency of pain recurrence in patients with non-cancer pain group, the need for repeated interventions for long-term pain control, and the necessity for further research on CP interventions in this cohort with a larger number of observations.

Disclosure

Conflict of Interest

The authors declare no conflict of interest.

Ethical Standards

All procedures performed on patients in the study comply with the ethical standards of the institutional and national ethics committees and the 1964 Helsinki Declaration and its later amendments or comparable ethical standards.

The study was approved by the Ethics and Bioethics Committee of the Romodanov Institute of Neurosurgery of the National Academy of Medical Sciences of Ukraine (minutes No. 3, dated December 16, 2020).

Informed Consent

Informed consent was obtained from all patients.

Funding

The study did not receive any sponsorship support.

References

1. Hoppenfeld J.D. Fundamentals of Pain Medicine: How to Diagnose and Treat your Patients. Lippincott Williams & Wilkins; 2014. 288 p.
2. Cuomo A, Cascella M, Forte CA, Bimonte S, Esposito G, De Santis S, Cavanna L, Fusco F, Dauri M, Natoli S, Maltoni M, Morabito A, Mediati RD, Lorusso V, Barni S, Porzio G, Mercadante S, Crispo A. Careful Breakthrough Cancer Pain Treatment through Rapid-Onset Transmucosal Fentanyl Improves the Quality of Life in Cancer Patients: Results from the BEST Multicenter Study. J Clin Med. 2020 Apr 2;9(4):1003. doi: 10.3390/jcm9041003
3. Urits I, Jones MR, Orhurhu V, Peck J, Corrigan D, Hubble A, Andrews M, Feng R, Manchikanti L, Kaye AD, Kaye RJ, Viswanath O. A Comprehensive Review of the Celiac Plexus Block for the Management of Chronic Abdominal Pain. Curr Pain Headache Rep. 2020 Jun 11;24(8):42. doi: 10.1007/s11916-020-00878-4
4. Koulouris AI, Banim P, Hart AR. Pain in Patients with Pancreatic Cancer: Prevalence, Mechanisms, Management and Future Developments. Dig Dis Sci. 2017 Apr;62(4):861-870. doi: 10.1007/s10620-017-4488-z
5. Castleberry AW, White RR, De La Fuente SG, Clary BM, Blazer DG 3rd, McCann RL, Pappas TN, Tyler DS, Scarborough JE. The impact of vascular resection on early postoperative outcomes after pancreaticoduodenectomy: an analysis of the American College of Surgeons National Surgical Quality Improvement Program database. Ann Surg Oncol. 2012 Dec;19(13):4068-77. doi: 10.1245/s10434-012-2585-y
6. Jadad AR, Browman GP. The WHO analgesic ladder for cancer pain management. Stepping up the quality of its evaluation. JAMA. 1995 Dec 20;274(23):1870-3. doi:10.1001/jama.1995.03530230056031
7. Kaufman M, Singh G, Das S, Concha-Parra R, Erber J, Micames C, Gress F. Efficacy of endoscopic ultrasound-guided celiac plexus block and celiac plexus neurolysis for managing abdominal pain associated with chronic pancreatitis and pancreatic cancer. J Clin Gastroenterol. 2010 Feb;44(2):127-34. doi: 10.1097/MCG.0b013e3181bb854d
8. Neuwersch-Sommeregger S, Köstenberger M, Stettner H, Pipam W, Breschan C, Feigl G, Likar R, Egger M. CT-Guided Coeliac Plexus Neurolysis in Patients with Intra-Abdominal Malignancy: A Retrospective Evaluation of 52 Palliative In-Patients. Pain Ther. 2021 Dec;10(2):1593-1603. doi: 10.1007/s40122-021-00317-1
9. Dumitrescu A, Aggarwal A, Chye R. A retrospective case series of patients who have undergone coeliac plexus blocks for the purpose of alleviating pain due to intra-abdominal malignancy. Cancer Rep (Hoboken). 2020 Oct;3(5):e1265. doi: 10.1002/cnr2.1265
10. Mantyh PW. Cancer pain and its impact on diagnosis, survival and quality of life. Nat Rev Neurosci. 2006 Oct;7(10):797-809. doi: 10.1038/nrn1914
11. Eroshkin AA, Romanukha DM. CT-guided Celiac Plexus Neurolysis in the Management of Severe Upper Abdominal Pain. Ukr Neurosurg J. 2020 Jun 18;26(2):34-45. doi: 10.25305/unj.201779
12. Tack J, Drossman DA. What's new in Rome IV? Neurogastroenterol Motil. 2017 Sep;29(9). doi: 10.1111/nmo.13053
13. Schmulson MJ, Drossman DA. What Is New in Rome IV. J Neurogastroenterol Motil. 2017 Apr 30;23(2):151-163. doi: 10.5056/jnm16214
14. Patrizi F, Freedman SD, Pascual-Leone A, Fregni F. Novel therapeutic approaches to the treatment of chronic abdominal visceral pain. ScientificWorldJournal. 2006 Apr 18;6:472-90. doi: 10.1100/tsw.2006.980
15. Goulden MR. The pain of chronic pancreatitis: a persistent clinical challenge. Br J Pain. 2013 Feb;7(1):8-22. doi: 10.1177/2049463713479230
16. Pezzilli R, Morselli-Labate AM, Fantini L, Campana D, Corinaldesi R. Assessment of the quality of life in chronic pancreatitis using Sf-12 and EORTC Qlq-C30 questionnaires. Dig Liver Dis. 2007 Dec;39(12):1077-86. doi: 10.1016/j.dld.2007.06.014
17. Wehler M, Nichterlein R, Fischer B, Farnbacher M, Reulbach U, Hahn EG, Schneider T. Factors associated with health-related quality of life in chronic pancreatitis. Am J Gastroenterol. 2004 Jan;99(1):138-46. doi: 10.1111/j.1572-0241.2004.04005.x
18. Eisenberg E, Carr DB, Chalmers TC. Neurolytic celiac plexus block for treatment of cancer pain: a meta-analysis. Anesth Analg. 1995 Feb;80(2):290-5. doi: 10.1097/00000539-199502000-00015
19. Vig S, Bhan S, Bhatnagar S. Celiac Plexus Block - An Old Technique with New Developments. Pain Physician. 2021 Aug;24(5):379-398.
20. Eroshkin OA, Romanukha DM. Minimally invasive interventions on celiac plexus in patients with persistent abdominal pain caused by pancreatic cancer. INT NEUROL J. Mar 20;20(1):13-22. doi: 10.22141/2224-0713.20.1.2024.1041
21. Mohamed RE, Amin MA, Omar HM. Computed tomography-guided celiac plexus neurolysis for intractable pain of unresectable pancreatic cancer. The Egyptian Journal of Radiology and Nuclear Medicine. 2017 Sep 1;48(3):627-37. doi: 10.1016/j.ejrnm.2017.03.027
22. Romanukha DM, Strokan AM, Biloshytsky VV. The use of different methods of celiac plexus neurolysis in the

treatment of pain syndrome associated with pancreatic cancer. Ukr Neurosurg J. 2022 Sep 29;28(3):52-6. doi: 10.25305/unj.257987
23. Rai P, Cr L, Kc H. Endoscopic ultrasound-guided celiac plexus neurolysis improves pain in gallbladder cancer. Indian J Gastroenterol. 2020 Feb 17. doi: 10.1007/s12664-019-01003-z
24. Jin G, Qiu X, Ding M, Dai M, Zhang X. Navigated magnetic resonance imaging-guided celiac plexus neurolysis using an open magnetic resonance system for pancreatic cancer patients with upper abdominal pain. J Cancer Res Ther. 2019;15(4):825-830. doi: 10.4103/jcrt.JCRT_38_19
25. Arcidiacono PG, Calori G, Carrara S, McNicol ED, Testoni PA. Celiac plexus block for pancreatic cancer pain in adults. Cochrane Database Syst Rev. 2011 Mar 16;2011(3):CD007519. doi: 10.1002/14651858.CD007519.pub23
26. Drossman DA, Hasler WL. Rome IV-Functional GI Disorders: Disorders of Gut-Brain Interaction. Gastroenterology. 2016 May;150(6):1257-61. doi: 10.1053/j.gastro.2016.03.035
27. Sperber AD, Drossman DA. Review article: the functional abdominal pain syndrome. Aliment Pharmacol Ther. 2011 Mar;33(5):514-24. doi: 10.1111/j.1365-2036.2010.04561.x
28. Drossman DA. Presidential address: Gastrointestinal illness and the biopsychosocial model. Psychosom Med. 1998 May-Jun;60(3):258-67. doi: 10.1097/00006842-199805000-00007
29. First HB, Frances A, Pincus HA. DSM-IV-TR Guidebook. Washington, DC: American Psychiatric Publishing, 2004.
30. Drossman DA. Medicine has become a business, but what is the cost? Gastroenterology. 2004 Apr;126(4):952-3. doi: 10.1053/j.gastro.2004.02.029
31. Grunkemeier DM, Cassara JE, Dalton CB, Drossman DA. The narcotic bowel syndrome: clinical features, pathophysiology, and management. Clin Gastroenterol Hepatol. 2007 Oct;5(10):1126-39; quiz 1121-2. doi: 10.1016/j.cgh.2007.06.0130
32. Drossman DA. Severe and refractory chronic abdominal pain: treatment strategies. Clin Gastroenterol Hepatol. 2008 Sep;6(9):978-82. doi: 10.1016/j.cgh.2008.04.024
33. McQuay HJ, Tramèr M, Nye BA, Carroll D, Wiffen PJ, Moore RA. A systematic review of antidepressants in neuropathic pain. Pain. 1996 Dec;68(2-3):217-27. doi: 10.1016/s0304-3959(96)03140-5
34. Sabo CM, Grad S, Dumitrascu DL. Chronic Abdominal Pain in General Practice. Dig Dis. 2021;39(6):606-614. doi: 10.1159/000515433
35. Keefer L, Drossman DA, Guthrie E, Simrén M, Tillisch K, Olden K, Whorwell PJ. Centrally Mediated Disorders of Gastrointestinal Pain. Gastroenterology. 2016 Feb 19:S0016-5085(16)00225-0. doi: 10.1053/j.gastro.2016.02.034
36. Rana MV, Candido KD, Raja O, Knezevic NN. Celiac plexus block in the management of chronic abdominal pain. Curr Pain Headache Rep. 2014 Feb;18(2):394. doi: 10.1007/s11916-013-0394-z
37. Choi JW, Joo EY, Lee SH, Lee CJ, Kim TH, Sim WS. Radiofrequency thermocoagulation of the thoracic splanchnic nerve in functional abdominal pain syndrome -A case report-. Korean J Anesthesiol. 2011 Jul;61(1):79-82. doi: 10.4097/kjae.2011.61.1.796
38. Liou H, Kong MJ, Alzubaidi SJ, Knuttinen MG, Patel IJ, Kriegshauser JS. Single-Center Review of Celiac Plexus/Retrocrural Splanchnic Nerve Block for Non-Cancer Related Pain. Acad Radiol. 2021 Nov;28 Suppl 1:S244-S249. doi: 10.1016/j.acra.2021.03.005
39. Laignel-Lavastine M. Pathologie du sympathique. Paris: Alcan, 1924.
40. Maratka Z. Celiac (solar) plexus syndrome. A frequently overlooked source of abdominal pain. J Clin Gastroenterol. 1993 Mar;16(2):95-7
41. Maratka Z. Comments on Rome criteria of functional gastrointestinal disorders. Hepatogastroenterology. 2007 Mar;54(74):454-7
42. Maťatka Z. Functional gastrointestinal disorders – 50 years' experience in comparison with the Rome criteria. Folia Gastroenterol Hepatol 2005;3(1):10-16.
43. Reidenberg MM, Portenoy RK. The need for an open mind about the treatment of chronic nonmalignant pain. Clin Pharmacol Ther. 1994 Apr;55(4):367-9. doi: 10.1038/clpt.1994.43
44. Gabbrielli A, Pandolfi M, Mutignani M, Spada C, Perri V, Petruzziello L, Costamagna G. Efficacy of main pancreatic-duct endoscopic drainage in patients with chronic pancreatitis, continuous pain, and dilated duct. Gastrointest Endosc. 2005 Apr;61(4):576-81. doi: 10.1016/s0016-5107(05)00295-6
45. Chauhan S, Forsmark CE. Pain management in chronic pancreatitis: A treatment algorithm. Best Pract Res Clin Gastroenterol. 2010 Jun;24(3):323-35. doi: 10.1016/j.bpg.2010.03.007
46. Fasanella KE, Davis B, Lyons J, Chen Z, Lee KK, Slivka A, Whitcomb DC. Pain in chronic pancreatitis and pancreatic cancer. Gastroenterol Clin North Am. 2007 Jun;36(2):335-64, ix. doi: 10.1016/j.gtc.2007.03.011
47. Lieb JG 2nd, Forsmark CE. Review article: pain and chronic pancreatitis. Aliment Pharmacol Ther. 2009 Apr 1;29(7):706-19. doi: 10.1111/j.1365-2036.2009.03931.x
48. Dumonceau JM, Costamagna G, Tringali A, Vahedi K, Delhaye M, Hittelet A, Spera G, Giostra E, Mutignani M, De Maertelaer V, Devière J. Treatment for painful calcified chronic pancreatitis: extracorporeal shock wave lithotripsy versus endoscopic treatment: a randomised controlled trial. Gut. 2007 Apr;56(4):545-52. doi: 10.1136/gut.2006.0968831
49. Zenz M, Strumpf M, Tryba M. Long-term oral opioid therapy in patients with chronic nonmalignant pain. J Pain Symptom Manage. 1992 Feb;7(2):69-77. doi: 10.1016/0885-3924(92)90116-y
50. Vera-Portocarrero L, Westlund KN. Role of neurogenic inflammation in pancreatitis and pancreatic pain. Neurosignals. 2005;14(4):158-65. doi: 10.1159/0000876548
51. Fusaroli P, Caletti G. Is there a role for celiac plexus block for chronic pancreatitis? Endosc Int Open. 2015 Feb;3(1):E60-2. doi: 10.1055/s-0034-13913924
52. Kapural L, Jolly S. Interventional Pain Management Approaches for Control of Chronic Pancreatic Pain. Curr Treat Options Gastroenterol. 2016 Sep;14(3):360-70. doi: 10.1007/s11938-016-0100-4
53. Maydeo A, Kamat N, Dalal A, Patil G. Advances in the Management of Pain in Chronic Pancreatitis. Curr Gastroenterol Rep. 2023 Oct;25(10):260-266. doi: 10.1007/s11894-023-00898-1
54. Cohen SM, Kent TS. Etiology, Diagnosis, and Modern Management of Chronic Pancreatitis: A Systematic Review. JAMA Surg. 2023 Jun 1;158(6):652-661. doi: 10.1001/jamasurg.2023.0367
55. Gress F, Schmitt C, Sherman S, Ciaccia D, Ikenberry S, Lehman G. Endoscopic ultrasound-guided celiac plexus block for managing abdominal pain associated with chronic pancreatitis: a prospective single center experience. Am J Gastroenterol. 2001 Feb;96(2):409-16. doi: 10.1111/j.1572-0241.2001.03551.x
56. Sey MS, Schmaltz L, Al-Haddad MA, DeWitt JM, Calley CS, Juan M, Lasisi F, Sherman S, McHenry L, Imperiale TF, LeBlanc JK. Effectiveness and safety of serial endoscopic ultrasound-guided celiac plexus block for chronic pancreatitis. Endosc Int Open. 2015 Feb;3(1):E56-9. doi: 10.1055/s-0034-13779193
57. Santosh D, Lakhtakia S, Gupta R, Reddy DN, Rao GV, Tandan M, Ramchandani M, Guda NM. Clinical trial: a randomized trial comparing fluoroscopy guided percutaneous technique vs. endoscopic ultrasound guided technique of coeliac plexus block for treatment of pain in chronic pancreatitis. Aliment Pharmacol Ther. 2009 May 1;29(9):979-84. doi: 10.1111/j.1365-2036.2009.03963.x
58. Cho NR, Kim YN, Kim JY, Ko YR, Hong TH, Moon HK, Park HJ. Celiac plexus block with botulinum toxin in severe chronic pancreatitis-A case report. J Clin Pharm Ther. 2020

Aug;45(4):848-851. doi: 10.1111/jcpt.13180
59. Park J, Chung ME. Botulinum Toxin for Central Neuropathic Pain. Toxins (Basel). 2018 Jun 1;10(6):224. doi: 10.3390/toxins100602248
60. Busch EH, Atchison SR. Steroid celiac plexus block for chronic pancreatitis: results in 16 cases. J Clin Anesth. 1989;1(6):431-3. doi: 10.1016/0952-8180(89)90006-8
61. Raj M, Chen RY. Interventional applications of endoscopic ultrasound. J Gastroenterol Hepatol. 2006 Feb;21(2):348-57. doi: 10.1111/j.1440-1746.2006.04214.x
62. Draganov P, Toskes PP. Chronic pancreatitis. Curr Opin Gastroenterol. 2002 Sep;18(5):558-62. doi: 10.1097/00001574-200209000-00006
63. Strand DS, Law RJ, Yang D, Elmunzer BJ. AGA Clinical Practice Update on the Endoscopic Approach to Recurrent Acute and Chronic Pancreatitis: Expert Review. Gastroenterology. 2022 Oct;163(4):1107-1114. doi: 10.1053/j.gastro.2022.07.079
64. Puli SR, Reddy JB, Bechtold ML, Antillon MR, Brugge WR. EUS-guided celiac plexus neurolysis for pain due to chronic pancreatitis or pancreatic cancer pain: a meta-analysis and systematic review. Dig Dis Sci. 2009 Nov;54(11):2330-7. doi: 10.1007/s10620-008-0651-x

Original article

Ukr Neurosurg J. 2024;30(3):30-37
doi: 10.25305/unj.303393

Impact of transpedicular fixation on thoracolumbar junction burst fracture stability: a biomechanical perspective

Oleksii S. Nekhlopochyn[1], Vadim V. Verbov[2], Ievgen V. Cheshuk[2], Milan V. Vorodi[2], Michael Yu. Karpinsky[3], Oleksandr V. Yaresko[3]

[1] Spine Neurosurgery Department, Romodanov Neurosurgery Institute, Kyiv, Ukraine
[2] Restorative Neurosurgery Department, Romodanov Neurosurgery Institute, Kyiv, Ukraine
[3] Biomechanics Laboratory, Sytenko Institute of Spine and Joint Pathology, Kharkiv, Ukraine

Received: 06 May 2024
Accepted: 03 June 2024

Address for correspondence:
Oleksii S. Nekhlopochyn, PhD, Senior Researcher of Spine Neurosurgery Department, Romodanov Neurosurgery Institute, 32 Platona Maiborody st., Kyiv, 04050, Ukraine, e-mail: AlexeyNS@gmail.com

Introduction. The treatment of burst fractures at the thoracolumbar junction remains a contentious issue in vertebrology. Despite a broad array of surgical interventions available, many surgeons favor isolated posterior stabilization, which can be performed using either minimally invasive or open approaches. However, the biomechanical properties of these methods have not been thoroughly investigated.

Objective: This study aims to evaluate the biomechanical stability of the thoracolumbar junction following transpedicular stabilization of a burst fracture at the Th12 vertebra, under different system configurations influenced by lateral flexion.

Materials and Methods: A mathematical finite element model of the human thoracolumbar spine, featuring a burst fracture at the Th12 vertebra, was developed. The model included a transpedicular stabilization system with eight screws, simulating "long" stabilization. We examined four variants of transpedicular fixation using both mono- and bicortical screws, with and without the inclusion of two cross-links.

Results: The study found that the load borne by the damaged Th12 vertebral body varied depending on the fixation system employed. Specifically, stress levels were 24.0 MPa, 27.3 MPa, 18.4 MPa, and 25.8 MPa for models with short screws without cross-links, long screws without cross-links, short screws with cross-links, and long screws with cross-links, respectively. At the screw entry points in the vertebral arch, the highest stress values were recorded at the L2 vertebra, showing 11.8 MPa, 14.0 MPa, 9.4 MPa, and 13.4 MPa for each respective model. Among the metal construct elements, the connecting rods consistently exhibited the highest stress, with values of 226.7 MPa, 313.4 MPa, 212.4 MPa, and 293.98 MPa, respectively.

Conclusion: The results underscore that utilizing cross-links in the stabilization of burst fractures at the thoracolumbar junction, which is only feasible through an open installation, somewhat mitigates stress within the stabilized spinal segment. Meanwhile, the modeling of lateral flexion revealed only minimal differences in stress values between open and minimally invasive installations.

Keywords: *burst fracture; thoracolumbar junction; transpedicular stabilization; finite element analysis; biomechanical properties; minimally invasive surgery*

Introduction. The first detailed morphological description of burst fractures (BF) was provided by Sir Frank Wild Holdsworth in 1963 [1]. Based on his dual-column theory, Holdsworth proposed that such injuries are stable, as the posterior support complex remains intact. In 1983, Francis Denis expanded on this by introducing a three-column theory of spinal stability [2]. According to Denis, the posterior column comprises the posterior support complex, including bone structures and ligaments; the anterior column consists of the anterior longitudinal ligament, the anterior part of vertebral body, and the intervertebral disc; and the middle column is defined by the vertebral body's posterior wall and the fibrous ring of the intervertebral disc, along with the posterior longitudinal ligament. Under this framework, BF that compromise two of the three columns are considered unstable. Despite extensive clinical data and a wealth of experimental research, the stability of BF remains an open question. Thus, the management strategies for patients with BF in the thoracolumbar spine continue to be highly debated [3].

A trend of the last few decades has been the active promotion and adherence to the principles of evidence-based medicine. Modern healthcare, particularly in relation to traumatic spinal injuries, faces two seemingly contradictory objectives. On one hand, the effectiveness of therapy is determined by the duration of disability, where surgical methods clearly have an advantage as they generally allow for a reduction in the duration of functional limitations under comparable conditions [4].

On the other hand, the economic aspect favors conservative methods as they are less costly [5].

The thoracolumbar junction is the most vulnerable region of the spine regarding traumatic injuries [6]. It is known that over 50% of all spinal injuries occur in the Th11-L2 vertebrae [7]. BF account for about 15-20% of these injuries. Due to the biomechanical characteristics of this section and the high frequency of injuries, therapeutic approaches to BF in this area are highly varied [8]. Posterior, anterior, combined, and hybrid surgical methods are commonly used. It should be noted that in cases where there are no neurological disorders and significant compression of the spinal canal—which is observed in 60-70% of all BF—the primary goal of surgical intervention is the preservation and, in some cases, correction of the spinal axis, and the elimination of instability until the consolidation of bone fragments [4]. So, the need for stabilization of such injuries is often temporary, and several authors have noted the appropriateness of removing metal constructs to remobilize previously fixed segments, which naturally leads to reduced pain and improved quality of life. This is why most practicing surgeons prefer isolated posterior transpedicular fixation as it is less traumatic during installation and more accessible for removal [9].

The ability to avoid open decompression of the spinal canal facilitates the widespread adoption of minimally invasive techniques for the placement of pedicle screws. This technique significantly reduces blood loss, shortens the duration of surgery, and consequently decreases the risks of postoperative complications and the length of hospital stays [10]. Most researchers report identical orthopedic outcomes using either minimally invasive or open screw placement methods [11]. However, some publications note a greater loss of spinal axis correction and vertebral body height specifically with minimally invasive screw placement [12, 13]. Such differences may be solely related to the features of the stabilization system, as minimally invasive placement does not involve the use of cross-links, which undoubtedly affects the load distribution in the stabilized section of the spine and may have specific clinical manifestations [14]. Meanwhile, a review of the literature reveals no studies evaluating the differences in BF stabilization with or without cross-links; moreover, the assessment of the depth of pedicle screw placement in the treatment of BF has also not been studied.

Objective: To analyze the load distribution in the thoracolumbar junction with a burst fracture of the Th12 vertebra under various modifications of the stabilizing transpedicular system influenced by lateral flexion.

Materials and Methods: In the Biomechanics Laboratory of Sytenko Institute of Spine and Joint Pathology, National Academy of Medical Sciences of Ukraine, a mathematical finite element model of the human thoracolumbar spine with a burst fracture at the Th12 vertebra was developed. The model incorporated a transpedicular stabilization system. An eight-screw "long" stabilization was simulated. Detailed descriptions and characteristics of the model have been provided in previous publications [15, 16].

To simulate the BF, the body of the Th12 vertebra was divided by several planes into separate fragments ***(see Fig. 1)***. The gaps between the fragments were filled with a material that simulated interfragmentary regenerate, to replicate the conditions of a real burst fracture.

Four variants of transpedicular fixation were modeled using both short fixation screws and long screws that pass through the anterior wall of the vertebral body, with and without the use of two cross-links ***(see Fig. 2)***.

In the simulation, the material was assumed to be homogeneous and isotropic [17]. A 10-node tetrahedral finite element with quadratic approximation was selected for the analysis. The mechanical properties of biological tissues (cortical and cancellous bone, intervertebral discs) for the mathematical modeling were chosen based on data from references [18, 19]. The material for the metal construct elements was titanium. Mechanical characteristics of artificial materials were selected according to technical literature [20]. For the analysis, characteristics such as the Young's modulus (E) and the Poisson's ratio (v) were used. Data on the mechanical properties of the materials are presented in ***Table 1***.

The stress-strain state of the models was investigated under the influence of a bending load acting from right to left, simulating a leftward tilt of the torso, with the distal surface of the L5 disc being rigidly fixed. The load was applied to the body of the Th9 vertebra and the right facet joint. The load magnitude was 350 N. The loading scheme for the models is shown in ***Fig. 3a***.

For the convenience of studying changes in the stress-strain state of the models depending on the method of transpedicular fixation, the stress magnitude was determined at multiple control points ***(see Figs. 3b, c, d)***.

The stress-strain state of the models was investigated using the finite element method. The criterion for assessing the stress state of the models was von Mises stress [21]. The modeling was performed using the SolidWorks computer-aided design system (Dassault Systèmes, France). Calculations of the stress-strain state of the models were carried out using the CosmosM software suite [22].

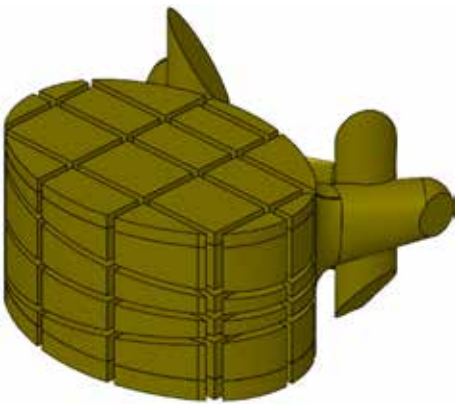

Fig. 1. *Th12 Vertebra Model*

This article contains some figures that are displayed in color online but in black and white in the print edition.

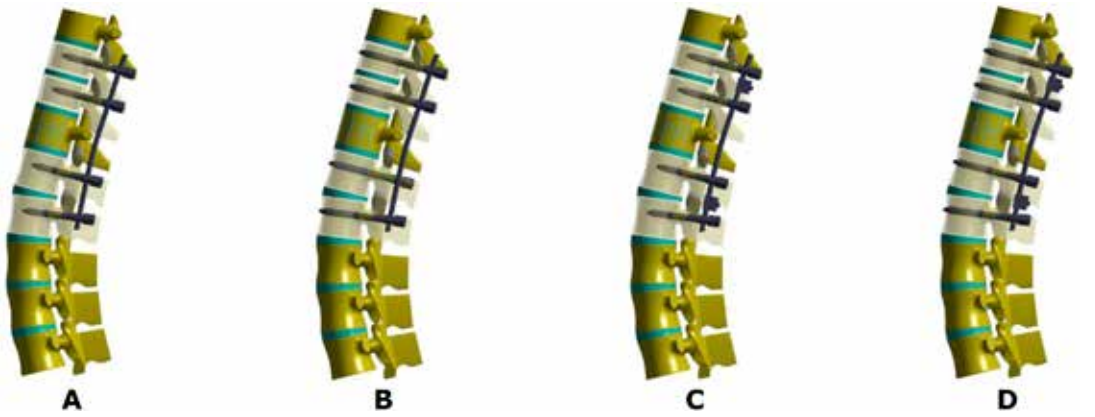

Fig. 2. Models with different variants of transpedicular fixation: a - short screws without cross-links; b - long screws without cross-links; c - short screws with cross-links; d - long screws with cross-links

Table 1. Mechanical Properties of Materials Used in Modeling

Material	Young's Modulus (MPa)	Poisson's Ratio
Cortical Bone	10,000	0.3
Cancellous Bone	450	0.2
Articular Cartilage	10.5	0.49
Intervertebral Discs	4.2	0.45
Interfragmentary Regenerate	1.0	0.45
Titanium VT-16	110,000	0.3

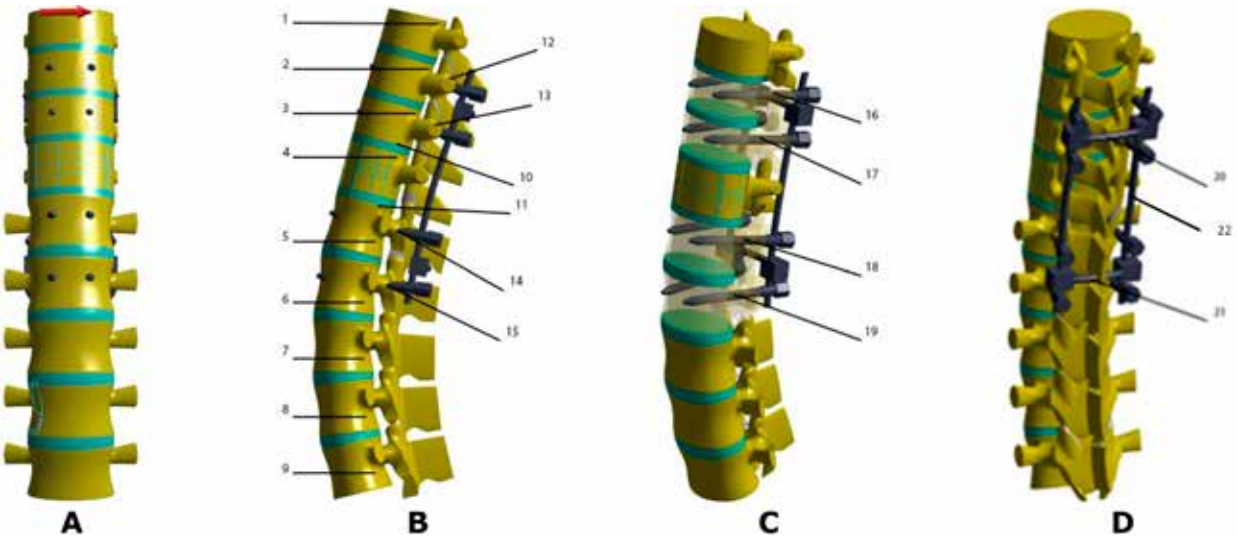

Fig. 3. Load scheme of models (a) and locations of control points (b, c, d): 1 - body of Th9 vertebra; 2 - body of Th10 vertebra; 3 - body of Th11 vertebra; 4 - body of Th12 vertebra; 5 - body of L1 vertebra; 6 - body of L2 vertebra; 7 - body of L3 vertebra; 8 - body of L4 vertebra; 9 - body of L5 vertebra; 10 - lower endplate of Th11 vertebra; 11 - upper endplate of L1 vertebra; 12 - entry point for screws in the arch of Th10 vertebra; 13 - entry point for screws in the arch of Th11 vertebra; 14 - entry point for screws in the arch of L1 vertebra; 15 - entry point for screws in the arch of L2 vertebra; 16 - screws in the body of Th10 vertebra; 17 - screws in the body of Th11 vertebra; 18 - screws in the body of L1 vertebra; 19 - screws in the body of L2 vertebra; 20 - crosslinks between screws in Th10 and Th11 vertebra bodies; 21 - crosslinks between screws in L1 and L2 vertebra bodies; 22 - rods

Results

In the model using transpedicular fixation with short screws without cross-links ***(see Fig. 4)***, the maximum stress values of 24.0 MPa were identified in the body of the Th12 vertebra. High stress levels of 21.5 and 20.1 MPa were also recorded in the bodies of the L2 and L3 vertebrae, respectively. Around the fixing screws, the highest stress value of 11.8 MPa was determined in the arches of the L2 vertebra. The stress around the screws in other vertebrae did not exceed 5.4 MPa.

In the metal structure components, the rods were the most stressed, experiencing stress levels of 226.7 MPa, indicating that they bear the primary load. Among the fixation screws, the maximum stress value of 27.3 MPa was observed in screws at the L2 vertebra, while the minimum was 14.3 MPa at the L1 vertebra. Screws in the thoracic vertebrae experienced uniform stress levels—22.1 MPa and 20.6 MPa at Th10 and Th11 vertebrae, respectively.

Using long screws without cross-links in the stabilization system ***(see Fig. 5)*** slightly reduced the stress levels in the bodies of intact vertebrae, whereas in the body of the Th12 vertebra, the stress increased to 27.3 MPa. Around the transpedicular screws, an increase in stress levels was also observed. The most significant doubling of stress was seen in the arches of the Th10 vertebra, where it was recorded at 9.0 MPa. In the arches of the Th11 and L2 vertebrae, stresses increased to 6.0 and 14.0 MPa, respectively. These findings correspond to the pattern of stress distribution changes on the transpedicular screws at Th10, Th11, and L2 vertebrae, where they also increased to values of 38.6 MPa, 20.3 MPa, and 34.8 MPa, respectively. The increased load on the transpedicular screws is transmitted to the rods, causing an increase in their stress levels to 313.4 MPa.

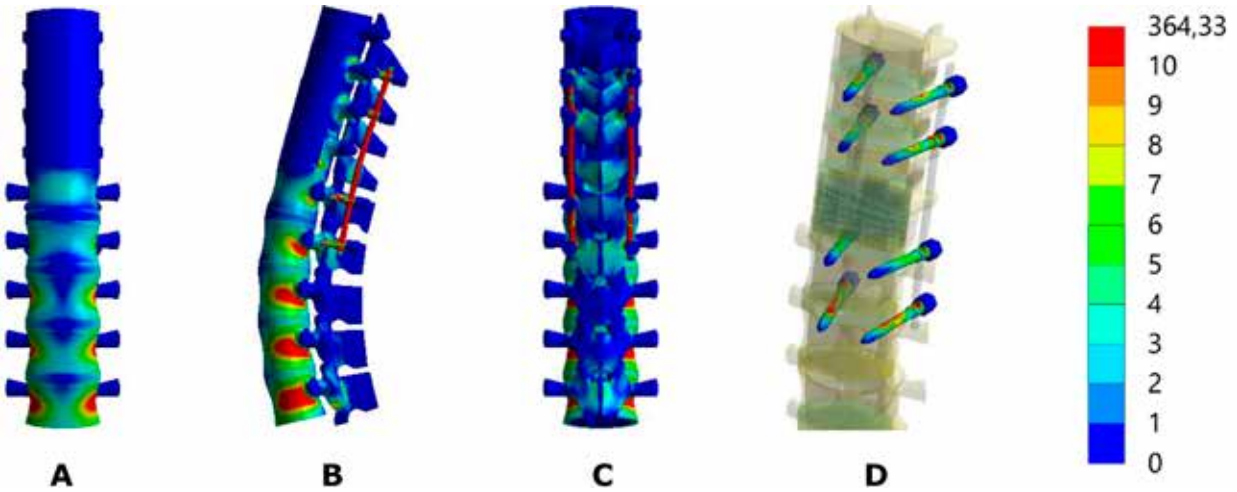

Fig. 4. Stress distribution in the model of the thoracolumbar spine with a burst fracture of the Th12 vertebra under load simulating leftward trunk tilt. Transpedicular fixation with short screws without crosslinks (model modification No. 1): a - front view; b - side view; c - rear view; d - screws

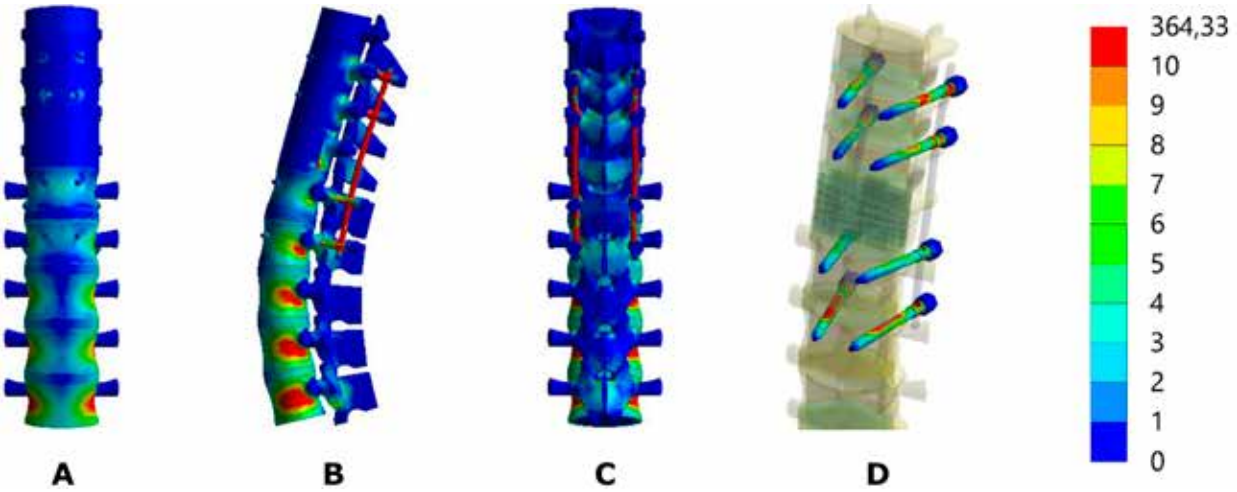

Fig. 5. Stress distribution in the model of the thoracolumbar spine with a burst fracture of the Th12 vertebra under load simulating leftward trunk tilt. Transpedicular fixation with bicortical screws without crosslinks (model modification No. 2): a - front view; b - side view; c - rear view; d - screws

The use of short fixation screws in combination with crosslinks, as shown in ***(Fig. 6)***, allowed for a reduction in the maximum stress values at all control points of the model and, most importantly, in the damaged Th12 vertebra, down to 18.4 MPa. A reduction in stress levels was also observed in all elements of the metal structure. The most significant changes occurred in the connecting rods, where stresses decreased to 212.4 MPa. The stresses on the crosslinks themselves were determined to be 7.8 MPa and 10.6 MPa at the upper and lower crosslinks, respectively.

The combination of crosslinks with long fixation screws ***(Fig. 7)*** during lateroflexion, compared to the model without crosslinks, also reduces stresses at all control points of the model, both in bone and metal components. However, compared to the model using short screws, the stress levels remain higher. The exception is the crosslinks themselves, where stress decreases to levels of 6.2 MPa and 5.4 MPa for the upper and lower crosslinks, respectively.

Data on the stress values at all control points of models with transpedicular fixation are presented in ***Table 2***.

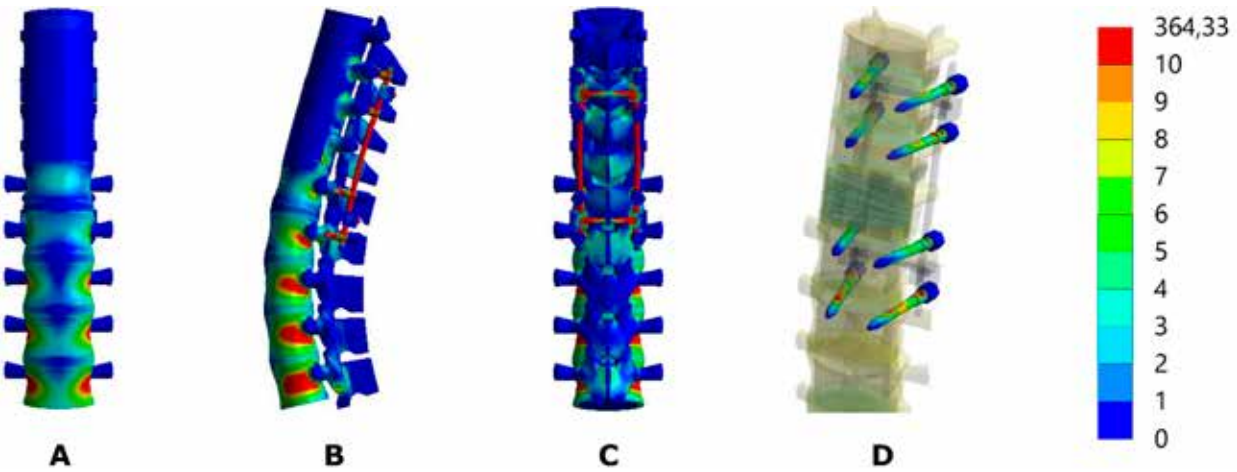

Fig. 6. Stress distribution in the model of the thoracolumbar spine with a burst fracture of the Th12 vertebra under load simulating leftward trunk tilt. Transpedicular fixation with monocortical screws and the presence of crosslinks in the system (model modification No. 3): a - front view; b - side view; c - rear view; d – screws

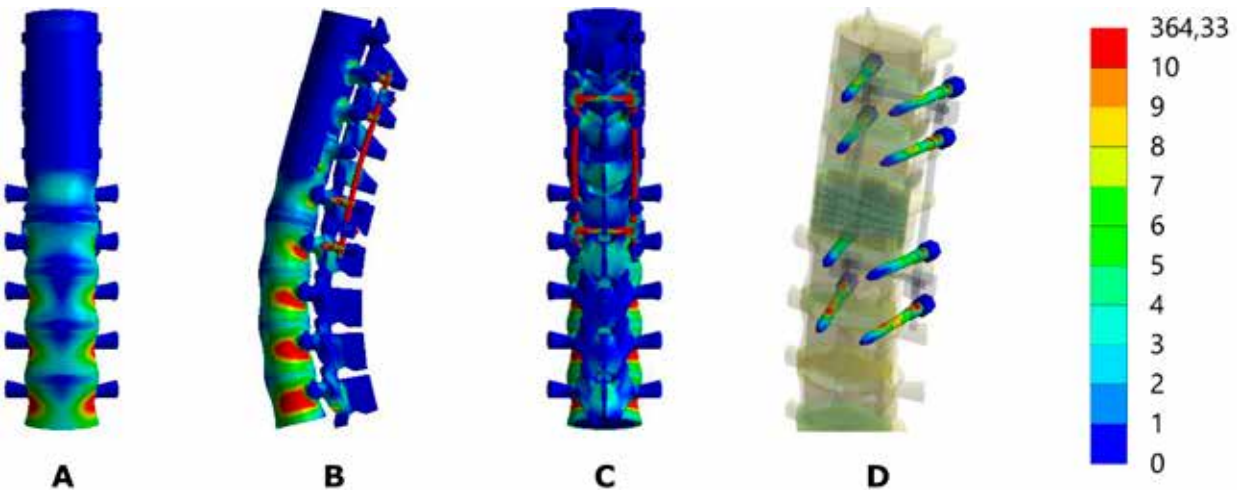

Fig. 7. Stress distribution in the model of the thoracolumbar spine with a burst fracture of the Th12 vertebra under load simulating leftward trunk tilt. Transpedicular fixation with bicortical screws and the presence of crosslinks in the system (model modification No. 4): a - front view; b - side view; c - rear view; d - screws

Table 2. Stress under load simulating leftward trunk tilt in models of the thoracolumbar spine with a burst fracture of the Th12 vertebra under various transpedicular fixation options

No	Control Points		Stress, MPa			
			Model without Crosslinks		Model with Crosslinks	
			Short Screws	Long Screws	Short Screws	Long Screws
1	Bone Tissue	Th9 Vertebra Body	1.1	1.0	1.1	1.0
2		Th10 Vertebra Body	10.4	7.6	10.2	5.8
3		Th11 Vertebra Body	6.5	5.4	6.3	5.2
4		Th12 Vertebra Body	24.0	27.3	18.4	25.8
5		L1 Vertebra Body	10.3	9.3	9.7	8.7
6		L2 Vertebra Body	21.5	18.2	20.0	17.6
7		L3 Vertebra Body	20.1	17.0	19.8	16.1
8		L4 Vertebra Body	25.0	21.1	23.8	20.5
9		L5 Vertebra Body	15.4	14.7	17.3	14.3
10		Lower Endplate of Th11	3.4	3.1	3.2	2.9
11		Upper Endplate of L1	5.8	5.3	5.5	4.9
12		Entry of Screws into Arch of Th10	4.1	9.3	3.8	9.0
13		Entry of Screws into Arch of Th11	5.4	3.6	4.5	3.5
14		Entry of Screws into Arch of L1	5.3	6.0	2.9	5.8
15		Entry of Screws into Arch of L2	11.8	14.0	9.4	13.4
16	Metal Constructs	Screws in Th10 Body	22.1	38.6	19.8	38.6
17		Screws in Th11 Body	20.6	20.3	20.3	19.9
18		Screws in L1 Body	14.3	15.5	11.4	13.2
19		Screws in L2 Body	27.3	34.8	26.5	33.0
20		Crosslinks between Th10 and Th11 Screws			7.8	6.2
21		Crosslinks between L1 and L2 Screws			10.6	5.4
22		Connecting rods	226.7	313.4	212.4	293.98

When conducting a comparative analysis of the obtained results, the following key features can be identified:

1. Stress Reduction Effectiveness:

- Crosslinks consistently reduce stress across all configurations, particularly beneficial in models involving both short and long screws. This effect is prominent in critical areas such as the fractured Th12 vertebra, where the reduction of stress can be crucial for stability and healing.

2. Screw Length:

- Long Screws with crosslinks tend to reduce stress more effectively than short screws without crosslinks, especially in thoracic vertebrae (Th10 and Th11). This suggests that for areas requiring robust stabilization, long screws with crosslinks might be more beneficial.

- However, in the case of the fractured Th12 vertebra, short screws with crosslinks show the best performance by significantly lowering the stress, illustrating that the optimal screw length may vary depending on the specific requirements of the fracture and anatomical location.

3. Load Distribution:

- Metal Constructs: Long screws without crosslinks exhibit the highest stress levels, particularly at critical points like in the Th10 vertebra body. This underscores the potential for higher mechanical loads leading to increased risk of screw loosening or breakage. The inclusion of crosslinks helps mitigate this risk by better distributing the load.

- Endplates and Screw Entry Points: The use of crosslinks not only reduces the stress on the vertebral bodies but also at the structural interfaces where screws enter the bone, enhancing the overall integrity of the fixation.

4. Rods:

The connecting rods, an integral part of the metal construct, show significantly reduced stress when crosslinks are used. This reduction highlights the importance of crosslinks in preventing overloading of the beams, which can prevent structural failure under load.

5. General Observations:

- The pattern of stress distribution suggests that while long screws are generally effective, the addition of crosslinks is critical for achieving optimal outcomes. This combination seems to provide the best balance between stability and stress reduction.

- The consistent reduction of stress in models with crosslinks, regardless of screw length, suggests that

crosslinks could be a universally beneficial addition to spinal fixation systems, especially in cases of severe trauma or instability.

It should be noted that the results we obtained are generally predictable and corroborated by a range of clinical and experimental biomechanical studies. For instance, it is indisputable that the use of crosslinks in transpedicular stabilization provides a more uniform distribution of loading across various sections of the stabilized spine, reducing the risks of fixation failure [23]. The data regarding the impact of the length of transpedicular screws on critical load indicators in the bone tissue-metal construct system also find their clinical confirmation. It is known, for example, that the modification with bicortical placement of screws is more preferable in osteoporotic spine [24, 25]. In our study, the loading of the vertebral bodies when using long transpedicular screws with crosslinks is minimal, which to some extent confirms the validity and informativeness of the finite element model we used.

However, when extrapolating these results to clinical practice, it's important to note that despite the clear advantages of models with crosslinks, the stress values obtained are not so critical as to favor open stabilization unequivocally. For example, even the most heavily loaded elements of the metal constructs—the connecting rods —show a maximum stress level of 313.4 MPa, while the calculated strength threshold for the titanium alloy VT16 ranges from 1030 MPa to 1225 MPa [26]. The empirical data suggest that, despite apparent biomechanical challenges, lateroflexion does not induce critical overloads at any of the control points analyzed, rendering an eight-screw fixation somewhat excessive. However, these findings are specific to the examined loading pattern, and conclusions regarding the suitability of any particular stabilization type can only be drawn after exploring all loading scenarios as well as modeling shorter fixation methods, which will be addressed in our future research. Moreover, based on the data, it should be noted that in cases with additional risks of fixation failure and non-consolidation of the fractured vertebral body, opting for an open installation of a transpedicular system enhanced with crosslinks may still be more advisable.

Conclusion: The results obtained illustrate that the use of crosslinks in the stabilization of burst fractures in the thoracolumbar junction, which is feasible only through open installation, contributes to a reduction in stress within the stabilized spinal segment. Meanwhile, in the modeling of lateroflexion, the difference in stress values between open and minimally invasive installations is minimal.

Information disclosure

Conflict of interest

The authors declare no conflict of interest.

Ethical standards

This article does not contain any studies involving humans or animals.

Funding

The research was conducted without sponsorship.

References

1. Holdsworth F. Fractures, dislocations, and fracture-dislocations of the spine. J Bone Joint Surg Am. 1970 Dec;52(8):1534-51.
2. Denis F. The three column spine and its significance in the classification of acute thoracolumbar spinal injuries. Spine (Phila Pa 1976). 1983 Nov-Dec;8(8):817-31. doi: 10.1097/00007632-198311000-00003
3. Dai LY, Jiang SD, Wang XY, Jiang LS. A review of the management of thoracolumbar burst fractures. Surg Neurol. 2007 Mar;67(3):221-31; discussion 231. doi: 10.1016/j.surneu.2006.08.081
4. Tanasansomboon T, Kittipibul T, Limthongkul W, Yingsakmongkol W, Kotheeranurak V, Singhatanadgige W. Thoracolumbar Burst Fracture without Neurological Deficit: Review of Controversies and Current Evidence of Treatment. World Neurosurg. 2022 Jun;162:29-35. doi: 10.1016/j.wneu.2022.03.061
5. Aras EL, Bunger C, Hansen ES, Søgaard R. Cost-Effectiveness of Surgical Versus Conservative Treatment for Thoracolumbar Burst Fractures. Spine (Phila Pa 1976). 2016 Feb;41(4):337-43. doi: 10.1097/BRS.0000000000001219.
6. Qiu TX, Tan KW, Lee VS, Teo EC. Investigation of thoracolumbar T12-L1 burst fracture mechanism using finite element method. Med Eng Phys. 2006 Sep;28(7):656-64. doi: 10.1016/j.medengphy.2005.10.011
7. Wang H, Zhang Y, Xiang Q, Wang X, Li C, Xiong H, Zhou Y. Epidemiology of traumatic spinal fractures: experience from medical university-affiliated hospitals in Chongqing, China, 2001-2010. J Neurosurg Spine. 2012 Nov;17(5):459-68. doi: 10.3171/2012.8.SPINE111003
8. Bruno AG, Burkhart K, Allaire B, Anderson DE, Bouxsein ML. Spinal Loading Patterns From Biomechanical Modeling Explain the High Incidence of Vertebral Fractures in the Thoracolumbar Region. J Bone Miner Res. 2017 Jun;32(6):1282-1290. doi: 10.1002/jbmr.3113
9. Ko S, Jung S, Song S, Kim JY, Kwon J. Long-term follow-up results in patients with thoracolumbar unstable burst fracture treated with temporary posterior instrumentation without fusion and implant removal surgery: Follow-up results for at least 10 years. Medicine (Baltimore). 2020 Apr;99(16):e19780. doi: 10.1097/MD.0000000000019780
10. Lu J, Chen Y, Hu M, Sun C. Systematic review and meta-analysis of the effect of using percutaneous pedicle screw internal fixation for thoracolumbar fractures. Ann Palliat Med. 2022 Jan;11(1):250-259. doi: 10.21037/apm-21-3736
11. Walker CT, Xu DS, Godzik J, Turner JD, Uribe JS, Smith WD. Minimally invasive surgery for thoracolumbar spinal trauma. Ann Transl Med. 2018 Mar;6(6):102. doi: 10.21037/atm.2018.02.10
12. Perna A, Santagada DA, Bocchi MB, Zirio G, Proietti L, Tamburrelli FC, Genitiempo M. Early loss of angular kyphosis correction in patients with thoracolumbar vertebral burst (A3-A4) fractures who underwent percutaneous pedicle screws fixation. J Orthop. 2021 Feb 21;24:77-81. doi: 10.1016/j.jor.2021.02.029
13. Alkosha HM, Omar SA, Albayar A, Awad BI. Candidates for Percutaneous Screw Fixation Without Fusion in Thoracolumbar Fractures: A Retrospective Matched Cohort Study. Global Spine J. 2020 Dec;10(8):982-991. doi: 10.1177/2192568219886320
14. Cornaz F, Widmer J, Snedeker JG, Spirig JM, Farshad M. Cross-links in posterior pedicle screw-rod instrumentation of the spine: a systematic review on mechanical, biomechanical, numerical and clinical studies. Eur Spine J. 2021 Jan;30(1):34-49. doi: 10.1007/s00586-020-06597-z
15. Nekhlopochyn O, Verbov V, Cheshuk I, Karpinsky M, Yaresko O. Mathematical Modeling of Variants of Transpedicular Fixation at the Thoracolumbar Junction after ThXII Vertebrectomy during Trunk Backward Bending. ORTHOPAEDICS TRAUMATOLOGY and PROSTHETICS. 2023;(2):43-49. doi: 10.15674/0030-59872023243-49
16. Nekhlopochyn OS, Verbov VV, Cheshuk IV, Karpinsky MY, Yaresko OV. Finite Element Analysis of Thoracolumbar Junction Transpedicular Fixation Variants after Resection of the Th12 Vertebra While Forward Bending. Bulletin of Problems Biology and Medicine. 2023;169(2):281-287. doi: 10.29254/2077-4214-2023-2-169-281-296
17. Ayturk UM, Puttlitz CM. Parametric convergence sensitivity and validation of a finite element model of the human lumbar spine. Comput Methods Biomech Biomed Engin. 2011

Aug;14(8):695-705. doi: 10.1080/10255842.2010.493517
18. Boccaccio A, Pappalettere C. Mechanobiology of Fracture Healing: Basic Principles and Applications in Orthodontics and Orthopaedics. In: Klika V, editor. Theoretical Biomechanics. Croatia: InTech; 2011. p. 21-48. doi: 10.5772/19420
19. Cowin SC. Bone Mechanics Handbook. 2nd ed. Boca Raton: CRC Press; 2001. 980 p.
20. ISO 5832-3:2021: Implants for Surgery: Metallic Materials. Part 3: Wrought titanium 6-aluminium 4-vanadium alloy [Internet]. International Organization for Standardization. Geneva: ISO; 2021. 17 p. https://www.iso.org/ru/standard/79626.html
21. Rao SS. The Finite Element Method in Engineering: Elsevier Science; 2005. 663 p.
22. Kurowski PM. Engineering Analysis with COSMOSWorks Professional 2007. SDC Publications; 2007. 263 p.
23. Mirzaei F, Iranmehr A, Shokouhi G, Khadivi M, Shakeri M, Namvar M, Rafiei E, Matloubi B. The role of cross-link augmentation on fusion rate and patient satisfaction among patients with traumatic thoracolumbar spinal fracture: A randomized clinical trial. Neurocirugia (Astur : Engl Ed). 2021 Mar 3:S1130-1473(21)00011-7. English, Spanish. doi: 10.1016/j.neucir.2021.01.002
24. Karami KJ, Buckenmeyer LE, Kiapour AM, Kelkar PS, Goel VK, Demetropoulos CK, Soo TM. Biomechanical evaluation of the pedicle screw insertion depth effect on screw stability under cyclic loading and subsequent pullout. J Spinal Disord Tech. 2015 Apr;28(3):E133-9. doi: 10.1097/BSD.0000000000000178
25. Shibasaki Y, Tsutsui S, Yamamoto E, Murakami K, Yoshida M, Yamada H. A bicortical pedicle screw in the caudad trajectory is the best option for the fixation of an osteoporotic vertebra: An in-vitro experimental study using synthetic lumbar osteoporotic bone models. Clin Biomech (Bristol, Avon). 2020 Feb;72:150-154. doi: 10.1016/j.clinbiomech.2019.12.013
26. Niinomi M. Mechanical biocompatibilities of titanium alloys for biomedical applications. J Mech Behav Biomed Mater. 2008 Jan;1(1):30-42. doi: 10.1016/j.jmbbm.2007.07.001

Original article

Ukr Neurosurg J. 2024;30(3):38-51
doi: 10.25305/unj.306363

Comparison of the effects of photodynamic exposure with the use of chlorine E6 on glioblastoma cells of the U251 line and human embryonic kidney cells of the HEK293 line *in vitro*

Volodymyr D. Rozumenko [1], Larysa D. Liubich [2], Larysa P. Staino [2], Diana M. Egorova [2], Andrii V. Dashchakovskyi [1], Victoriya V. Vaslovych [3], Tatyana A. Malysheva [3]

[1] Department of Neurooncology and Pediatric Neurosurgery, Romodanov Neurosurgery Institute, Kyiv, Ukraine
[2] Tissue Culture Laboratory, Department of Neuropathomorphology, Romodanov Neurosurgery Institute, Kyiv, Ukraine
[3] Department of Neuropathomorphology, Romodanov Neurosurgery Institute, Kyiv, Ukraine

Received: 17 June 2024
Accepted: 17 July 2024

Address for correspondence*:*
Larysa D. Liubich, Tissue Culture Laboratory, Romodanov Neurosurgery Institute, 32 Platona Maiborody st., Kyiv, 04050, Ukraine, e-mail: lyubichld@gmail.com

Malignant gliomas of the brain are a global medical and social problem with a trend toward a steady increase in morbidity and mortality rates. A method that enables the visual identification of tumor tissue and simultaneously selectively destroys it is photodynamic therapy, which involves the introduction of a photosensitizer (PS) followed by its activation at a certain wavelength of light. The selectivity of the accumulation of PS in the tumor tissue of the malignant gliomas is one of the key issues in the problem of increasing the effectiveness of photodynamic therapy.

Objective: to compare the effects of photodynamic exposure using PS chlorin E6 on human glioblastoma (GB) cells of the U251 line and non-malignant human embryonic kidney cells of the HEK293 line.

Material and methods. Groups of cell cultures were formed depending on the conditions of cultivation and exogenous influence: 1) control - cultivated in a standard nutrient medium (*Modified Eagle's Medium (*MEM)) with L-glutamine, 1 mmol of sodium pyruvate, 10% fetal bovine serum) and experimental: 2) cultivated under the conditions of adding chlorin E6 (concentrations 1.0 and 2.0 μg/ml); 3) cultivated on a nutrient medium without the addition of PS and exposed to laser irradiation (LI) (λ=660 nm, power in the range 0.4-0.6 W, dose in the range 10-75 J/cm^2, continuous or pulse mode); 4) cultured under conditions of chlorin E6 addition and subsequent exposure to LI (power in the range 0.4-0.6 W, dose in the range 10-75 J/cm^2, continuous or pulse mode). After exposure to the specified experimental factors, dynamic observation with microphotographic registration was performed for 24 h, followed by microscopic and micrometric studies (number of viable cells, total number of cells, mitotic index (MI,%)).

Results. PS chlorin E6 is incorporated into the cytoplasm of cells of U251 and HEK293 cell lines, the intensity of fluorescence is comparable. Upon exposure to chlorin E6 (1.0 and 2.0 μg/ml), cytodestructive and antimitotic effects are increased in a dose-dependent manner in the culture of human GB cells of the U251 line. The cytodestructive effect of chlorin E6 on cell cultures of the HEK293 line is less pronounced, but the antimitotic effect is comparable in both types of cell cultures. Under the influence of LI, cytodestructive and antimitotic effects increase in a dose-dependent manner in the culture of human GB cells of the U251 line. The level of cytodestructive and antimitotic effects is significantly lower in the cultures of non-neoplastic HEK293 cells. The most significant drop in the mitotic activity of GB U251 cells (~100%) was recorded at the lowest LI dose of 25 J/cm^2, power of 0.6 W in pulse mode. For HEK293 cells, the most significant decrease in mitotic activity (~80%) was recorded at LI with a power of 0.6 W and dose of 75 J/cm^2 in continuous mode. Under the combined effect of chlorin E6 (1 and 2 μg/ml, pre-incubation of 4 h) and LI in different modes, the viability of tumor cells in U251 culture decreases in a dose-dependent manner; the smallest dose of LI to achieve the maximum cytotoxic effect is 25 J/cm^2, with a power of 0.6 W in pulse mode when using chlorin E6 at a concentration of 2 μg/ml. The specified characteristics of photodynamic exposure do not cause irreversible effects in HEK293 cultures (reference cells).

Conclusions. An effective mode of photodynamic exposure to achieve a cytodestructive and antimitotic effect in the culture of human GB cells of the U251 line, which is relatively safe for non-malignant cells, has been established: the combined application of a laser irradiation dose of 25 J/cm^2, with a power of 0.6 W in pulse mode during the preliminary incubation of the cell culture with chlorin E6 at a concentration of 2 μg/ml for 4 h.

Key words: *laser irradiation; photosensitizer; malignant gliomas; glioblastoma; U251; HEK293; mitotic index*

Introduction

The treatment of malignant gliomas (MG) remains a serious challenge globally, despite research into the causes of their occurrence and mechanisms of progression. Malignant brain tumors are a global medical and social problem, with a trend towards increasing incidence and mortality rates (primarily due to the progression of MG) [1-5]. Traditional surgical approaches with ad oculus imaging may leave unnoticed tumor cells in the zone of invasive spread that migrate over significant distances. Consequently, MG recurrence often occurs near the marginal (perifocal) area of the surgical cavity [6]. Additionally, in functionally critical areas of the brain, the radical surgical removal of tumors is impossible. Photodynamic therapy (PDT), a two-stage process involving the introduction of a photosensitive chemical agent (photosensitizer) followed by its intraoperative activation at a certain wavelength of light, is a method that allows to identify the tumour tissue visually intraoperatively and simultaneously destroy it with maximum clarity (objectively) [6, 7].

The principle of PDT is based on the cytotoxic effects induced by the generation of singlet molecular oxygen and free radicals by the activated photosensitizer (PS), which trigger photochemical reactions in the tumor cells, leading to the destruction of basic cytoskeletal proteins. The tumor tissue is believed to have a higher affinity for the PS, which selectively incorporates into neoplasm cells [8, 9]. The simultaneous use of fluorescence-guided surgery and PDT allows for the visualization and targeted destruction of tumor cells [9-11], optimizing the determination of tumor spreading boundaries for maximal removal [12].

Analysis of clinical trial data suggests that using PDT as an adjunct treatment for MG immediately after maximal resection is safe, reduces the risk of recurrence by targeting residual tumor cells in the resection cavity, and improves patient survival and quality of life [10,13-21]. The lack of information on the development of resistance to multiple PDT sessions suggests the potential for repeated treatment of tumor cells that were not removed during surgery.

Since the efficiency of photodynamic damage to sensitized cells is determined by the intracellular concentration of the PS, its localization within the cell, photochemical activity, and the dose of laser irradiation (LI), developing *in vitro* experimental models to evaluate PDT effectiveness is a relevant task. Photosensitizers must cross the blood-brain barrier, selectively localize in tumor tissue without significant accumulation in healthy tissues, exhibit maximum cytotoxic activity against tumor cells, and be rapidly excreted from the body [22, 23]. In researching PS, the focus is on compounds of natural origin, one of which is chlorin E6 — a second-generation PS, representing natural pigments obtained from green algae. Chlorin E6 is combined with polyvinylpyrrolidone (a biocompatible polymer that imparts water solubility to the hydrophobic chlorin E6), which promotes tumor accumulation due to the increased permeability of defective tumor vessels and reduced lymphatic drainage [24]. The selective accumulation of the PS in MG tumor tissue is one of the key issues for improving the effectiveness of PDT.

Objective: to compare the effects of photodynamic therapy using the photosensitizer chlorin E6 on human GB cells of the U251 line and non-malignant human embryonic kidney cells of the HEK293 line.

Materials and Methods

The study was conducted on cultures of human glioblastoma (GB) cells of the U251 line and human embryonic kidney HEK293 cell line. Cryopreserved cell samples (kindly provided by the "Cell Bank of Human and Animal Tissue Lines," R.E. Kavetsky Institute of Experimental Pathology, Oncology and Radiobiology, NAS of Ukraine, Kyiv) were thawed in a water bath for 30 min at 38°C, suspended in 10 ml of Modified Eagle's Medium (MEM) with L-glutamine (Biowest, France) without serum, and centrifuged (5 min at 1000 rpm, MICROmed CM-3). The cell pellet was suspended in MEM medium with L-glutamine (1 mmol sodium pyruvate, 10% fetal calf serum (Biowest, France)), and placed in culture plastic flasks (25 cm^3, Cellstar, Germany) at a concentration of $0.1 \cdot 10^6$ cells/8 ml of the culture medium. Cultures were maintained in a CO_2 incubator (Nuve, Turkey) under standard conditions (95% humidity, 37°C, 5% CO_2). The culture medium was changed every three days. Dynamic observation with microphotoregistration was performed using a "Nikon S-100" inverted microscope (Japan).

Cells in the amount of $2 \cdot 10^6$ were transferred to plastic Petri dishes (d = 35 mm, Sarstedt, Germany) on coverslips pre-coated with polyethyleneimine (Sigma-Aldrich, GmbH, Germany), the culture medium (2 ml) was added, and cells were cultured until a monolayer (75-80%) was achieved.

To investigate the immediate effects of chlorin E6 in the cell culture with a formed monolayer, the PS was added at a concentration of 1 or 2 μg/ml. To investigate the direct effects of LI, plates with cultures were placed under the vertical fiber-optic laser output (h = 5 cm) of the "LIKA-surgeon" device ("Photonics-Plus", Ukraine) and irradiated with uniform coverage of the monolayer surface area with light beams (λ – 660 nm) under various modes (power range - 0.4 - 0.6 W, dose (exposure - surface energy density relative to the irradiated surface area) - 10 - 75 J/cm^2, continuous or pulse mode). The exposure time of LI to the cell culture depended on the applied power and mode (the maximum duration of irradiation was 240 s for LI 0.6 W, 75 J/cm^2, pulse mode). The irradiated cultures were kept at room temperature during this time, while the cultures of the comparison groups were kept under similar conditions. To study the combined effects of chlorin E6 and LI, the PS was added to the cell culture with a formed monolayer (at concentrations of 1 and 2 μg/ml) and held in a CO_2 incubator (Nuve, Turkey) for 4 h, after which the cultures were irradiated under various modes as indicated above. The variants of experimental exposure combinations on cell cultures are presented in the ***Table***.

After exposure to the specified experimental factors, the cultures were kept in a CO_2 incubator (Nuve,

This article contains some figures that are displayed in color online but in black and white in the print edition.

Turkey) and subjected to dynamic observation with microphotoregistration using an inverted microscope "Nikon S-100" (Japan) for 24 h. Microphotoregistration of fluorescence was conducted using an Axiophot microscope (Opton, Germany) with fluorescent filters (λ - [500-680] nm).

To determine the cytotoxic effects of chlorin E6 and laser irradiation, the cell cultures were exposed to various research conditions with the addition of a vital dye (0.2% trypan blue solution (Merck, Germany)) to the culture medium, and the growth of cultures was observed using an inverted microscope for 24 h.

For further analysis, cell culture groups were formed based on cultivation conditions and exogenous exposure: 1) control - cultured in a standard nutrient medium (MEM with L-glutamine, 1 mmol sodium pyruvate, 10% fetal calf serum) and experimental: 2) chlorin E6 addition (concentrations of 1.0 and 2.0 μg/ml); 3) cultured in a nutrient medium without addition of a PS and exposed to LI (power - 0.4–0.6 W, dose - 10–75 J/cm², continuous or pulse mode); 4) cultured with the addition of chlorin E6 and exposed to LI (power - 0.4–0.6 W, dose - 10–75 J/cm², continuous or pulse mode).

Table. Conditions for experimental exposure to cell cultures

№	Exposure conditions				Number of cell cultures	
					U251	HEK293
1	Control				10	9
2	Chlorin E6			1,0 μg/ml	9	13
				2,0 μg/ml	10	14
3	Laser irradiation (LI)	0,4 W	10 J/cm2	continuous mode	3	3
				pulse mode	3	3
			25 J/cm2	continuous mode	3	3
				pulse mode	3	3
		0,6 W	10 J/cm2	continuous mode	3	3
				pulse mode	3	3
			25 J/cm2	continuous mode	7	3
				pulse mode	7	3
			50 J/cm2	continuous mode	3	3
				pulse mode	3	3
			75 J/cm2	continuous mode	3	3
				pulse mode	3	3
4	Chlorin E6 (1 μg/ml) + LI	0,4 W	10 J/cm2	continuous mode	3	3
				pulse mode	3	3
			25 J/cm2	continuous mode	3	3
				pulse mode	3	3
		0,6 W	10 J/cm2	continuous mode	3	3
				pulse mode	3	3
			25 J/cm2	continuous mode	3	3
				pulse mode	3	3
	Chlorin E6 (2 μg/ml) + LI	0,4 W	10 J/cm2	continuous mode	3	3
				pulse mode	3	3
			25 J/cm2	continuous mode	3	3
				pulse mode	3	3
		0,6 W	10 J/cm2	continuous mode	3	3
				pulse mode	3	3
			25 J/cm2	continuous mode	7	3
				pulse mode	7	3
			50 J/cm2	continuous mode	3	3
				pulse mode	3	3
			75 J/cm2	continuous mode	3	3
				pulse mode	3	3

Cell cultures were fixed in 10% neutral formalin (Bio-Optica, Italy) and stained with hematoxylin and eosin by the Carazzi method. Microscopic examination and photoregistration of cytological preparations were carried out using a light-optical photomicroscope "Nikon Eclipse E200" (Japan). In each preparation, the structural features of experimental cultures were compared with the control ones. The analysis included cell shape, the presence and branching of processes, chromatin structure and distribution, nuclear morphology, and intercellular interactions.

Quantitative studies of experimental cultures compared to the control were conducted in 10 representative fields of view using a standard measuring scale (object micrometer). Morphometric analysis was performed by processing digital images of cultures in 10 randomly selected fields of view (0.04 mm^2) for each sample at the same magnification (800x) using ImageView software (2020). The test area determined the number of viable cells, the total number of cells, and the number of cells in the mitotic division state. The mitotic index (MI, %) was calculated as the percentage of cells undergoing mitosis per 100 cells.

Statistical analysis of the obtained data was performed using a licensed statistical software package (StatSoft Inc., 2022). The normality of data distribution was determined by the Shapiro-Wilk test. Non-parametric methods of variation statistics were applied (Kruskal-Wallis rank-based ANOVA for multiple comparisons of several independent groups, Mann-Whitney U-test for pairwise comparison of independent groups, and Wilcoxon test for pairwise comparison of dependent groups over time). Data are presented per unit of test area (0.04 mm^2) as (M±m), where M is the arithmetic mean, m is the standard deviation from the arithmetic mean. Differences were considered statistically significant at $p<0.05$.

Results and Discussion

As an *in vitro* model of MG, we used cultures of human GB cells of the U251 line, which was obtained from a malignant human brain GB tumor by explantation. The cell type of the tumor was identified as pleomorphic/astrocytoid [25].

Human GB cells of the U251 line in culture demonstrated typical growth dynamics: starting from the formation of chains and dense monolayer cell conglomerates alongside individual cells without distinct signs of differentiation (with narrow cytoplasm and moderate nuclear polymorphism) and astrocytic cells with processes during the 1st day after explantation ***(Fig. 1A)*** to the expansion of the monolayer of tumor cells (large in size with distinct contours, clear cytoplasm, large nucleus, astrocytic structure, unipolar, triangular, rhomboid, polygonal shape with elongated processes) on the 5^{th}-7^{th} day ***(Fig. 1B)***. At the stage of confluent growth, the cultures showed reticular proliferation of densely packed tumor cells with high polymorphism. Histological preparations in the growth zone of the cultures revealed 2-3 tumor cells in the mitotic division stage within the field of view ***(Fig. 1C)***. On the 7^{th} day of cultivation in the control cultures of U251 cell line, in the growth zones of undifferentiated tumor cells, the mitotic index (MI) averaged (0.88±0.05) %.

To compare the efficiency of photodynamic effects on non-tumor tissues, we used the HEK293 cell line - an immortalized line artificially created by transforming a culture of human embryonic kidney cells with fragments of adenovirus 5 DNA [26]. HEK293 cells have an epithelial-like structure and form monolayer cultures. They usually have a flattened elongated shape with well-defined cell boundaries and high adhesion. HEK293 cells do not express tissue-specific genes but do express markers of renal progenitor cells, neuronal cells, and adrenal cells [27]. The presence of specific gene products and mRNA, typically detected in neurons, along with the potential for induced synaptogenesis, the functionality of endogenous neuron-specific voltage-dependent channels, and responses to various agonists involved in neuron signaling, support considering HEK293 as cells with a neuronal phenotype [27]. HEK293 cells have a complex phenotype due to a heterogeneous unstable atypical karyotype: they have two or more copies of each chromosome, with a modal chromosome number of 64-hypotriploid karyotype (containing more than two copies (diploid), but less than three); three copies of the X chromosome and four copies of chromosomes 17 and 22) [28]. The average number of chromosomes and chromosomal aberrations vary in HEK293 cells and their derivatives, as well as in HEK293 cells from different cell banks/laboratories [27].

In our studies, in the first 24 h, we observed an adherent population of small, mostly slightly rounded cells growing dispersed, as well as a small number of polygonal and distinctly elongated cells ***(Fig. 2A)***.

When cultured for 5-7 days, HEK293 cells formed a continuous monolayer of epithelial-like structure, arranged quite densely, with a large number of intercellular contacts. Most cells exhibited regular, balanced shapes, with occasional round, cylindrical, and polygonal forms. The cells had dense cytoplasm and a centrally located large oval-round nucleus containing 1-2 (rarely 3) nucleoli ***(Fig. 2B)***. A significant number of proliferatively active cells were observed ***(Fig. 2D)***. On the 7^{th} day of cultivation in control cultures of HEK293 cells line in the growth zones, the MI averaged (0.61±0.07)%. In the trypan blue test, a small proportion of spontaneously degenerated cells were noted ***(Fig. 2C)***.

Effects of chlorin E6 in cultures of U251 and HEK293 cell lines. After applying chlorin E6 at a concentration of 1 μg/mL for 24 h in U251 cell line cultures, a thinning of the growth zone was observed, with the appearance of large lacunae in the cellular monolayer ***(Fig. 3A)***. Among intact cells, diffusely located dystrophic or necrobiotically altered tumor cells were found, characterized by reduction of processes, rounded cytoplasm with signs of progressive lipid and hydropic dystrophy, and hyperchromatic nuclei. Some tumor cells turned into shadow cells or "naked" nuclei, forming small clusters. The number of cells in the mitotic state decreased to 1-2 in the field of view (MI averaged (0.71±0.08) %, $p=0.14$ compared to control, Mann-Whitney U-test). Blocked forms of K-mitoses were noted among the figures of mitotic division of tumor cells.

With an increased concentration of chlorin E6 (2 μg/ml), within just 6 h, there was noticeable thinning of U251 cell culture masses due to retraction of the growth zone and reduction of processes in damaged cells. After

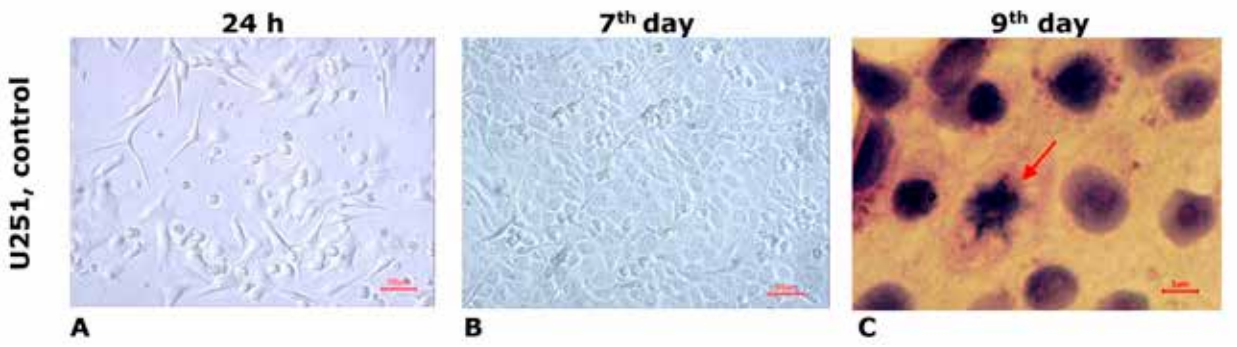

Fig. 1. Microphotos of human GB U251 cell cultures grown in standard culture medium (control). Light microscopy, unstained culture (A, B); staining with hematoxylin and eosin (C). The arrow indicates a cell in the mitotic phase (prophase)

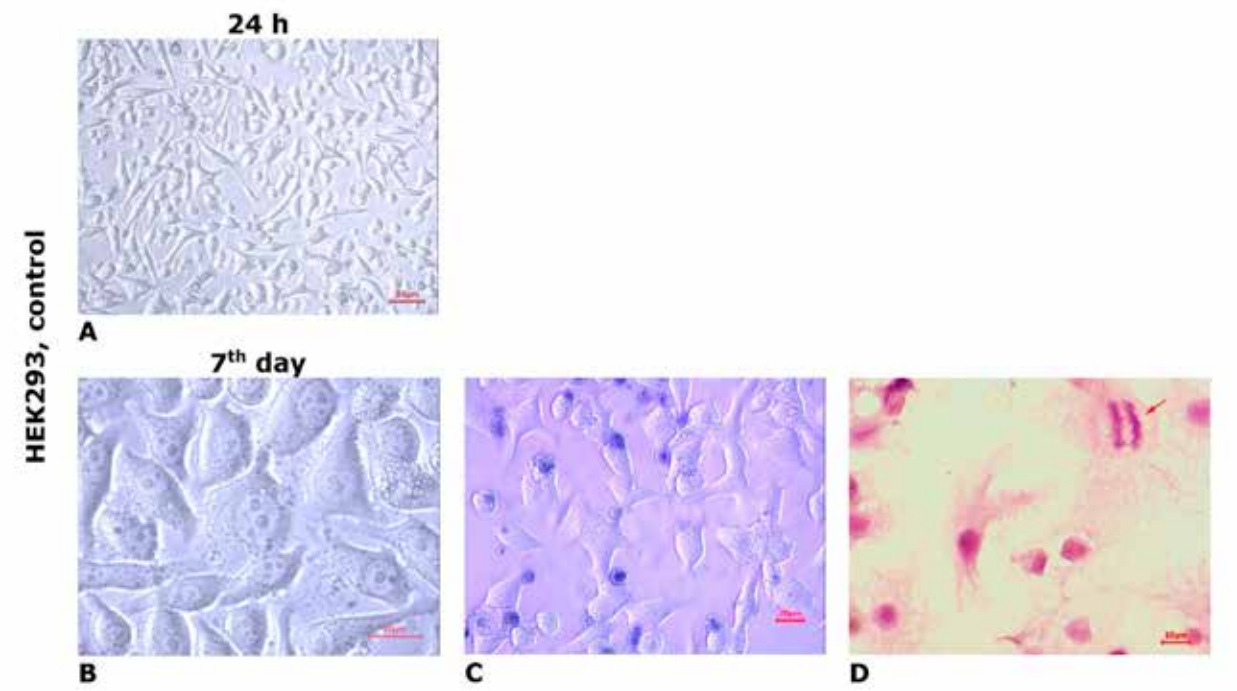

Fig. 2. Microphotos of HEK293 cell line cultures grown in standard culture medium (control). Light microscopy, unstained culture (A, B); staining with trypan blue vital dye (C); staining with hematoxylin and eosin (D). The arrow indicates a cell in the mitotic phase (anaphase)

24 h, intercellular adhesion was lost, leading to the formation of small and large lacunae in the monolayer of cells in the growth zone, dilution of cell masses, and desquamation of some dead cells. In some areas, the growth zone of U251 cells was almost completely depleted with only a few degenerated round-shaped cells remaining. Reticulated structures with degenerating cells (with cytoplasmic vacuolization and loss of processes) persisted in isolated areas ***(Fig. 3A)***. In the preserved areas of the growth zone monolayer, mitotic activity of some tumor cells was maintained (one cell in mitosis was observed in several fields of view, MI decreased to (0.15±0.02)%, $p=1\cdot10^{5}$ compared to control, p=0.04 compared with the value when exposed to chlorin E6 (1 μg/ml), Mann-Whitney U-test) ***(Fig. 4)***.

Unlike the U251 cell line, the growth zone of HEK293 cells remained intact 24 h after exposure to chlorin E6 at a concentration of 1 μg/ml. While cell density remained high, pathological changes were observed, including reduction of processes, cytoplasmic rounding, nuclear displacement to the periphery of the cytoplasm, and vacuolization ***(Fig. 3C)***. HEK293 cells maintained a low level of mitotic activity (MI was, on average, (0.33±0.04)%, p=0.04 compared to control, Mann-Whitney U-test). Increasing the concentration of chlorin E6 to 2 μg/ml had little effect on the HEK293 cell monolayer density but did result in an increase in the number of rounded cells with reduced processes, vacuolated cytoplasm, and decentered nuclei ***(Fig. 3C)***. A few mitotically active cells were observed in the growth

zone (MI decreased to (0.23±0.03)% ***(Fig. 4)***, p=0.01 compared to control, p=0.6 compared to the effect of chlorin E6 (1 μg/ml), Mann-Whitney U-test), among which pathological forms (asymmetric mitoses) were observed, leading to telophase disruption, resulting in the appearance of binucleated and multinucleated cells in the monolayer.

According to the data of fluorescence study, in experimental cultures of U251 and HEK293 cells, chlorin E6 accumulated in the cytoplasm, and the fluorescence intensity in different cell types was nearly identical ***(Figs. 3B, 3D)***, likely due to the heterogenous phenotype characteristics of HEK2 cells [27]. Other authors have reported localization of the photosensitizer in cytoplasmic organelles as well [29].

In contrast to cell lines U251 and HEK293, the fluorescence intensity of chlorin E6 incorporated into non-malignant rat brain cells (E14-16) was much weaker [30], which aligns with data regarding the higher affinity and selective accumulation of photosensitizers in tumor tissues [22].

Thus, the results of testing chlorin E6 exposure indicate a dose-dependent cytotoxic effect on tumor cells of the U251 line. Unlike the U251 cell line, HEK293 cell cultures did not experience such destruction of the growth zone when exposed to chlorin E6, as the majority of cells remained intact. However, the anti-mitotic effect of chlorin E6 was relatively comparable in both types of cell cultures.

Effects of laser irradiation at various modes on U251 and HEK293 cell line cultures

After 24 h of LI exposure (0.4 W power, 10 J/cm² dose, continuous mode), a retraction of the growth zone with the formation of lacunae of varying sizes and compaction of the tumor cell monolayer was observed in U251 cell cultures ***(Fig. 5A)***. Under the same conditions, HEK293 cell cultures did not exhibit significant monolayer disruption; the cells maintained characteristic sizes and shapes ***(Fig. 5C)***. Under pulse mode LI (0.4 W, 10 J/cm²), no additional changes were observed in both studied cell lines compared to previous observations ***(Fig. 5B)***.

Under LI exposure at 0.4 W, 25 J/cm² in continuous mode, further retraction of the growth zone occurred in cultures of cell line U251, with intact monolayer regions preserved ***(Fig. 5A)***. In HEK293 cell line cultures, no damage to the growth zone was detected under these conditions; the trypan blue test revealed a small number of degenerated cells ***(Fig. 5C)***. With LI (0.4 W, 25 J/cm²) in pulse mode, there was further compaction of the U251 cell monolayer, an increase in lacunae in the growth zone, and the number of degenerated cells ***(Fig. 5B)***, along with a significant reduction in mitotic activity (***Fig. 6A***; $p=3\cdot10^{-6}$ compared to control, p=0.007 compared to the indicator under continuous LI mode, Mann-Whitney U-test). No significant changes were observed in HEK293 cell line cultures under the same conditions ***(Figs. 6B, 6D)***.

Under higher power laser irradiation (0.6 W, 10 J/cm², continuous mode) in U251 cell cultures, a substantial reduction in the total number of cells in the monolayer was observed, with most cells rounding up and losing intercellular contacts, leading to the depletion of the growth zone ***(Fig. 5A)***. Meanwhile, the HEK293 cell monolayer did not undergo significant changes ***(Fig. 5C)***. Laser irradiation (0.6 W, 10 J/cm²) in pulse mode caused the destruction of the U251 cell growth zone: most cells had reduced processes and lost contacts with each other and the surface, leading to monolayer degradation with the formation of unformed cell aggregates and fragments ***(Fig. 6B)***. The mitotic activity of U251 cells was at a low level (***Fig. 6A***; $p=1\cdot10^{-6}$ compared to control, Mann-Whitney U-test). In HEK293 cell cultures under the same conditions, the appearance of pathologically altered cells was noted (with loss of characteristic shape and rounding), as well as the presence of binucleated cells and displacement of nuclei to the cytoplasm's periphery ***(Fig. 5D)***. The mitotic activity of HEK293 cells changed little ***(Fig. 6B)***, and the monolayer cell density slightly decreased compared to the control.

When exposed to LI (0.6 W, 25 J/cm², continuous mode), there was a significant reduction in the total number of U251 cells in the damaged growth zone, with large areas devoid of cells or containing only a few cells at different stages of degeneration ***(Fig. 5A)***. In cultures of the cell line HEK293 under the same conditions, nuclear displacement to the periphery of the cytoplasm was observed in most cells, with an increase in the number of rounded cells but without a loss in monolayer density or the overall cell count in the growth zone ***(Fig. 5C)***. LI (0.6 W, 25 J/cm²) in pulse mode intensified the destructive processes in U251 cell cultures ***(Fig. 5B)*** and practically eliminated mitotic activity (***Fig. 6A***; $p=3\cdot10^{-6}$ compared to control, p=0.34 compared to the index in continuous LI mode, Mann-Whitney U-test). In cultures of HEK293 cells under the same conditions, significant damage to the cell mass was not observed, and the monolayer density remained high, although the number of rounded degenerated cells increased ***(Fig. 5D)*** and mitotic activity indices significantly decreased (***Fig. 6B***; p=0.02 compared to control, p=0.27 compared to continuous LI mode, Mann-Whitney U-test).

Increasing the LI dose to 50 J/cm² in continuous mode at 0.6 W led to an increase in dystrophic and necrobiotic changes in the cells of U251 line and the appearance of a significant number of apoptotic bodies ***(Fig. 5A)***. Under the same conditions, LI (0.6 W, 50 J/cm²) in pulse mode intensified destructive processes in the U251 cell growth zone ***(Fig. 5B)***. Necrobiotic processes of spontaneous cell death affected most cells in the growth zone, and MI significantly decreased ($p=1\cdot10^{-6}$ compared to control, p=0.55 compared to the index of continuous LI mode, Mann-Whitney U-test). In HEK293 cell cultures under the same conditions, LI led to a reduction in cell density in the monolayer growth zone compared to control cultures ($p<0.05$, Mann-Whitney U-test, **Fig. 6B**). Cells maintained their characteristic shape, but vacuolization in the cytoplasm was observed ***(Fig. 5C, 5D)***, and mitotic activity significantly decreased (p=0.03, p=0.04 compared to control, Mann-Whitney U-test).

After exposure to a LI dose of 75 J/cm² (power 0.6 W) in both continuous and pulse modes, an increase in growth zone destruction and dystrophic and necrobiotic changes were observed in cultures of cell line U251 ***(Fig. 5A, 5B)***. In some areas, the growth zone was completely devastated with almost total cell destruction. Chromatin coagulation was observed in some cells, turning into a sharply basophilic

homogeneous mass (pyknosis), indicating membrane integrity disruption. Mitotic activity almost disappeared ($p=1\cdot10^{-6}$ compared to control, p=0.41 compared to the index in continuous LI mode, Mann-Whitney U-test). Cytological preparations of preserved areas of the growth zone recorded an increase in the proportion of pathologically altered cells with a large number of cell shadows and "bare nuclei" against a sharp decrease in the total cell count ***(Fig. 6A)***.

In HEK293 cell cultures, LI (0.6 W 75 J/cm²) in continuous mode led to the rounding and separation of cells in the dense monolayer, enlargement of nuclei, cytoplasmic vacuolization, decreased cell adhesion, and, consequently, disruption of the growth zone ***(Fig. 5C)***. LI with the same parameters in pulse mode led to vacuolization of HEK293 cells, loss of intercellular contacts, cell rounding, and lysis, which reduced the monolayer density ***(Fig. 5D).*** Mitotic activity was low

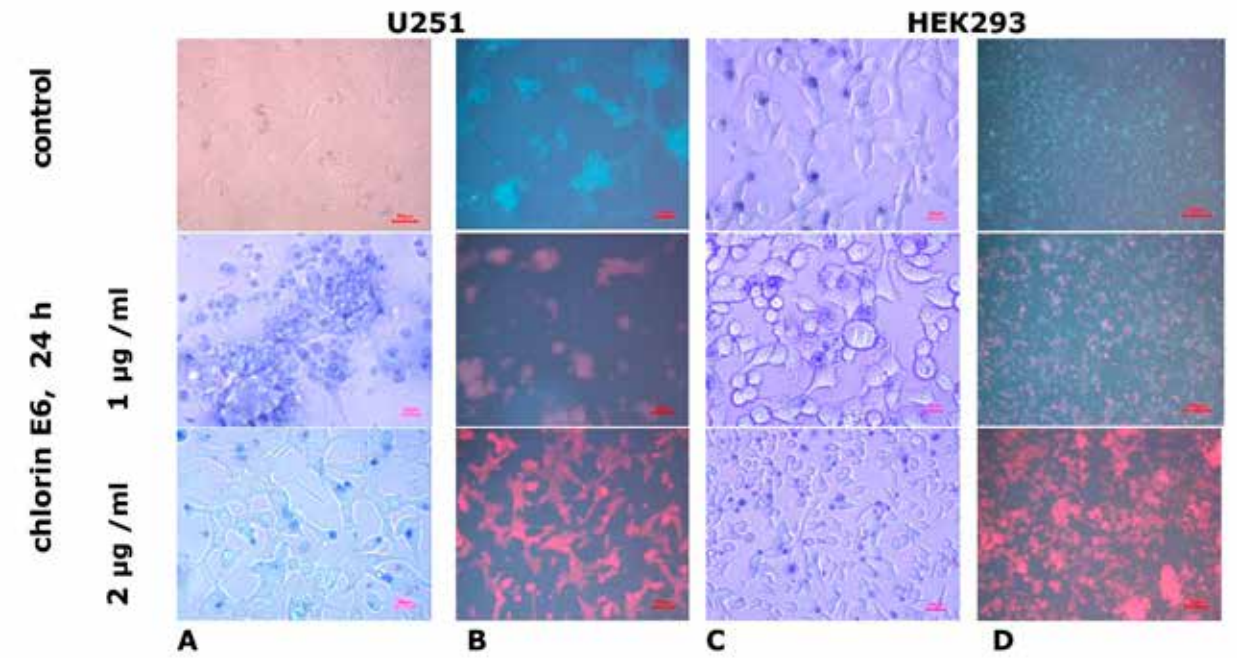

Fig. 3. Microphotos of U251 human glioblastoma cell cultures and HEK293 cell cultures grown in standard medium and after the addition of chlorin E6 at different concentrations. Light (A, C) and fluorescence (B, D) microscopy. Staining with trypan blue vital dye

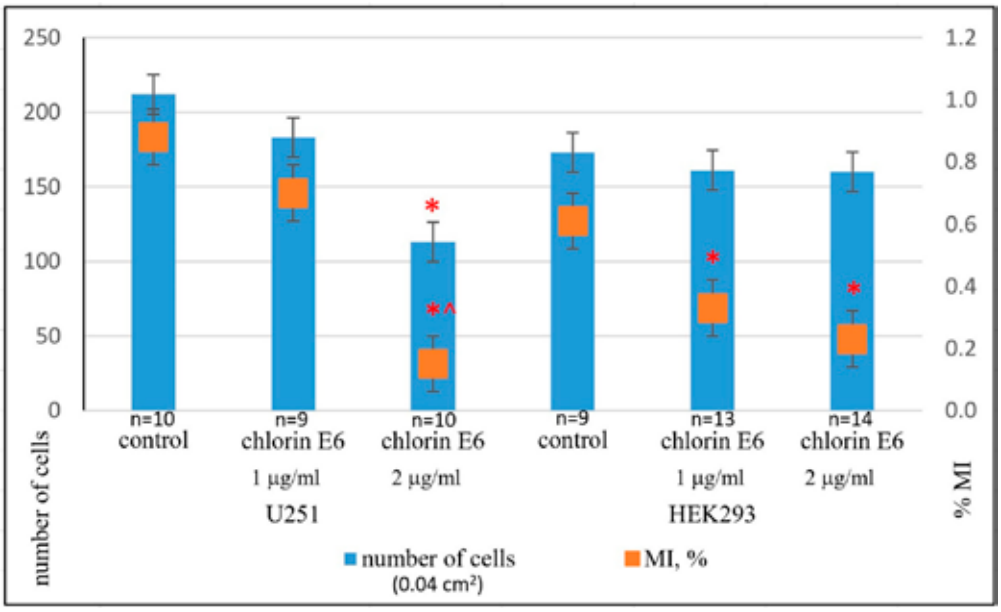

Fig. 4. Average number of cells and mitotic index (MI, %) in U251 human GB cell cultures and HEK293 cell cultures 24 h after the addition of chlorin E6 at different concentrations: * – p<0.05 compared to control; ^ – p<0.05 compared to chlorin E6 (1 μg/ml); Mann-Whitney U-test

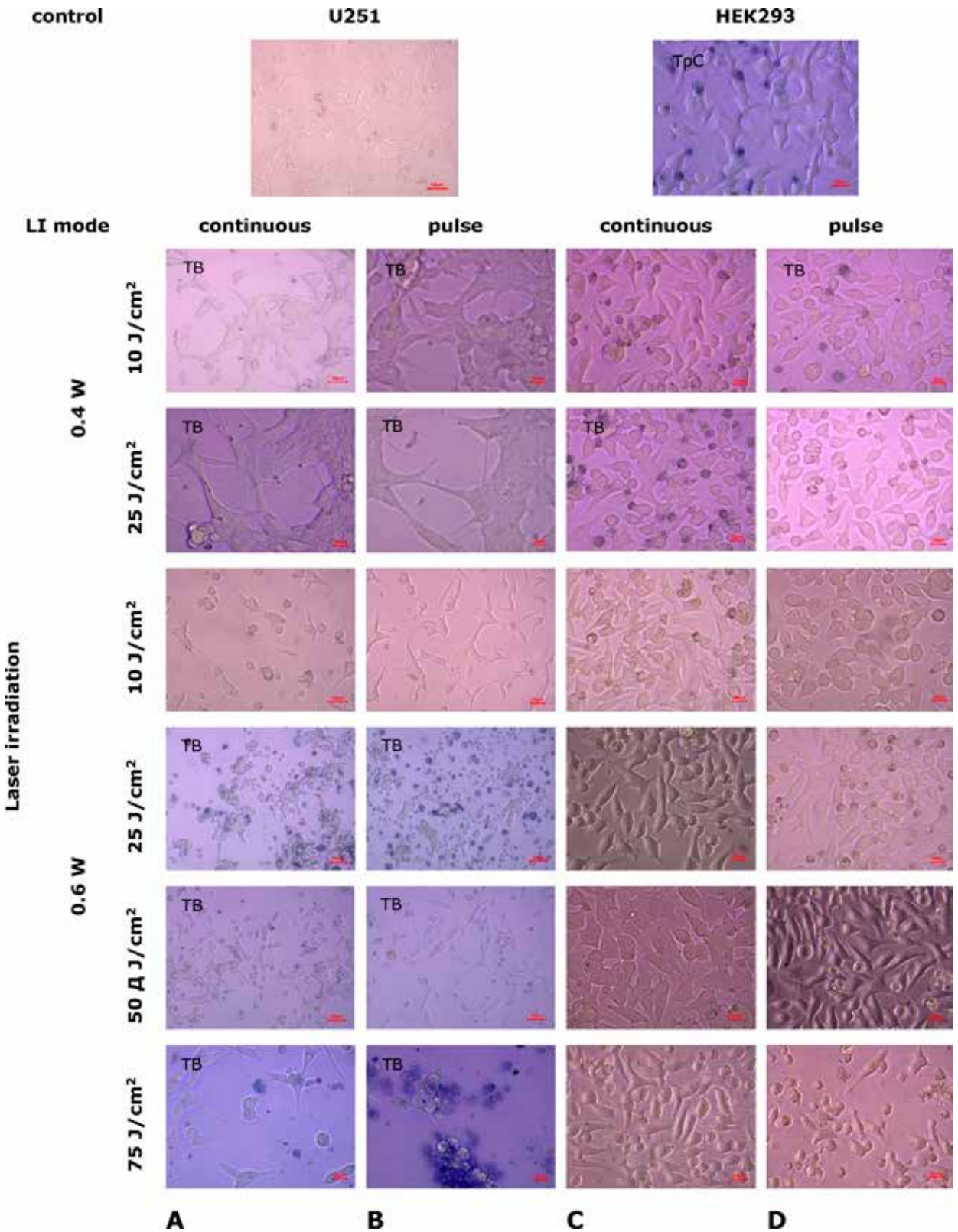

Fig. 5. Microphotos of U251 human glioblastoma cell cultures and HEK293 cell cultures 24 h after exposure to laser irradiation under various modes. Light microscopy. Unstained cultures and staining with trypan blue vital dye (TB)

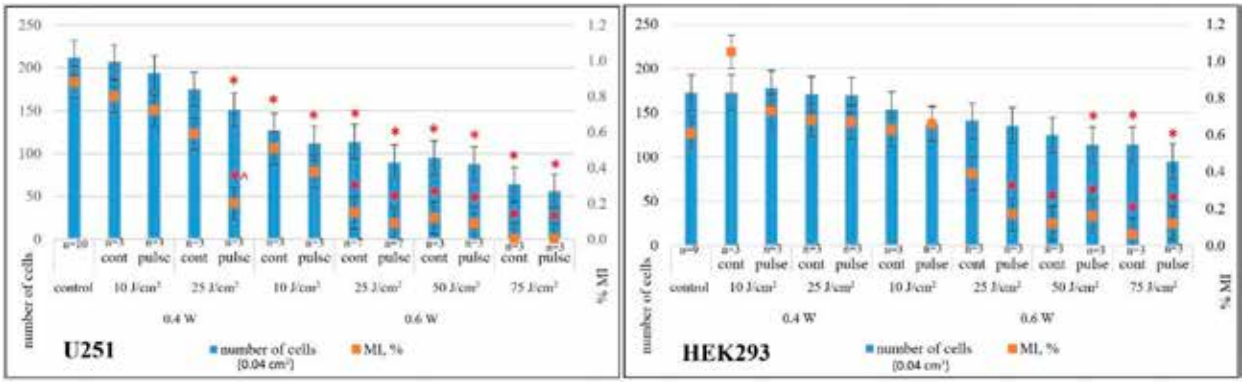

A **B**

Fig. 6. Average cell count and mitotic index (MI, %) in U251 human GB cell cultures (A) and HEK293 cell cultures (B) 24 h after laser irradiation under various modes: * - p<0.05 compared to control; ^ - p<0.05 compared to continuous mode of laser irradiation, Mann-Whitney U-test

(p=0.01 compared to control, p=0.58 compared to the index in continuous LI mode, Mann-Whitney U-test; ***Fig. 6B***).

Therefore, studies testing the effects of LI on U251 human GB cell cultures demonstrate a dose-dependent cytotoxic effect. Increasing the power from 0.4 to 0.6 W and the dose from 10 to 75 J/cm² in continuous mode leads to destructive changes in the growth zone's architectonics (from growth zone retraction with lacunae formation of varying sizes at the lowest LI parameters to severe destruction and significant cell mass depletion at the highest parameters). There was also a gradual decrease in mitotic activity of tumor cells and accumulation of necrobiotic changes up to irreversible degeneration with subsequent desquamation of dead cells. This effect tends to intensify with the same laser irradiation characteristics in pulse mode, significantly differing from the effect of laser irradiation at 0.4 W, 25 J/cm² (p=0.007, Mann-Whitney U-test).

In contrast to tumor cells of U251 line, the degree of LI influence in the applied modes on non-tumor cells of HEK293 line was significantly less: the first pathological changes of HEK293 line cells without changes in the growth zone were detected starting with LI power of 0.6 W (dose 10 J/cm²) in pulse mode, and significant monolayer density changes occurred with an increase in LI dose to 75 J/cm² in pulse mode.

Based on the dynamics of the mitotic activity indicator, it was found that the most significant reduction in U251 human GB cell culture was registered starting with laser irradiation power of 0.6 W (dose 25 J/cm²). In this mode, HEK293 cell cultures retained mitotic activity.

The most significant decrease in mitotic activity of U251 human GB cells (~100%) was recorded at a minimum LI dose of 25 J/cm², power 0.6 W in pulse mode ($p=3\cdot10^{-6}$ compared to control, p=0.34 compared to continuous LI mode, Mann-Whitney U-test; ***Fig. 6A***). For HEK293 cells, the most significant reduction in mitotic activity (~80%) was recorded at LI power 0.6 W (dose 75 J/cm²) in continuous mode (p=0.01 compared to control, Mann-Whitney U-test; ***Fig. 6B***).

Effects of combined exposure to chlorin E6 and laser irradiation in different modes on U251 human GB cell cultures and HEK293 cell lines. In U251 cell cultures, after 24-h incubation with chlorin E6 (1 μg/mL) followed by LI (0.4 W, 10 J/cm², continuous and pulse mode), retraction of the growth zone and a significant decrease in cell monolayer density occurred ***(Fig. 7A, 7B)***. The cells in the growth zone were characterized by high permeability to the vital dye (trypan blue), even at the nucleus, indicating membrane integrity damage. Under the same conditions, the density of the cell monolayer in HEK293 cell cultures also decreased significantly, with some cells losing contact with each other and the surface, becoming rounded **(Fig. 7C, 7D)**. However, only some HEK293 cells (mainly rounded, necrotized, floating ones) stained with trypan blue. In the cells of the HEK293 line, the accumulation of lipid droplets in the cytoplasm was observed, which caused cellular cytotoxicity.

Similar changes described in cells of both cell lines were observed after 24-h incubation with chlorin E6 (1 μg/mL) followed by LI (0.4 W, 25 J/cm², continuous and pulse mode) ***(Fig. 7)***.

When exposed to LI of higher power (0.6 W, 10 J/cm², continuous mode), cultures of U251 cell line showed a marked depletion of the growth zone, with cells degenerating, rounding, and losing processes ***(Fig. 7A)***. Small complexes of spread cells with processes that lost their characteristic shapes remained in the field of view, among them were bi- and tri-nucleated cells. In the growth zone of HEK293 cells under the same conditions, areas of depletion were observed, with cells losing contact with each other and the surface, leading to desquamation. A large number of rounded cells at various stages of degeneration were observed in the field of view ***(Fig. 7C)***.

When exposed to LI (0.6 W, 10 J/cm², pulse mode), U251 cells underwent degenerative changes: loss of processes, decreased adhesion, loss of characteristic cell shapes, and lipid accumulation in the cytoplasm. The growth zone was depleted, leaving clusters of cells with multiple nuclei and reduced processes ***(Fig. 7B)***. Mitotic activity decreased ($p=1\cdot10^{-6}$ compared to control, p=0.59 compared to the index under continuous LI mode, Mann-Whitney U-test).

Under the same conditions, the cell density in the HEK293 growth zone remained higher, although they underwent degenerative changes: lipid accumulation, cytoplasmic vacuolization, loss of characteristic morphological features, rounding, and the presence of multiple nuclei ***(Fig. 7D)***. Similar changes occurred in the growth zone of HEK293 cell cultures with increasing laser dose irradiation to 25 J/cm² ***(Fig. 7C, 7D)***. In pulse mode, LI led to greater depletion of the growth zone and an increase in the number of degeneratively altered cells compared to continuous mode. Mitotic activity remained at a low level (p=0.003 compared to control, for both LI modes, Mann-Whitney U-test).

The use of chlorin E6 at a concentration of 2 μg/mL followed by LI with gradual increases in power and dose resulted in even more destructive changes in the cell monolayer. In U251 cell cultures, after 24-h incubation with chlorin E6 (2 μg/mL) and subsequent LI (0.6 W, 10 J/cm², continuous mode), depletion of the growth zone was observed with residual clusters of degeneratively altered cells ($p=1 \cdot 10^{-6}$ compared to control, Mann-Whitney U-test; ***Fig. 8A***). Similar consequences under these conditions were also found in HEK293 cell cultures ***(Fig. 8C)***. Pulse mode LI was associated with a tendency to intensify the identified changes (p=0.08 compared to the index for continuous LI mode, Mann-Whitney U-test).

When the irradiation dose was increased to 25 J/ cm² in both continuous and pulse modes, destruction of the growth zone with cell remnants at various stages of degeneration was observed in cultures of both studied cell lines, but with significantly lower intensity in HEK293 cell cultures ***(Fig. 8)***. Under these conditions, mitotic

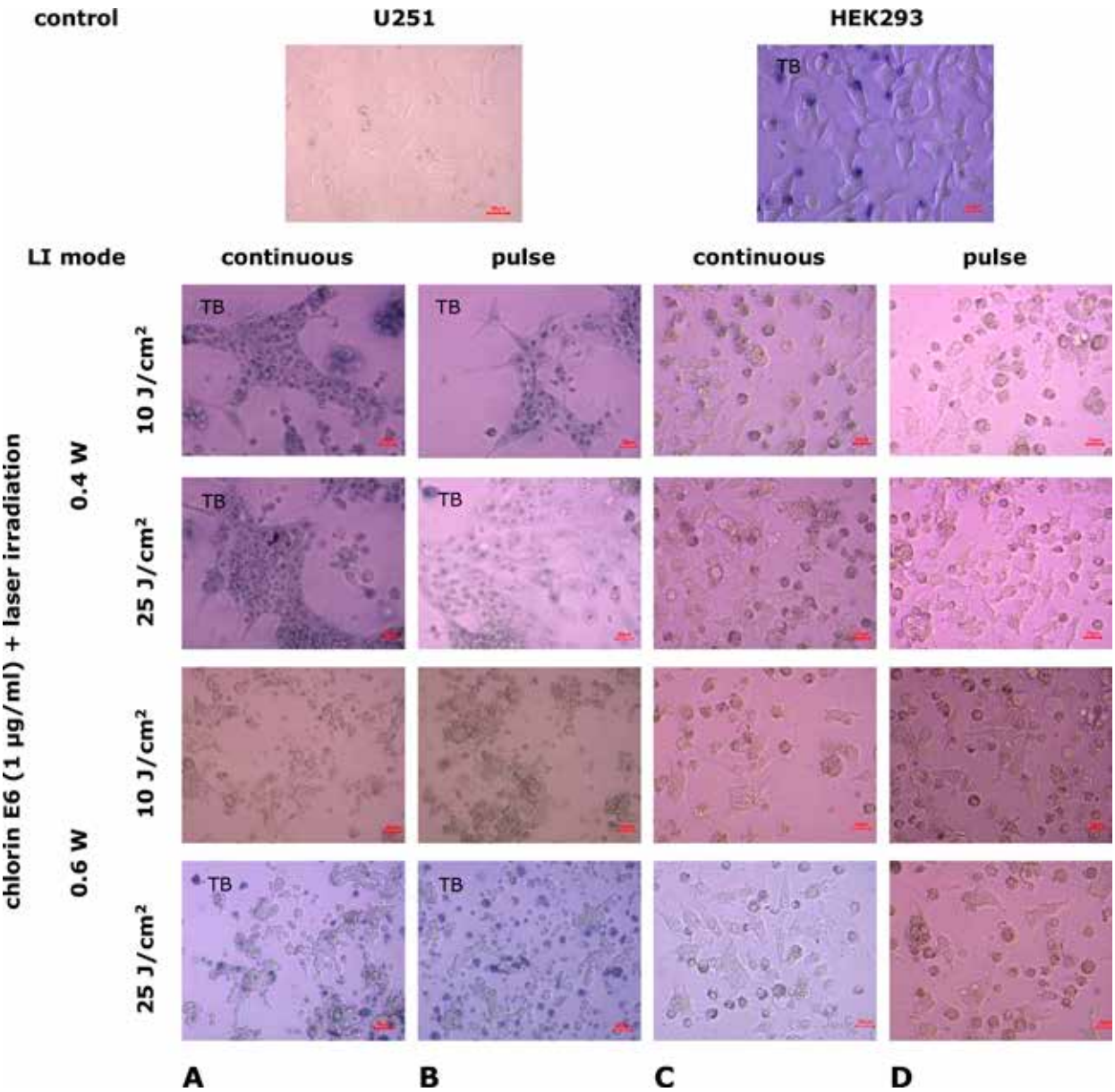

Fig. 7. Microphotographs of U251 human glioblastoma cell cultures and HEK293 cell cultures under combined exposure to chlorin E6 (1 μg/mL) and laser irradiation in different modes. Light microscopy. Unstained cultures and staining with trypan blue vital dye (TB)

activity was preserved in individual cells, especially in HEK293 lines (p=0.04 compared to control, p=0.09 compared to the index in continuous LI mode, Mann-Whitney U-test; ***Fig. 9A, 9B***).

Increasing the LI dose to 50 and 75 J/cm², in both continuous and pulse modes, slightly increased the degree of growth zone destruction in U251 cell lines. In addition to the completely destroyed areas of the growth zone, complexes and layers of adhered cells, particularly with processes, were found. However, most of these cells exhibited degenerative changes, such as loss of processes, characteristic morphological forms, cytoplasmic vacuolization, accumulation of lipid granules, and membrane integrity disruption ***(Fig. 8A, 8B)***. Similar changes in the growth zone under the same experimental conditions occurred in HEK293 cell cultures ***(Fig. 8C, 8D)***.

Mitotic activity of cells in cell cultures of U251 cell line was practically undetectable, starting from 25 J/cm² LI (0.6 W, pulse mode) ($p=3\cdot10^{-6}$ compared to control, p=0.17 compared to continuous LI mode, Mann-Whitney U-test) ***(Fig. 9A)***, whereas, in HEK293 cell cultures, mitotic activity was not recorded starting from 50 J/cm² LI (0.6 W, pulse mode) (p=0.04 compared to control, p=0.29 compared to continuous LI mode, Mann-Whitney U-test ***Fig. 9B***).

Consequently, studies on the combined effects of chlorin E6 and LI on U251 human glioblastoma cell cultures indicate a cumulative dose-dependent cytotoxic effect. Increasing the concentration of chlorin E6 from 1 to 2 μg/mL and increasing the LI power from 0.4 to 0.6 W and dose from 10 to 75 J/cm² in continuous mode consistently lead to destructive changes in the architectonics of the growth zone (these changes range from the retraction of the growth zone with the formation of lacunae of varying sizes at the lowest LI levels to gross destruction of the architectonics and significant

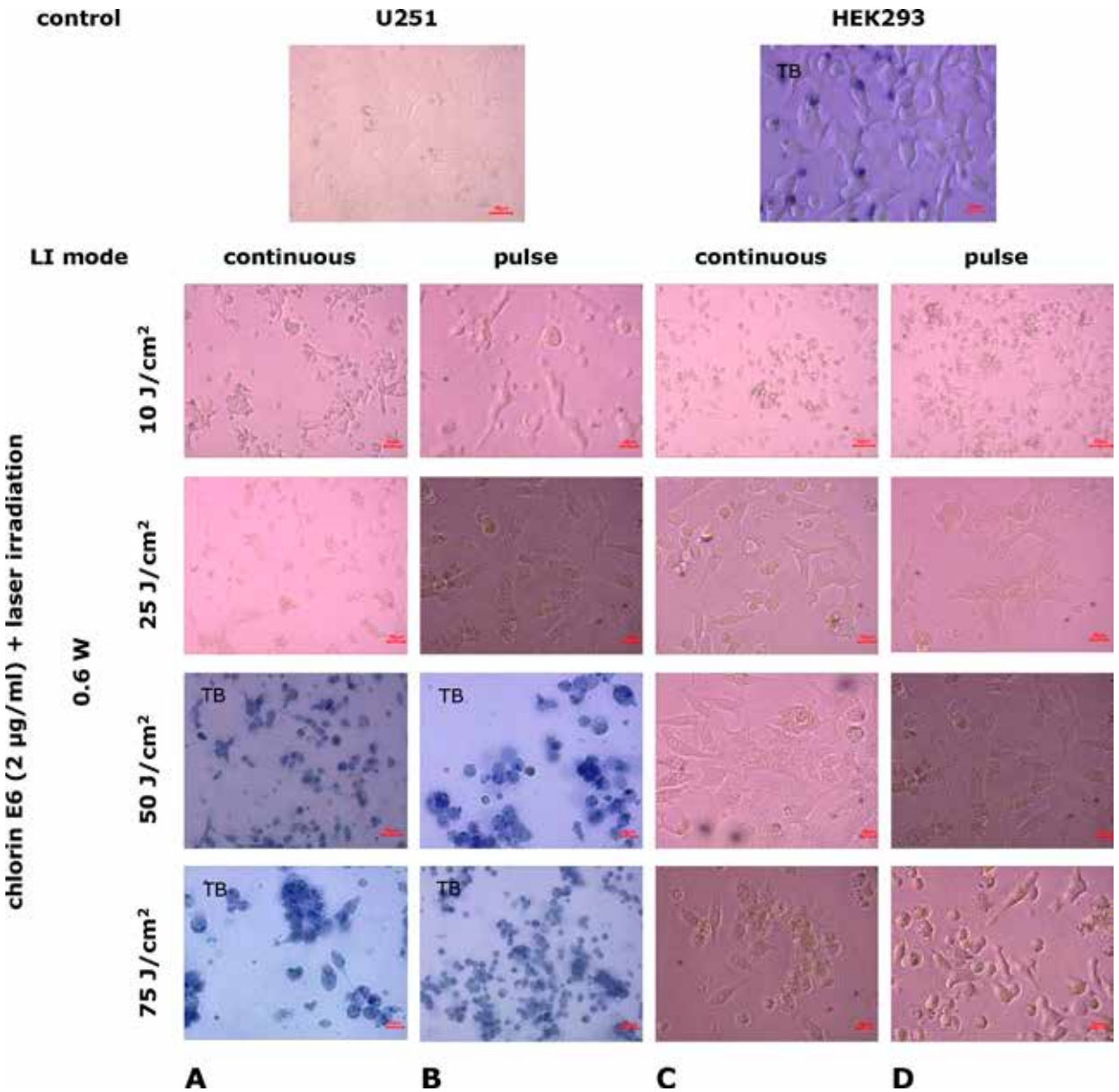

Fig. 8. Microphotographs of U251 human glioblastoma cell cultures and HEK293 cell cultures under combined exposure to chlorin E6 (2 μg/mL) and laser irradiation in different modes. Light Microscopy. Unstained cultures and staining with trypan blue vital dye (TB)

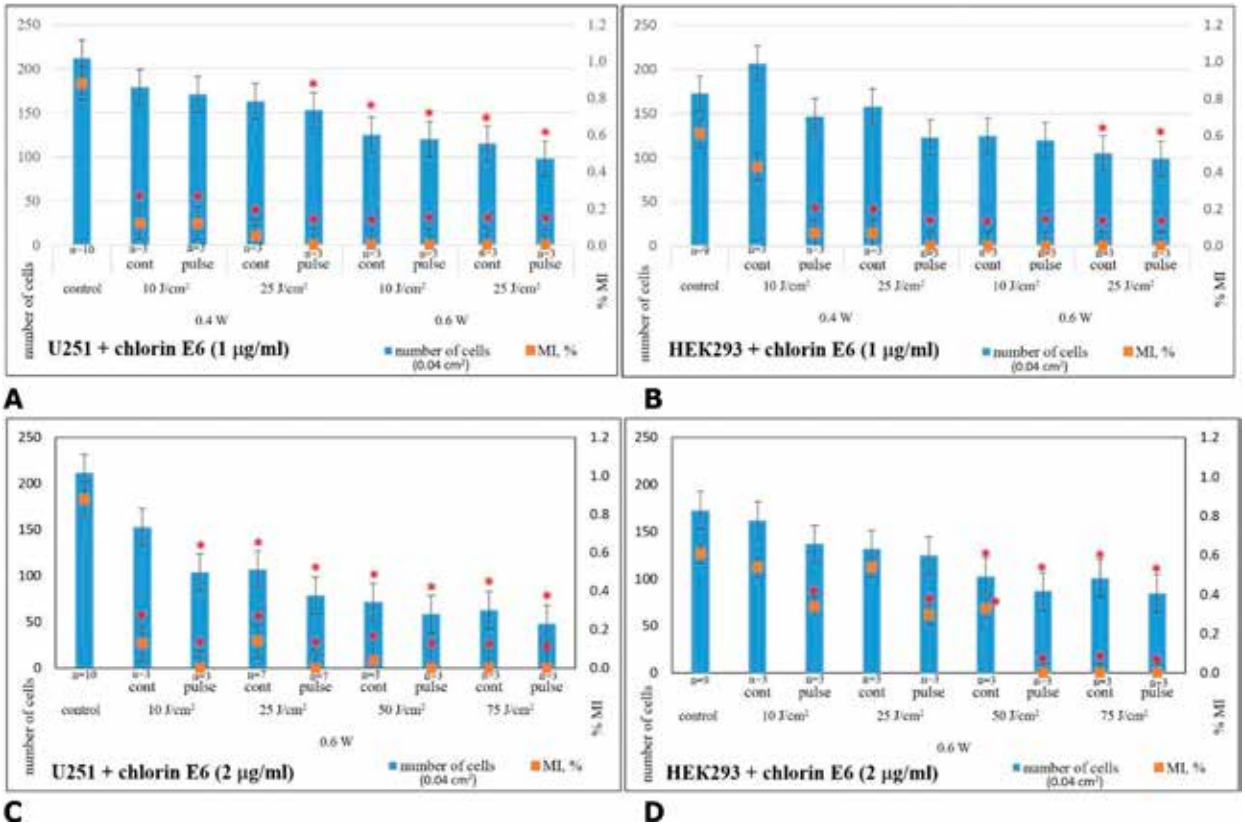

Fig. 9. Average cell count and mitotic index (MI, %) in cell cultures of U251 human GB cell line (A,C) and HEK293 cell line (B,D) 24 h after combined exposure to chlorin E6 (1 μg/mL, 2 μg/mL, 4-h pre-incubation) and various laser irradiation modes: * – $p<0.05$ compared to control; Mann-Whitney U-test

depletion of cell masses at the highest levels, as well as a dynamic reduction in the mitotic activity of tumor cells ($p=(1–3)\cdot10^{-6}$ compared to control), accumulation of necrobiotic changes, irreversible degeneration, and desquamation of dead cells. This effect tends to intensify with the use of LI in pulse mode ($p=0.37$, $p=0.17$, $p=0.45$, $p=0.50$, respectively, for LI doses of 10, 25, 50, and 75 J/ cm² compared to quantitative indicators of cultures under the combined influence of chlorin E6 and continuous LI mode, Mann-Whitney U-test). It is precisely with the combined effect of chlorin E6 (2 μg/ mL) and LI that the quantitative indicators of reduced mitotic activity in U251 human GB cell cultures become statistically significant compared to the corresponding indicators with direct LI exposure, starting at a dose of 25 J/cm² ($p=0.05$, $p=0.047$, $p=0.013$, respectively, for LI doses of 25, 50, and 75 J/cm², Mann-Whitney U-test).

The nature of the changes in HEK293 cell cultures under the combined influence of chlorin E6 and LI in the same modes is similar to that of U251 cells, but unlike tumor cells, the dynamics of the changes were not as pronounced, and their level was significantly lower. Significant pathological changes in HEK293 cells, their monolayer density, and mitotic activity were detected starting at LI mode of 0.6 W, dose of 25 J/cm² in pulse mode with the application of 1 μg/mL of chlorin E6 or LI mode of 0.6 W, dose of 50 J/cm² in pulse mode with the use of 2 μg/mL of chlorin E6. For U251 cell line, the threshold value was the following LI characteristics: power 0.4 W, dose 25 J/cm², pulse mode with the application of 1 μg/mL of chlorin E6 or power 0.6 W, dose 10 J/cm², pulse mode using 2 μg/mL of chlorin E6 ***(Fig. 9)***.

The results of the study on the combined effects of chlorin E6 (1 and 2 μg/mL, 4-h pre-incubation) and LI in various modes (λ=660 nm, power 0.4–0.6 W, dose 10–75 J/cm², continuous or pulsed mode) provide a basis for concluding the efficiency of the cytodestructive and antimitotic effects in U251 human GB cell cultures. Specifically, the application of an irradiation dose of 25 J/cm² at 0.6 W in pulse mode with chlorin E6 at a concentration of 2 μg/mL (after 4-h pre-incubation of the cell culture) is effective. The use of combined effect of PS and LI with the indicated characteristics in the culture of cells of the HEK293 cell line, which has a similar neuronal phenotype, did not entail such significant cytodestructive effects as in the culture of tumour cells of the U251 cell line, i.e. human GB cells of the line U251 are more sensitive to the photodynamic effect of chlorin E6 and LI compared to cells of the HEK293 line. One explanation for this may be the higher metabolism level of MG tumor cells compared to non-transformed cells [31, 32], as well as their faster accumulation of the photosensitizer compared to neuro cells. The selective accumulation of the PS in tumor cells is associated with low pH levels due to excess lactic acid production during active glycolysis compared to normal cells. Photosensitizers dissolve better in acidic environments and consequently accumulate more effectively in tumor cells [33].

The antimitotic effect of the applied photodynamic exposure modes using chlorin E6 in U251 human GB cell cultures is consistent with data showing reduced proliferation and clonogenic capacity in glioblastoma cell lines (T98G, MO59, LN229, U87-MG) after photodynamic exposure with the use of phthalocyanines ZnPc and TAZnPc [29].

Thus, according to the results of morphological and morphometric study, it was found that PS chlorin E6 is incorporated into the cytoplasm of human GB cell lines U251 and cells of HEK293 line, and the fluorescence intensity is comparable. The direct exposure of chlorin E6 (1.0 and 2.0 μg/ml) for 24 h dose-dependently enhanced cytodestructive and antimitotic effects in human GB culture of U251 line. In contrast to cell line U251, the cytodestructive effect of chlorin E6 on cultures of cell line HEK293 is less pronounced, but the antimitotic effect is relatively comparable in both types of cell cultures. When exposed to LI (λ=660 nm, power 0.4-0.6 W, dose 10-75 J/cm², continuous or pulse mode), cytodestructive and antimitotic effects in human GB cell culture line U251 are increased in a dose-dependent manner. The level of cytodestructive and antimitotic effects is significantly lower in cultures of the non-tumour cell line HEK293. The most significant reduction of mitotic activity of human GB cells of U251 line (~100%) was recorded at the lowest dose of LI 25 J/cm², power 0.6 W, in pulse mode, whereas for HEK293 line cells (~80%) - at LI power 0.6 W, dose 75 J/cm², in continuous mode. The combination of exposure to chlorin E6 and LI as the dose increases leads to complete destruction of tumour cells in human GB cell culture cell line U251. Total cytodestructive and antimitotic effect in the culture of human GB cell line U251 is achieved at the combination of the lowest irradiation dose 25 J/cm², power 0.6 W, in pulse mode and chlorin E6 in concentration of 2 μg/ml. In contrast to human GB cells of U251 line, the specified mode of photodynamic exposure is not irreversibly destructive for cultures of HEK293 line cells: against the background of a 1.3-fold decrease in the total number of cells, reference cells retain mitotic activity (MI~0.3%).

Consequently, human GB cells of the U251 line are more sensitive to the cumulative effect of photodynamic exposure to chlorin E6 and LI compared to HEK293 cells. An effective mode of photodynamic exposure to achieve sufficient cytodestructive and antimitotic effect in human GB cell culture of the U251 line is the combined application of irradiation with a dose of 25 J/cm², power 0.6 W, in pulse mode with pre-incubation of cell culture with chlorin E6 at a concentration of 2 μg/ml for 4 h. This mode is much less destructive, and therefore, relatively safe for cultures of HEK293 line.

Conclusions

As a result of the morphological and morphometric study, an effective photodynamic exposure has been established for achieving cytodestructive and antimitotic effects in human GB cell culture of the U251 line. The mode is relatively safe for non-malignant cells: involving the combined application of a laser irradiation dose of 25 J/cm² at 0.6 W in pulse mode, in pre-incubation of the cell culture with chlorin E6 at a concentration of 2 μg/ml for 4 h.

Acknowledgments

The authors express their sincere gratitude to Oleksandra Lykhova, Ph.D., Senior Research Fellow of the Department of Tumor Process Monitoring and Therapy Design, R.E. Kavetsky Institute of Experimental Pathology, Oncology and Radiobiology of the NAS of Ukraine, for kindly providing the U251 and HEK293 cell line samples for cultivation and research.

Disclosure

Conflict of Interest

The authors declare no conflicts of interest.

Funding

This research was not supported by any sponsorship.

The study is part of a research project (State Registration No. 0122U000331).

References

1. Sung H, Ferlay J, Siegel RL, Laversanne M, Soerjomataram I, Jemal A, Bray F. Global Cancer Statistics 2020: GLOBOCAN Estimates of Incidence and Mortality Worldwide for 36 Cancers in 185 Countries. CA Cancer J Clin. 2021 May;71(3):209-249. doi: 10.3322/caac.21660
2. Ostrom QT, Price M, Neff C, Cioffi G, Waite KA, Kruchko C, Barnholtz-Sloan JS. CBTRUS Statistical Report: Primary Brain and Other Central Nervous System Tumors Diagnosed in the United States in 2016-2020. Neuro Oncol. 2023 Oct 4;25(12 Suppl 2):iv1-iv99. doi: 10.1093/neuonc/noad149. PMID: 377931257
3. Louis DN, Perry A, Wesseling P, Brat DJ, Cree IA, Figarella-Branger D, Hawkins C, Ng HK, Pfister SM, Reifenberger G, Soffietti R, von Deimling A, Ellison DW. The 2021 WHO Classification of Tumors of the Central Nervous System: a summary. Neuro Oncol. 2021 Aug 2;23(8):1231-1251. doi: 10.1093/neuonc/noab106
4. Ostrom QT, Cioffi G, Waite K, Kruchko C, Barnholtz-Sloan JS. CBTRUS Statistical Report: Primary Brain and Other Central Nervous System Tumors Diagnosed in the United States in 2014-2018. Neuro Oncol. 2021 Oct 5;23(12 Suppl 2):iii1-iii105. doi: 10.1093/neuonc/noab200
5. Fedorenko Z, Goulak L, Gorokh Ye, Ryzhov A, Soumkina O. CANCER IN UKRAINE, 2021-2022: Incidence, mortality, prevalence and other relevant statistics. Bulletin of the National Cancer Registry of Ukraine. 2023;24. http://ncru.inf.ua/publications/BULL_24/PDF_E/bull_eng_24.pdf
6. van Solinge TS, Nieland L, Chiocca EA, Broekman MLD. Advances in local therapy for glioblastoma - taking the fight to the tumour. Nat Rev Neurol. 2022 Apr;18(4):221-236. doi: 10.1038/s41582-022-00621-0
7. Mahmoudi K, Garvey KL, Bouras A, Cramer G, Stepp H, Jesu Raj JG, Bozec D, Busch TM, Hadjipanayis CG. 5-aminolevulinic acid photodynamic therapy for the treatment of high-grade gliomas. J Neurooncol. 2019 Feb;141(3):595-607. doi: 10.1007/s11060-019-03103-4
8. Muller PJ, Wilson BC. Photodynamic therapy for malignant newly diagnosed supratentorial gliomas. J Clin Laser Med Surg. 1996 Oct;14(5):263-70. doi: 10.1089/clm.1996.14.263
9. Cramer SW, Chen CC. Photodynamic Therapy for the Treatment of Glioblastoma. Front Surg. 2020 Jan 21;6:81. doi: 10.3389/fsurg.2019.00081
10. Muragaki Y, Akimoto J, Maruyama T, Iseki H, Ikuta S, Nitta M, Maebayashi K, Saito T, Okada Y, Kaneko S, Matsumura A, Kuroiwa T, Karasawa K, Nakazato Y, Kayama T. Phase II clinical study on intraoperative photodynamic therapy with talaporfin sodium and semiconductor laser in patients with malignant brain tumors. J Neurosurg. 2013 Oct;119(4):845-52. doi: 10.3171/2013.7.JNS13415
11. Quirk BJ, Brandal G, Donlon S, Vera JC, Mang TS, Foy AB, Lew SM, Girotti AW, Jogal S, LaViolette PS, Connelly JM, Whelan HT. Photodynamic therapy (PDT) for malignant brain tumors--where do we stand? Photodiagnosis Photodyn Ther. 2015 Sep;12(3):530-44. doi: 10.1016/j.pdpdt.2015.04.009
12. Senders JT, Muskens IS, Schnoor R, Karhade AV, Cote DJ,

Smith TR, Broekman ML. Agents for fluorescence-guided glioma surgery: a systematic review of preclinical and clinical results. Acta Neurochir (Wien). 2017 Jan;159(1):151-167. doi: 10.1007/s00701-016-3028-5
13. Stummer W, Pichlmeier U, Meinel T, Wiestler OD, Zanella F, Reulen HJ; ALA-Glioma Study Group. Fluorescence-guided surgery with 5-aminolevulinic acid for resection of malignant glioma: a randomised controlled multicentre phase III trial. Lancet Oncol. 2006 May;7(5):392-401. doi: 10.1016/S1470-2045(06)70665-9
14. Kostron H, Obwegeser A, Jakober R. Photodynamic therapy in neurosurgery: a review. J Photochem Photobiol B. 1996 Nov;36(2):157-68. doi: 10.1016/s1011-1344(96)07364-2
15. Kaneko S, Fujimoto S, Yamaguchi H, Yamauchi T, Yoshimoto T, Tokuda K. Photodynamic Therapy of Malignant Gliomas. Prog Neurol Surg. 2018;32:1-13. doi: 10.1159/000469675
16. Schipmann S, Müther M, Stögbauer L, Zimmer S, Brokinkel B, Holling M, Grauer O, Suero Molina E, Warneke N, Stummer W. Combination of ALA-induced fluorescence-guided resection and intraoperative open photodynamic therapy for recurrent glioblastoma: case series on a promising dual strategy for local tumor control. J Neurosurg. 2020 Jan 24;134(2):426-436. doi: 10.3171/2019.11.JNS192443
17. Vermandel M, Dupont C, Lecomte F, Leroy HA, Tuleasca C, Mordon S, Hadjipanayis CG, Reyns N. Standardized intraoperative 5-ALA photodynamic therapy for newly diagnosed glioblastoma patients: a preliminary analysis of the INDYGO clinical trial. J Neurooncol. 2021 May;152(3):501-514. doi: 10.1007/s11060-021-03718-6
18. Eljamel MS, Goodman C, Moseley H. ALA and Photofrin fluorescence-guided resection and repetitive PDT in glioblastoma multiforme: a single centre Phase III randomised controlled trial. Lasers Med Sci. 2008 Oct;23(4):361-7. doi: 10.1007/s10103-007-0494-2
19. van Linde ME, Brahm CG, de Witt Hamer PC, Reijneveld JC, Bruynzeel AME, Vandertop WP, van de Ven PM, Wagemakers M, van der Weide HL, Enting RH, Walenkamp AME, Verheul HMW. Treatment outcome of patients with recurrent glioblastoma multiforme: a retrospective multicenter analysis. J Neurooncol. 2017 Oct;135(1):183-192. doi: 10.1007/s11060-017-2564-z
20. Lietke S, Schmutzer M, Schwartz C, Weller J, Siller S, Aumiller M, Heckl C, Forbrig R, Niyazi M, Egensperger R, Stepp H, Sroka R, Tonn JC, Rühm A, Thon N. Interstitial Photodynamic Therapy Using 5-ALA for Malignant Glioma Recurrences. Cancers (Basel). 2021 Apr 7;13(8):1767. doi: 10.3390/cancers13081767
21. Kobayashi T, Nitta M, Shimizu K, Saito T, Tsuzuki S, Fukui A, Koriyama S, Kuwano A, Komori T, Masui K, Maehara T, Kawamata T, Muragaki Y. Therapeutic Options for Recurrent Glioblastoma-Efficacy of Talaporfin Sodium Mediated Photodynamic Therapy. Pharmaceutics. 2022 Feb 2;14(2):353. doi: 10.3390/pharmaceutics14020353
22. Muller PJ, Wilson BC. Photodynamic therapy of brain tumors--a work in progress. Lasers Surg Med. 2006 Jun;38(5):384-9. doi: 10.1002/lsm.20338
23. Zavadskaya TS. Photodynamic therapy in the treatment of glioma. Exp Oncol. 2015 Dec;37(4):234-41.
24. Hamaliya MF, Shyshko YD, Shton' IO, Kholin VV, Shcherbakov OB, Usatenko OV. [Photodynamic activity of second-generation photosensitizer fotolon (chlorin e6) and its golden nanocomposite: experiments in vitro and in vivo]. Photobiology and Photomedicine. 2012;9(1-2):99-103. Ukrainian. https://periodicals.karazin.ua/photomedicine/article/view/13195
25. U-251 MG (formerly known as U-373 MG) (ECACC 09063001). Culture Collections. UK Health Security Agency; 2024. https://www.culturecollections.org.uk/products/celllines/generalcell/detail.jsp?refId=09063001&collection=ecacc_gc
26. HEK293 (ECACC 85120602). Culture Collections. UK Health Security Agency; 2024. https://www.culturecollections.org.uk/nop/product/293
27. Lin YC, Boone M, Meuris L, Lemmens I, Van Roy N, Soete A, Reumers J, Moisse M, Plaisance S, Drmanac R, Chen J, Speleman F, Lambrechts D, Van de Peer Y, Tavernier J, Callewaert N. Genome dynamics of the human embryonic kidney 293 lineage in response to cell biology manipulations. Nat Commun. 2014 Sep 3;5:4767. doi: 10.1038/ncomms5767
28. Stepanenko AA, Dmitrenko VV. HEK293 in cell biology and cancer research: phenotype, karyotype, tumorigenicity, and stress-induced genome-phenotype evolution. Gene. 2015 Sep 15;569(2):182-90. doi: 10.1016/j.gene.2015.05.065
29. Velazquez FN, Miretti M, Baumgartner MT, Caputto BL, Tempesti TC, Prucca CG. Effectiveness of ZnPc and of an amine derivative to inactivate Glioblastoma cells by Photodynamic Therapy: an in vitro comparative study. Sci Rep. 2019 Feb 28;9(1):3010. doi: 10.1038/s41598-019-39390-0
30. Rozumenko VD, Liubich LD, Staino L.P., Egorova D.M., Vaslovych VV, Rozumenko AV, Komarova OS, Dashchakovskyi AV, Kluchka VM, Malysheva TA. Effects of photodynamic exposure using chlorine E6 on U251 glioblastoma cell line in vitro. Ukrainian Neurosurgical Journal. 2023; 29(2): 11-21. doi: 10.25305/unj.273699
31. Márquez J, Alonso FJ, Matés JM, Segura JA, Martín-Rufián M, Campos-Sandoval JA. Glutamine Addiction In Gliomas. Neurochem Res. 2017 Jun;42(6):1735-1746. doi: 10.1007/s11064-017-2212-1
32. Rivera JF , Sridharan SV , Nolan JK , Miloro SA , Alam MA , Rickus JL , Janes DB . Real-time characterization of uptake kinetics of glioblastoma vs. astrocytes in 2D cell culture using microelectrode array. Analyst. 2018 Oct 8;143(20):4954-4966. doi: 10.1039/c8an01198b
33. Moan J, Peng Q. An outline of the history of PDT. Patrice T, editor. Photodynamic Therapy. London: The Royal Society of Chemistry; 2003. p. 1–18. doi: 10.1039/9781847551658-00001

Case Report

Ukr Neurosurg J. 2024;30(3):52-55
doi: 10.25305/unj.306743

Meningocele manqué. Case report of a rare disorder

Ajay Sebastian Carvalho [1], Vijay Kumar Gupta [2], Chinmaya Srivatsava [1], Deepak Dwivedi [3]

[1] Department of Neurosurgery, Command Hospital Eastern Command, Kolkata, India
[2] Department of Neurosurgery, National Institute of Medical Sciences and Research (NIMS), Jaipur, Rajasthan, India
[3] Department of Anaesthesia and Critical Care, Command Hospital Eastern Command, Kolkata, India

Received: 23 June 2024
Accepted: 31 July 2024

Address for correspondence*:*
Ajay Sebastian Carvalho, Department of Neurosurgery, Command Hospital Eastern Command, 17/1E, Alipore Rd, Alipore Police Line, Alipore, Kolkata, West Bengal 700027, India, e-mail:ajayneuro0404@gmail.com

A case of meningocele manqué with its management is presented and the literature of this rarely reported condition is reviewed.

A one-year-old child was admitted with a small sac like lesion in the upper dorsal region with a soft swelling in the dorso lumbar region, was also associated with congenital bilateral talipes equinovarus which was being treated by a paediatric orthopedic surgeon.

Methods. Craniospinal MRI was suggestive of dorso lumbar lipomyelomeningocele, and corresponding to the dorsal sinus/sac at DV3/DV4 level there was another tethering seen on the MRI due to a band and associated with syrinx of the dorsal cord below that, s/o meningocele manqué.

Treatment. This patient underwent in 1st stage, DV2 to DV5 laminoplasty, excision of the sinus, durotomy, dissection of the multiple arachnoid cysts, and cutting of the dorsal band. In second stage will undergo surgery for Lipomyelomeningocele

Conclusion: Meningocele Manque is rare, it can present in isolation or associated with other spinal dysraphism. With other spinal dysraphism they can be either at the same or at another location, as was seen in our case. Before operating all cases of spinal dysraphism it is of paramount importance to MRI screen the entire neuraxis and study images thoroughly. In our case along with the dorso lumbar lipomyelomeningocele, there was a Meningocele manqué at DV3/DV4 level. It is essential that the meningocele manqué be addressed first; if not the returning/recoiling cord after de-tethering at the lower level can get tugged/sheared at the tethered meningocele manqué causing deficits.

Key words: *meningocele manqué; spinal dysraphism; tethered cord; lipomyelomeningocele*

Introduction

Meningocele Manque is a rare anomaly and is also rarely reported. It can present in isolation or with other spinal dysraphism. With other spinal dysraphism they can be either at the same or, as was in our case at another location. Before operating all cases of spinal dysraphism it is of paramount importance to MRI screen the entire neuraxis and study images thoroughly. In our case along with the dorso lumbar lipomyelomeningocele, there was a Meningocele manqué at the DV3/DV4 level. It is essential that the meningocele manqué is detected in all spinal dysraphism and addressed first; if not the returning/recoiling cord, after de-tethering at the lower level can get tugged/sheared at the tethered meningocele manqué causing deficits.

Clinical profile

One year old male child, first born of non-consanguineous marriage, a known case of Talipes equinovarus (TEV) on regular Paediatric Orthopedic consultation, was presented to paediatric OPD with the parents giving history of a soft swelling on the lower back region and a small sac like lesion on the upper back, they also reported history of reduced movements of the left lower limb as compared to the right lower limb. Urine stream was good. There were no associated delayed milestones. On examination there was a small sac like lesion (atretic meningocele) at DV3/DV4 level in the dorsal spine ***(Fig. 1A)***, lipomyelomeningocele in the dorso lumbar region ***(Fig. 1B)*** and TEV, there were no other cutaneous stigmata, neurologically the power in left lower limb was less as compared to right.

MRI of entire neuraxis revealed a lipomyelomeningocele ***(Fig. 2)*** with associated low lying cord with tethering. However at DV3/DV4 level corresponding to the dorsal sinus/sac there was another tethering of the dorsal cord due to a fibrous band associated with syrinx ***(Fig. 3)***, there was no associated Chiari malformation.

The plan was to operate in two setting in view of the age and low weight of the child, the first stage, the patient underwent DV2 to DV5 laminoplasty and durotomy, per-op there was protuberant arachnoid membranes forming multiple arachnoid cysts which was dissected out and a single dorsal band arising from the dorsal aspect of the cord to the dura ***(Fig.4)***, which was carefully cut and after these dissections the cord settled down. Post-op the patient was managed in the paediatric ICU, there were no fresh neurological deficits, drain was removed on the third day and the patient was discharged on the 7th post-op day.

Fig. 1. A - showing the dormant sinus/sac upper dorsal level (green arrow), B –showing the lipoma (part of lipomyelomeningocele) (blue arrow)

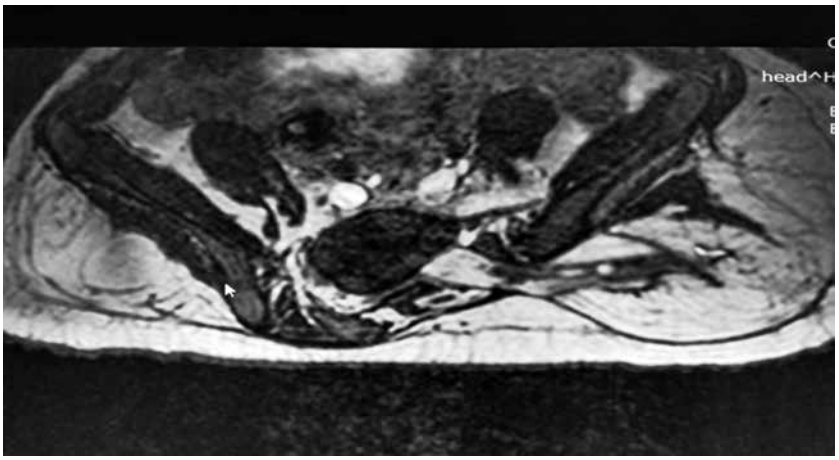

Fig. 2. Representative T2W axial cuts of the Lumbosacral spine showing the lipomyelomeningocele

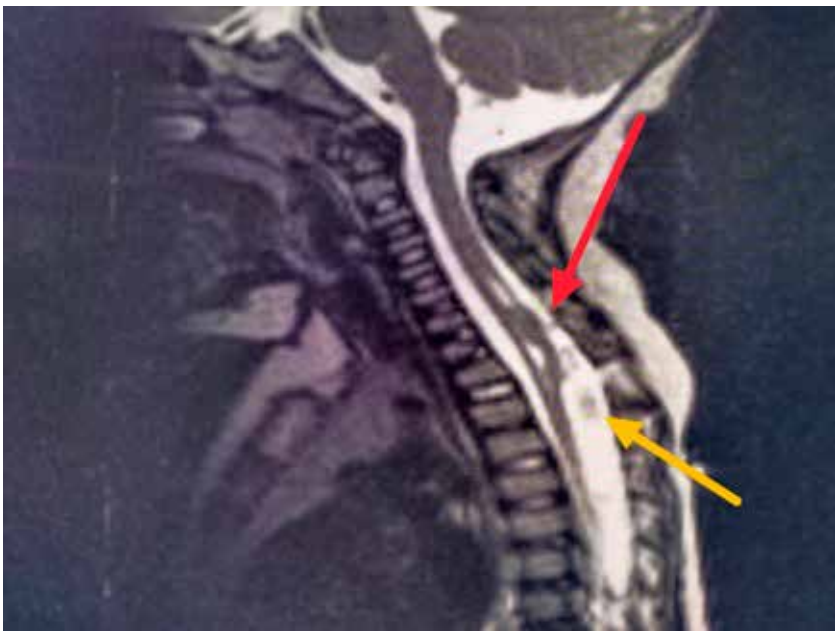

Fig. 3. Representative T2W MRI cut showing tethering at D3/D4 due to a band (red arrow) level with associated syrinx, yellow arrow points to protuberant arachnoid

This article contains some figures that are displayed in color online but in black and white in the print edition.

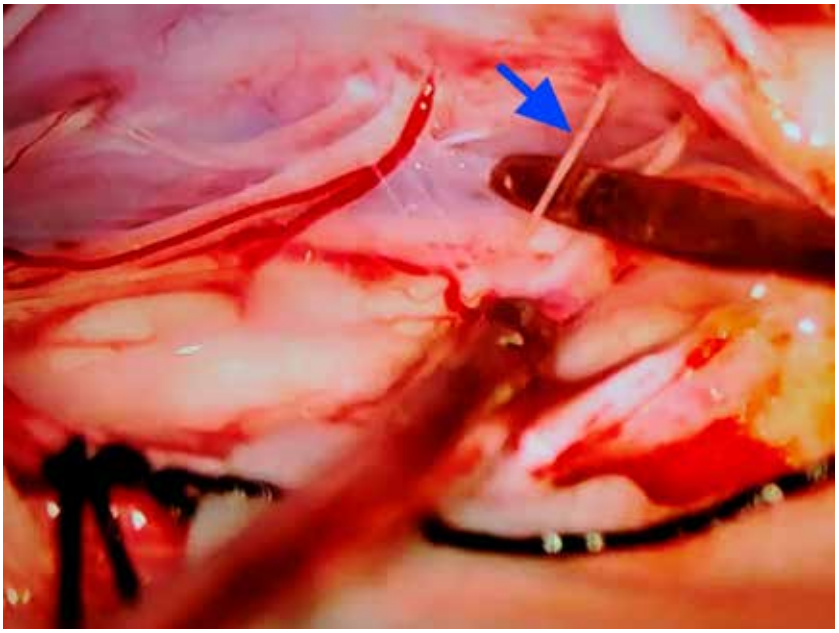

Fig. 4. Per-op photograph showing the dorsal band above the dissector on the right of the frame (blue arrow)

Review of literature

Meningocele manqué is basically tethering due to fibrous bands having atretic neural tissue. It is an incidental finding seen in spinal dysraphism [1, 2].

"Meningocele manque" was coined by James and Lassman in 1972. This was used to describe in patients with spina bifida occulta who had atretic meningoceles, and since there was no meningocele sac, this term was chosen. "Manque" which in French means 'might have been but it is not' [3].

Initially this term was used only to refer dorsal tethering bands found in cases of spina bifida occulta, but recently it's also being used in dorsal tethering bands associated with meningocele. It is also seen associated with diastematomyelia and dermoid cysts. Literature on meningocele manqué is very limited [4].

Embryonic theory of meningocele manqué is not clearly defined; a possible hypothesis is the dysraphic defect in meningocele formation which atrophies and the remaining embryonic remnants of the atrophied meningocele form dysplastic nervous and fibrous tissue tethering the cord [5]. The exact cause of meningocele manqué is not known, the causes could be congenital malformation of the spinal cord, Vitamin B12 deficiency or could be an association with diastematomyelia. In meningocele manque, the herniated lesion can contain atretic neural tissue, meninges and CSF [6].

Symptomatology is usually neurological symptoms of tethered cord with cutaneous stigmata.

The differential diagnoses for meningocele manqué are meningocele and meningomyelocele. Meningocele manqué in isolation carries a good prognosis [7]. It is essential to detect it in the screening MRI and will have to be addressed before the formal surgery for other dysraphism, if not the retracting cord after de-tethering can get sheared/tugged at the site of meningocele manqué. A similar situation was found in our case; the child underwent successful release of the meningocele manqué at DV2/DV3 level and in second stage will undergo surgery for Lipomyelomeningocele.

Conclusion

Meningocele Manque is rare, it can present in isolation or associated with other spinal dysraphism. With other spinal dysraphism they can be either at the same or at another location, as was seen in our case. Before operating all cases of spinal dysraphism it is of paramount importance to MRI screen the entire neuraxis and study images thoroughly. In our case along with the dorso lumbar lipomyelomeningocele, there was a Meningocele manqué at DV3/DV4 level. It is essential that the meningocele manqué be addressed first; if not the returning/recoiling cord after de-tethering at the lower level can get tugged/sheared at the tethered meningocele manqué causing deficits.

Disclosure

Conflict of interest

None reported.

Informed consent

The patient's parents provided informed consent for the publication of data and images.

Funding

The author declares no financial support of any kind received for this study.

References

1. Kriss VM, Kriss TC, Warf BC. Dorsal tethering bands of the meningocele manque: sonographic findings. AJR Am J Roentgenol. 1996 Nov;167 (5):1293-4. doi: 10.2214/ajr.167.5.8911198. PMID: 8911198.
2. Kaffenberger DA, Heinz ER, Oakes JW, Boyko O. Meningocele manqué: radiologic findings with clinical correlation. AJNR Am J Neuroradiol. 1992 Jul-Aug;13 (4):1083-8. PMID: 1636517; PMCID: PMC8333584.
3. JAMES CC, LASSMAN LP. Spinal dysraphism. An orthopaedic

syndrome in children accompanying occult forms. Arch Dis Child. 1960 Aug;35 (182):315-27. doi: 10.1136/adc.35.182.315. PMID: 13789286; PMCID: PMC2012570.
4. Iskandar BJ, Oakes WJ, McLaughlin C, Osumi AK, Tien RD. Terminal syringohydromyelia and occult spinal dysraphism. J Neurosurg. 1994 Oct;81 (4):513-9. doi: 10.3171/jns.1994.81.4.0513. PMID: 7931583.
5. Lassman LP, James CC. Meningocoele manqué. Childs Brain. 1977;3 (1):1-11. doi: 10.1159/000119644. PMID: 321190.
6. Warder DE. Tethered cord syndrome and occult spinal dysraphism. Neurosurg Focus. 2001 Jan 15;10 (1):e1. doi: 10.3171/foc.2001.10.1.2. PMID: 16749753.
7. Artul S, Nseir W, Artoul F, Bisharat B, Habib G. Atretic meningocele: Etiopathogenesis, frequency, anomaly associations and imaging findings. Austin J Radiol. 2015;2 (1):1011. https://austinpublishinggroup.com/radiology/fulltext/ajr-v2-id1011.php

Case report

Ukr Neurosurg J. 2024;30(3):56-60
doi: 10.25305/unj.307877

Surgical Treatment of Spinal Intra-Extradural Meningioma: A Clinical Case

Vitaliy Y. Molotkovets [1,2], Oleksii S. Nekhlopochyn [3], Myroslava O. Marushchenko [1]

[1] Department of Neurosurgery, Bogomolets National Medical University, Kyiv, Ukraine
[2] Extracerebral Tumor Department, Romodanov Neurosurgery Institute, Kyiv, Ukraine
[3] Spine Neurosurgery Department, Romodanov Neurosurgery Institute, Kyiv, Ukraine

Received: 05 July 2024
Accepted: 31 July 2024

Address for correspondence*: Vitaliy Y. Molotkovets, Extracerebral Tumor Department, Romodanov Neurosurgery Institute, 32 Platona Maiborody st., Kyiv, 04050, Ukraine, e-mail: molotkovets@gmail.com*

Spinal meningiomas are rare, predominantly benign tumors that exhibit slow growth and typically have a non-invasive pattern of development. They originate from arachnoid cells and fibroblasts of the dura mater. Despite their benign nature, some meningiomas can exhibit intra-extradural extension, complicating both diagnosis and treatment. This article presents a clinical case involving a patient with an intra-extradural spinal meningioma. Despite radiological imaging suggesting a neurinoma, the final diagnosis confirmed a meningioma.

Case Report: A female patient underwent surgical tumor resection through a posterolateral approach with laminectomy and facetectomy at the C4-C5 vertebral levels. The tumor, extending through the intervertebral foramen, was completely resected along with the affected nerve root. Histological examination verified a Grade 2 meningioma.

Discussion: Despite advancements in neuroimaging and surgical techniques, intraoperative findings can be unpredictable, necessitating an adaptive approach to tumor resection. The article emphasizes the importance of adequate preoperative planning and the use of intraoperative neurophysiological monitoring to reduce the risk of complications and improve treatment outcomes.

Conclusions: The primary treatment for spinal meningiomas is surgical. For dorsal and lateral localizations, total resection with the involved dura mater (Simpson Grade I) is optimal. For ventral localizations, tumor resection with coagulation of the dural attachment site (Simpson Grade II) is preferred. Preoperative and intraoperative use of electrophysiological methods is recommended to assess the functional status of neural structures. Intra-extradural localization of meningiomas is rare and presents significant challenges in preoperative diagnosis, requiring specific skills for effective removal.

Keywords: *meningioma; spinal tumor; intradural extramedullary location; neurosurgery*

Introduction

Meningiomas are slowly progressing benign neoplasms. They originate from arachnoid cells and fibroblasts of the dura mater (DM) [1]. They are characterized mainly by a non-invasive growth pattern but can extend to adjacent tissues. Meningiomas account for 25–46% of primary extramedullary spinal tumors [2,3] and 1.2–12.0% of all meningiomas of the central nervous system [3, 4]. In terms of their location relative to the spinal cord, they can be lateral (55%), ventral (29%), dorsal (13%), or "dumbbell"-shaped (3%) [4], and in relation to the DM, they can be intradural and extradural. In some cases, only extradural localization is observed [5], which complicates radiological assessment during preoperative diagnosis. Arachnoid tissue migration with islet aberrations in the case of extracranial meningiomas and distant sites (e.g., the nose or skin) is assumed [6, 7]. This mechanism of spread may occur with isolated extradural spinal meningiomas.

They occur more frequently in women aged 50–80, which is associated with hormone receptor expression [8, 9]. Meningiomas are the second most common benign extramedullary tumor after schwannomas in women aged 40–70 [10]. About 9% of spinal meningiomas are asymptomatic [11]. Depending on the location and size of the tumor, the clinical picture may manifest as pain, motor and sensory disorders, ataxia, and pelvic organ dysfunction [12]. Pain occurs in 42–87% of cases and may be either local or irradiated [13]. The clinical picture in extradural spread does not significantly differ from that of an intradural tumor.

Magnetic resonance imaging (MRI) with intravenous contrast enhancement is the diagnostic standard. Since extradural localization is relatively rare for meningiomas,

careful evaluation of the radiological picture is required. For example, foraminal extension is grounds for suspecting schwannoma or neurofibroma [12]. In the presence of young patients or multiple lesions, a genetic disease (neurofibromatosis type 2) is possible [14]. Meningiomas should be primarily differentiated from schwannomas, metastatic tumors, lymphomas, and tuberculomas. Preoperative differentiation and intraoperative histological examination allow the optimal surgical approach to be determined [15].

The use of the modified McCormick scale is advisable to assess functional impairments in spinal neoplasms (I - neurologically intact patients who move normally, with minimally expressed sensory disorders possible, II - mild motor or sensory deficits, functionally independent patients, III - independent of external assistance, IV – gross motor or sensory deficits, functional limitations, patients dependent on external assistance, V - paraplegia or tetraplegia) [16].

Clinical Case

Patient K., a 36-year-old military servicewoman, presented with complaints of pain in the cervical spine, slight muscle weakness in the left arm, dizziness, and impaired sensetion in the left arm. Neurological examination revealed a slight decrease in muscle strength (4 points) during shoulder abduction, characteristic of C5 root involvement.

MRI with contrast agent showed an intra-extravertebral tumor extending through the intervertebral foramen. The radiological picture most closely resembled a schwannoma ***(see Fig. 1).***

Surgery was performed to remove the tumor (Simpson II). Posterolateral approach was chosen for access to the tumor. C4 and C5 vertebral arches and articular processes together with the joint were identified through a midline incision. A laminectomy at the C4-C5 vertebrae and a left C4-C5 facetectomy were performed. The expanded intervertebral foramen and the dural cuff, showing signs of significant tension, were noteworthy. The intradural portion of the tumor was removed in the first stage. The nerve root was dissected and separated from the tumor tissue. The dural cuff was incised, and the portion of the tumor located in the intervertebral foramen and extending extravertebrally was removed. Within the dural cuff, the nerve root was structurally destroyed, making it impossible to preserve the nerve. After removing the tumor along with the affected nerve root, the DM was coagulated at the tumor growth site. Hermetic suture of the DM was performed at the site of the nerve root opening and tumor spread.

The postoperative period was uneventful. Neurologically, the patient did not experience any deterioration. She was referred for further rehabilitation treatment. Subsequently, the patient returned to her duties.

A meningioma (Grade 2) was verified by pathohistological examination.

MRI performed six months after surgery showed no signs of pathological accumulation of contrast agent which could indicate tumor recurrence ***(Fig. 2)***.

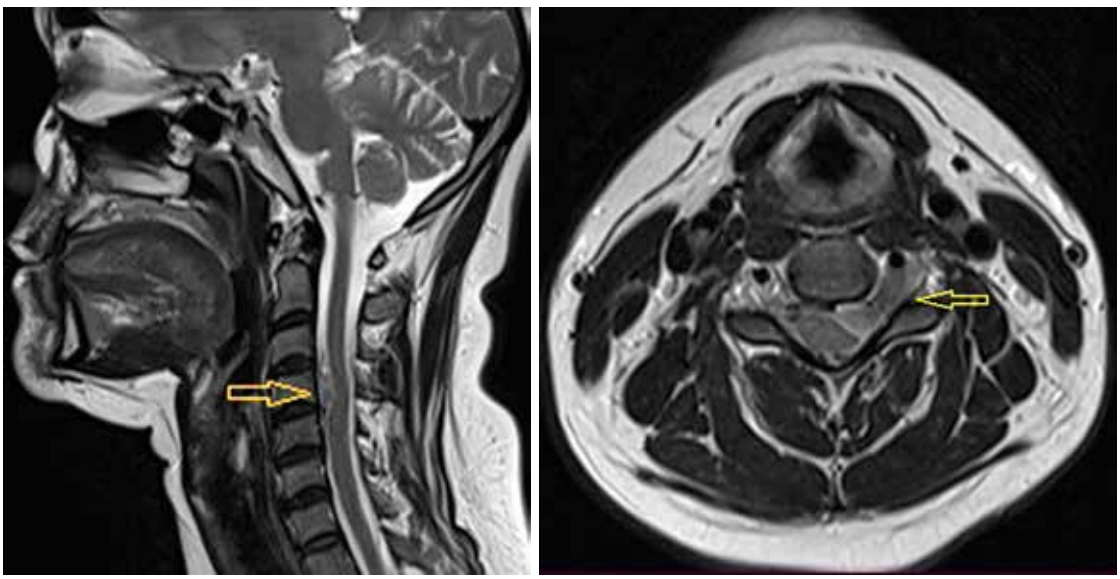

Fig. 1. MRI of the cervical spine with contrast in T2-mode. The arrow indicates an intra-extravertebral tumor extending through the intervertebral foramen. Tumor size: 13.0×22.0×8.5 mm

This article contains some figures that are displayed in color online but in black and white in the print edition.

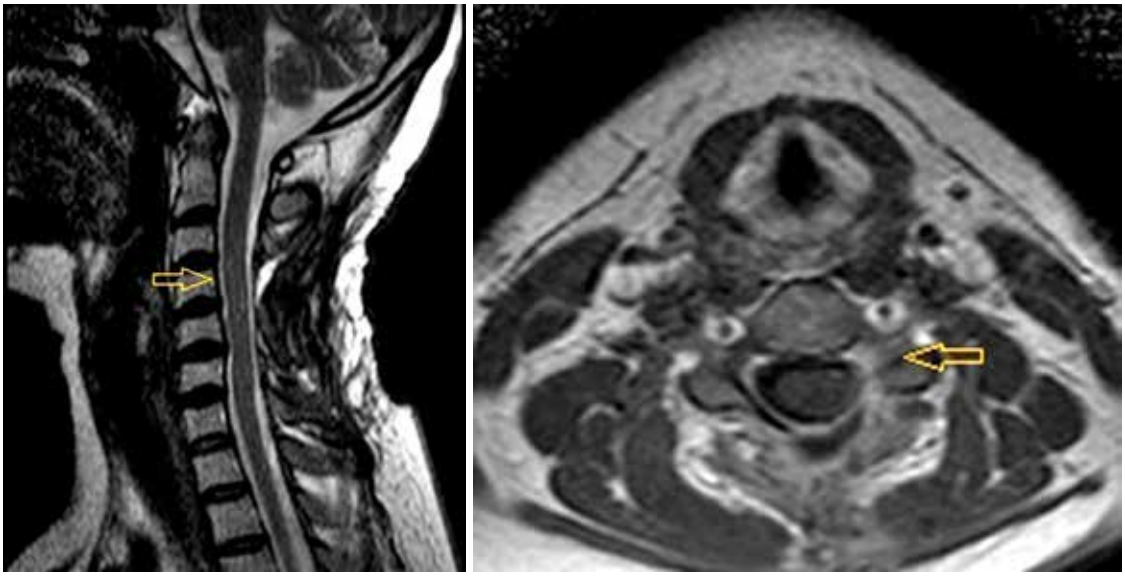

Fig. 2. MRI of the cervical spine with contrast, T2 mode. Postoperative follow-up six months after meningioma removal. Simpson II

Discussion

The primary treatment for spinal meningiomas is surgical, which is the most effective method for reducing recurrence rates (3-15%) after removal [10,17]. The generally accepted surgical strategy is radical removal of CNS meningiomas (Simpson I), as subtotal resection is a recurrence factor. Proven additional recurrence factors of spinal meningiomas include young age (<18 years), cervical spine location, extensive "dural tails," and male gender [18–20]. Given the complexity of DM plasty and the risk of damage to neural structures and disruption of DM integrity, spinal meningiomas are predominantly removed using the Simpson II method. However, there is no significant increase in recurrence rates as with cranial meningiomas. The recurrence rate for Simpson II removal is 1–8% [4, 17, 21]. The type of removal (Simpson I or Simpson II) is debated in the case of spinal meningiomas due to the low risk of recurrence and the increase in complications. No significant difference in survival has been established between different removal types (Simpson I or Simpson II) [4].

In most cases, total removal of meningiomas is achieved [22]. To some extent, the radicality of removal depends on the location. Dorsal and dorsolateral meningiomas are more often successfully removed with DM resection and reconstruction [4]. When removal of the growth area is impossible, dissection and splitting of DM leaves are recommended to increase radicality and maintain sheath integrity [23]. It has been established that one-third of spinal meningiomas invade the DM, specifically spreading between the inner and outer leaves, and 47% have "dural tails," as confirmed by pathohistological studies [24]. In the study by K. Kobayashi et al., of 116 spinal meningiomas, 3 had a dumbbell shape with transforaminal, extravertebral spread. After Simpson II removal, recurrences were observed in these three cases [4].

Considering the need to preserve neural structures during radical tumor removal, it is recommended to use intraoperative neurophysiological monitoring, including transcranial motor evoked potentials, and during preoperative diagnosis, to conduct electroneuromyography with an assessment of the degree of conduction impairment in the proximal sections of the nerve and innervation [25].

The main surgical treatment methods are [26]:

the most commonly used classical open approach and microsurgical removal.

minimally invasive surgery.

endoscopic surgery.

The choice of surgical method depends on many factors, such as tumor aggressiveness and complex spreading patterns (e.g., anterior spinal cord localization in the thoracic spine or anterolateral localization relative to the upper cervical spine, which may compress the vertebral artery [27]).

Optimal surgical access to ventral extra-intravertebral meningiomas of the cervical spine is challenging [28]. Both anterior approaches with corpectomy and corporodesis and posterior approaches with laminectomy and partial unilateral facetectomy are equally effective [28]. The main principle for choosing an approach to ventral extra-intravertebral meningiomas of the cervical spine is the level of involvement: for upper cervical localization, a posterior approach is preferred, and for lower cervical localization, an anterior approach is preferred.

Postoperative mortality for spinal meningiomas is generally low, ranging from 0 to 4.7%, according to various authors [29,30].

Radiation therapy can be applied in cases of high-grade malignancy or recurrence [31].

The presented clinical case shows that despite significant improvements in neuroimaging methods and adequate preoperative planning of the intervention volume, intraoperative findings can sometimes be unpredictable. The presence of classic, almost pathognomonic signs of schwannoma (dumbbell

shape accompanied by anatomical enlargement of the intervertebral foramen) is the basis for even experienced surgeons to choose a certain volume of intervention. The detection of a meningioma localized intraextracanalically requires significantly more effort for its adequate removal, minimizing the risks of neurological consequences and general surgical complications, such as cerebrospinal fluid leakage or the formation of cerebrospinal fluid cysts. Awareness of such situations is of important practical significance both for the radical removal of the tumor and for the necessary handling of the DM, which is critical to reducing the risk of recurrence.

Conclusions

The main treatment method for spinal meningiomas is surgical intervention. For dorsal and lateral localization, the optimal approach is total removal along with the involved DM (Simpson I). In the case of ventral localization, preference is given to tumor removal and coagulation of the site of derivative growth (Simpson II).

Electrophysiological methods are recommended during the preoperative and intraoperative periods to assess the functional state of neural structures.

Intra-extracanal localization of meningiomas is rare. It can significantly complicate preoperative diagnosis and may require specialized skills for the removal of such meningioma.

Disclosure

Conflict of Interest

The authors declare no conflicts of interest.

Informed consent

Informed consent for data disclosure was obtained from the patient.

References

1. Tuli J, Drzymalski DM, Lidov H, Tuli S. Extradural en-plaque spinal meningioma with intraneural invasion. World Neurosurg. 2012 Jan;77(1):202.e5-13. doi: 10.1016/j.wneu.2011.03.047
2. Saraceni C, Harrop JS. Spinal meningioma: chronicles of contemporary neurosurgical diagnosis and management. Clin Neurol Neurosurg. 2009 Apr;111(3):221-6. doi: 10.1016/j.clineuro.2008.10.018
3. Ravindra VM, Schmidt MH. Management of Spinal Meningiomas. Neurosurg Clin N Am. 2016 Apr;27(2):195-205. doi: 10.1016/j.nec.2015.11.010
4. Kobayashi K, Ando K, Matsumoto T, Sato K, Kato F, Kanemura T, Yoshihara H, Sakai Y, Hirasawa A, Nakashima H, Imagama S. Clinical features and prognostic factors in spinal meningioma surgery from a multicenter study. Sci Rep. 2021 Jun 2;11(1):11630. doi: 10.1038/s41598-021-91225-z
5. Takeuchi H, Kubota T, Sato K, Hirose S. Cervical extradural meningioma with rapidly progressive myelopathy. J Clin Neurosci. 2006 Apr;13(3):397-400. doi: 10.1016/j.jocn.2005.05.018. PMID: 16542842
6. Sato N, Sze G. Extradural spinal meningioma: MRI. Neuroradiology. 1997 Jun;39(6):450-2. doi: 10.1007/s002340050444
7. Fortuna A, Gambacorta D, Occhipinti EM. Spinal extradural meningiomas. Neurochirurgia (Stuttg). 1969 Sep;12(5):166-80. doi: 10.1055/s-0028-1095299
8. Westwick HJ, Shamji MF. Effects of sex on the incidence and prognosis of spinal meningiomas: a Surveillance, Epidemiology, and End Results study. J Neurosurg Spine. 2015 Sep;23(3):368-73. doi: 10.3171/2014.12.SPINE14974
9. Wigertz A, Lönn S, Mathiesen T, Ahlbom A, Hall P, Feychting M; Swedish Interphone Study Group. Risk of brain tumors associated with exposure to exogenous female sex hormones. Am J Epidemiol. 2006 Oct 1;164(7):629-36. doi: 10.1093/aje/kwj254
10. Levy WJ Jr, Bay J, Dohn D. Spinal cord meningioma. J Neurosurg. 1982 Dec;57(6):804-12. doi: 10.3171/jns.1982.57.6.0804
11. Engelhard HH, Villano JL, Porter KR, Stewart AK, Barua M, Barker FG, Newton HB. Clinical presentation, histology, and treatment in 430 patients with primary tumors of the spinal cord, spinal meninges, or cauda equina. J Neurosurg Spine. 2010 Jul;13(1):67-77. doi: 10.3171/2010.3.SPINE09430
12. Hong W, Kim ES, Lee Y, Lee K, Koh SH, Song H, Kwon MJ. Spinal Extradural Meningioma: A Case Report and Review of the Literature. J Korean Soc Radiol. 2018 Jul;79(1):11-17. doi: 10.3348/jksr.2018.79.1.11
13. Postalci L, Tugcu B, Gungor A, Guclu G. Spinal meningiomas: recurrence in ventrally located individuals on long-term follow-up; a review of 46 operated cases. Turk Neurosurg. 2011;21(4):449-53. doi: 10.5137/1019-5149.jtn.3518-10.2
14. Sandalcioglu IE, Hunold A, Müller O, Bassiouni H, Stolke D, Asgari S. Spinal meningiomas: critical review of 131 surgically treated patients. Eur Spine J. 2008 Aug;17(8):1035-41. doi: 10.1007/s00586-008-0685-y
15. Jeong SK, Seong HY, Roh SW. Extra-intradural Spinal Meningioma: A Case Report. Korean J Spine. 2014 Sep;11(3):202-4. doi: 10.14245/kjs.2014.11.3.202
16. Muravskiy AV. [Surgical treatment of intramedullary spinal cord ependymoma]. Ukrainian Neurosurgical Journal. 2002; (2):48-52. Ukrainian. https://theunj.org/article/view/91831
17. Solero CL, Fornari M, Giombini S, Lasio G, Oliveri G, Cimino C, Pluchino F. Spinal meningiomas: review of 174 operated cases. Neurosurgery. 1989 Aug;25(2):153-60. doi: 10.1227/00006123-198908000-00001
18. Sarıkaya C, Ramazanoğlu AF, Yaltırık CK, Etli MU, Önen MR, Naderi S. Short-Term Results of Simpson Grade 2 Resection in Spinal Meningiomas. World Neurosurg. 2023 Mar;171:e792-e795. doi: 10.1016/j.wneu.2022.12.115
19. Naito K, Yamagata T, Arima H, Takami T. Low recurrence after Simpson grade II resection of spinal benign meningiomas in a single-institute 10-year retrospective study. J Clin Neurosci. 2020 Jul;77:168-174. doi: 10.1016/j.jocn.2020.04.113
20. Maiti TK, Bir SC, Patra DP, Kalakoti P, Guthikonda B, Nanda A. Spinal meningiomas: clinicoradiological factors predicting recurrence and functional outcome. Neurosurg Focus. 2016 Aug;41(2):E6. doi: 10.3171/2016.5.FOCUS16163
21. Yoon SH, Chung CK, Jahng TA. Surgical outcome of spinal canal meningiomas. J Korean Neurosurg Soc. 2007 Oct;42(4):300-4. doi: 10.3340/jkns.2007.42.4.300
22. Iacob G. Spinal meningiomas. Personal experience and review of literature. Romanian Neurosurgery. 2014 Jun 1;21(2):147–61. doi: 10.2478/romneu-2014-0016
23. Saito T, Arizono T, Maeda T, Terada K, Iwamoto Y. A novel technique for surgical resection of spinal meningioma. Spine (Phila Pa 1976). 2001 Aug 15;26(16):1805-8. doi: 10.1097/00007632-200108150-00017
24. Nakamura M, Tsuji O, Fujiyoshi K, Hosogane N, Watanabe K, Tsuji T, Ishii K, Toyama Y, Chiba K, Matsumoto M. Long-term surgical outcomes of spinal meningiomas. Spine (Phila Pa 1976). 2012 May 1;37(10):E617-23. doi: 10.1097/BRS.0b013e31824167f1
25. Zheng C, Nie C, Zhu Y, Xu M, Lyu F, Jiang J, Xia X. Preoperative electrophysiologic assessment of C5-innervated muscles in predicting C5 palsy after posterior cervical decompression. Eur Spine J. 2021 Jun;30(6):1681-1688. doi: 10.1007/s00586-021-06757-9
26. Arima H, Takami T, Yamagata T, Naito K, Abe J, Shimokawa N, Ohata K. Surgical management of spinal meningiomas: A retrospective case analysis based on preoperative surgical grade. Surg Neurol Int. 2014 Aug 28;5(Suppl 7):S333-8. doi: 10.4103/2152-7806.139642
27. Parsa AT, Lee J, Parney IF, Weinstein P, McCormick PC, Ames C. Spinal cord and intradural-extraparenchymal spinal tumors: current best care practices and strategies. J Neurooncol. 2004 Aug-Sep;69(1-3):291-318. doi: 10.1023/b:neon.0000041889.71136.62
28. Eroglu U, Bahadır B, Tomlinson SB, Ugur HC, Sayaci EY, Attar A, Caglar YS, Cohen Gadol AA. Microsurgical

Management of Ventral Intradural-Extramedullary Cervical Meningiomas: Technical Considerations and Outcomes. World Neurosurg. 2020 Mar;135:e748-e753. doi: 10.1016/j.wneu.2019.12.145
29. Raco A, Pesce A, Toccaceli G, Domenicucci M, Miscusi M, Delfini R. Factors Leading to a Poor Functional Outcome in Spinal Meningioma Surgery: Remarks on 173 Cases. Neurosurgery. 2017 Apr 1;80(4):602-609. doi: 10.1093/neuros/nyw092
30. Boström A, Bürgel U, Reinacher P, Krings T, Rohde V, Gilsbach JM, Hans FJ. A less invasive surgical concept for the resection of spinal meningiomas. Acta Neurochir (Wien). 2008 Jun;150(6):551-6; discussion 556. doi: 10.1007/s00701-008-1514-0
31. Roux FX, Nataf F, Pinaudeau M, Borne G, Devaux B, Meder JF. Intraspinal meningiomas: review of 54 cases with discussion of poor prognosis factors and modern therapeutic management. Surg Neurol. 1996 Nov;46(5):458-63; discussion 463-4. doi: 10.1016/s0090-3019(96)00199-1